REVERSIBLE MICROBALLOON SYSTEM FOR HANDLING BIOANALYTICAL ASSAYS ON CENTRIFUGAL MICROFLUIDIC PLATFORM

MOHAMMAD MAHDI AEINEHVAND

THESIS SUBMITTED IN FULFILMENT OF THE REQUIREMENTS FOR THE DEGREE OF DOCTOR OF PHILOSOPHY

FACULTY OF ENGINEERING
UNIVERSITY OF MALAYA
KUALA LUMPUR

2016

UNIVERSITY OF MALAYA

ORIGINAL LITERARY WORK DECLARATION

Name of Candidate: MOHAMMAD MAHDI AEINEHVAND

Registration/Matric No.: KHA120101

Name of Degree: Doctor of Philosophy (Ph.D.)

Title of Thesis: Reversible Microballoon System for Handling Bioanalytical Assays on Centrifugal Microfluidic Platform

Field of Study: BIOMEMS

I do solemnly and sincerely declare that:

(1) I am the sole author/writer of this Work;
(2) This Work is original;
(3) Any use of any work in which copyright exists was done by way of fair dealing and for permitted purposes and any excerpt or extract from, or reference to or reproduction of any copyright work has been disclosed expressly and sufficiently and the title of the work and its authorship have been acknowledged in this Work;
(4) I do not have any actual knowledge or ought I reasonably to know that the making of this Work constitutes an infringement of any copyright work;
(5) I hereby assign all and every rights in the copyright to this Work to the University of Malaya ("UM"), who henceforth shall be owner of the copyright in this Work and that any reproduction or use in any form or by any means whatsoever is prohibited without the written consent of UM having been the first had and obtained;
(6) I am fully aware that if in the course of making this Work I have infringed any copyright whether intentionally or otherwise, I may be subject to legal action or any other action as may be determined by UM.

Candidate's Signature Date:

Subscribed and solemnly declared before,

Witness's signature Date:

Name:

Designation:

ABSTRACT

The unidirectional nature of centripetal flow, the predominant laminar flow in microfluidic systems, and the unreliability of the capillary valves are three main limitations exist in centrifugal microfluidics. This thesis presents the development of reversible microballoon pump, mixer and valve that enhance the control over the manipulation of liquids in bioanalytical assay on centrifugal microfluidic platforms. The high elasticity of the microballoon allows for an efficient conversion of centrifugally and externally induced forces to pumping, mixing and valving forces. The first liquid handling element presented in this thesis is a microballoon pump that relies on elastic energy stored in a latex membrane. It operates at low rotational speeds (< 1500 rpm) and pumps various liquid volumes towards the centre of the CD. The second presented liquid handling element is a microballoon mixer that operates by the expansion and relaxation of the membrane to provide for a consistent periodical 3D reciprocating flow. The third presented microballoon liquid handling element is a reversible thermo-pneumatic valve (RTPV) that seals or reopens an inlet when a trapped air volume is heated or cooled, respectively. It employs the deflection of a latex membrane to control liquid flow and prevent evaporation of reagents over a wide range of spinning speeds (up to 6000 rpm) and temperatures (up to the operational temperature of the disk materials), respectively.

To illustrate their practicality in real life applications, microballoon pump, mixer, and valves are used for the actuation of a siphon channel, biosensing enhancement of dengue virus, and controlling fluid flow in a continuous liquid circulation process, respectively. Finally, an array of RTPVs and a microballoon pump/mixer are imbedded in a microfluidic cartridge to automate a lab protocol required for the multiplexing of temperature-controlled assays. As a pilot study, the cartridge is used for the conversion of multiple dengue virus RNA to cDNA, and reused for the preparation of multiple separated PCR reaction mixtures.

ABSTRAK

Tiga kekurangan utama bagi system mickofluildik emparan adalah aliran sehala oleh daya emparan, aliran utama adalah aliran laminar dan ketidakberkesanan injap kapilari. Thesis ini membentangkan pembangunan sistem pam mikrobaloon dua-hala, pencampur/pembancuh dan injap yang akan mempertingkatkan keberkesanan kawalan untuk memanipulasi cecair dalam platfom mikrofluidk empran untuk kegunaan asai bioanalitik. Mikroballoon mempunyai anjalan yang kuat membolehkan penukaran daya empar dan luaran yang cekap mendorong untuk mengepam, mencampur dan daya injap. Unsur pengendalian cecair pertama yang dibentangkan dalam tesis ini adalah pam mikroballoon yang bergantung kepada tenaga elastik tersimpan dalam membran lateks. Ia boleh beroperasi pada kelajuan putaran yang rendah (< 1500 rpm) dan mengepam cecair pelbagai isipadu ke arah pusat CD. Unsur pengendalian cecair kedua yang dibentangkan adalah pengadun microballoon yang boleh beroperasi dengan pengembangan dan pengecutan membran lateks untuk aliran salingan 3D yang konsisten dan berkala. Microballoon pengendalian cecair unsur yang ketiga adalah injap thermo-pneumatik dua-hala (RTPV) yang dimeteraikan atau dibuka semula apabila jumlah udara yang terperangkap dipanaskan atau disejukkan. Ia menggunakan defleksi membran lateks untuk mengawal aliran cecair dan mengelakkan penyejatan reagen terhadap pelbagai kelajuan berputar (sehingga 6000 rpm) dan suhu (sehingga suhu operasi bahan-bahan di dalm cakera).

Untuk menggambarkan situasi praktikal dalam aplikasi sebenar, pam mikroballoon, pengadun dan injap telah digunakan untuk menggerakkan sebuah saluran siphon, peningkatan biosensing virus Denggi, dan mengawal aliran bendalir dalam satu proses peredaran cecair yang berterusan. Akhirnya, beberapa RTPVs dan pam mikroballoon /pencampur dalam kartrij mikrofluidik untuk kegunaan mengautomasikan protokol makmal yang diperlukan untuk pemultipleksan daripada asai suhu yang terkawal

telah dilakukan. Sebagai satu kajian rintis, kartrij digunakan untuk penukaran pelbagai RNA virus Denggi kepada cDNA, dan diguna semula untuk penyediaan pelbagai campuran tindak balas PCR.

`

ACKNOWLEDGMENTS

First, I want to thank my supervisors, Prof. Fatimah Ibrahim and Prof. Sulaiman Wadi Harun at University of Malaya and Prof. Marc Madou at University of California, Irvine, for their guidance and motivations throughout my study.

I would like to thank the University of Malaya High Impact Research Grant UM-MOHE UM.C/625/1/HIR/MOHE/05 from Ministry of Higher Education Malaysia (MOHE) for supporting my study and research work. I also would like to thank Faculty of Engineering and Faculty of Medicine for providing the facilities and the components required for undertaking this project.

Warm thanks to all my colleagues in the Centre for Innovation in Medical Engineering (CIME) and BioMEMS lab who support me through this whole journey, and in particular Karunan Joseph, Shah Mukim, Samira Hosseini, Wisam Al-Faqheri, Elham Farahmand, Bashar Yafouz, Amin Kazemzadeh, Gilbert Thio, Riwdwan, Jacob Moebius, Maria Bauer, Ling Kong and Prof. Jongman Cho.

Finally, I would like to thank my family. My family have been so supportive and have given me unconditional encouragement throughout. I have a big family, it includes Aeinehvands, Kalamis, Madou, Zarabi, Qochinyans, Fraihats, Alfered, Movses, Mozafari, Liew, and Martinezes. I would not have been able to start and/or complete a PhD without them.

TABLE OF CONTENTS

LIST OF FIGURES

LIST OF TABLES

LIST OF ABBREVIATIONS

CD	Compact disk
CM	Cellulose membrane
CNC	Computer numerical controlled
CP	Centrifugo pneumatic
ELISA	Enzyme linked-immunosorbent assays
LAMP	Loop mediated isothermal amplification
LOC	Lab-on-a-Chip
LOD	Lab-on-a-Disk
MA	Magnetically actuated
NASBA	Nucleic acid sequence-based amplification
NTD	Neglected tropical disease
PCR	Polymerase chain reaction
PDMS	Poly(dimethylsiloxame)
PMMA	Poly(methylmethacrylate)
POC	Point of care
PS	Polystyrene
PSA	Pressure sensitive adhesive
RPA	Recombinase polymerase amplification
RPM	Revolutions per minute
RTPV	Reversible thermo-pneumatic valve
SEM	Scanning electron microscopy
TP	Thermo-pneumatic

LIST OF APPENDICES

CHAPTER 1: INTRODUCTION

1.1 Overview

Lab-on-a-Chip (LOC) microfluidic platforms that enable rapid diagnostics near the patient's community are crucial to strengthen active surveillance, reduce mortality rates and minimize the window period of disease transmission (Briand et al., 2014; Chowell, Castillo-Chavez, Krishna, Qiu, & Anderson, 2015; Dhillon, Srikrishna, Garry, & Chowell, 2015). LOCs are microfluidic devices that integrate several laboratory functions (e.g., centrifugation, detection, separation, metering, valving, and mixing) on a plastic/silicon chip to automate bioanalytical assays. (Dittrich & Manz, 2006; Haeberle & Zengerle, 2007).

Centrifugal microfluidics is a subcategory of the LOC technology where liquid pumping force (the centrifugal force) is generated through spinning a microfluidic platform using a simple spindle motor (Robert Gorkin et al., 2010; M. Madou et al., 2006b). Manipulation of liquids by the centrifugal force prevents the need for an expensive syringe pump and its external interconnections. Centrifugal microfluidic platforms have been given several different names including lab-on-a-discs, LabDisks, microfluidic compact discs (CDs) and spinning microfluidic cartridges (Andreasen et al., 2015; Roy et al., 2015a; Oliver Strohmeier et al., 2014; Templeton & Salin, 2014). The centrifugally-induced pseudo forces (centripetal, Euler and Coriolis) exist everywhere on a microfluidic CD and facilitates the automation of parallel fluidic procedures. However, the unidirectional nature of the centrifugal force, the slow mixing/homogenization process, and the unreadability (unrobustness) of the capillary valves remain as three main problems in the centrifugal microfluidics. (Gorkin III, Clime, Madou, & Kido, 2010; Robert Gorkin et al., 2010; Stetten, 2012). The next section describes these three drawbacks, the fluidic techniques developed to overcome them and the limitations of the commonly used fluidic techniques.

1.2 Problem Statement

The first problem that exists in centrifugal microfluidics is the unidirectional nature of the centrifugal force as it always pumps liquids towards the outer rim of the CD. It limits the possible number of sequential fluidic steps or the usable space on microfluidic CDs (Abi-Samra et al., 2011; Gorkin III et al., 2010). To overcome this drawback, various methods have been developed to generate pumping forces to propel liquid towards the disc centre. Capillary force of a hydrophilized microchannel (Kitsara et al., 2014), pneumatic pressure of a compressed air bubble (Gorkin III et al., 2010), and thermo-pneumatic (TP) pressure of a heated air bubble are typical pumping forces employed to propel liquids against the direction of the centrifugal force (Thio, Ibrahim, et al., 2013). However, the implementation of these forces involves surface modification procedures, spinning of the CD at high spinning speeds (e.g., 6500 rpm) and the need of an additional power source (e.g., heat source), which introduce complexity and high cost of fabrication, elevated power consumption and the disturbance to other fluidic components.

The dominant flow regime in the micro- and nano-scale domain is laminar, limiting the mixing efficiency and slowing chemical reactions (Grumann, Geipel, Riegger, Zengerle, & Ducrée, 2005; Noroozi et al., 2009; van Reenen, de Jong, den Toonder, & Prins, 2014). Many recent inventions pertain to enhance the mixing on microfluidic CDs by the application of forces different from the centripetal force. By using a combination of the Euler and Coriolis forces an effective mixing mean (shake mode mixing) was demonstrated (Grumann et al., 2005). To enhance the quality of heterogeneous immunoassays, Noroozi et al. (2009) developed a flow reciprocation mixing method based on the compression/expansion of a trapped bubble. Other mixing techniques (e.g., magnet stirring) employ extra external equipment (e.g., magnetic platform) to provide high mixing efficiency. The high accelerations (e.g., 1920 rpm s^{-1}), high spinning speeds (e.g., 7500 rpm), large air chamber and additional equipment used

to mix liquids introduce the need for an expensive spindle motor, risk of contamination and CD delamination.

The third problem is the unreliability of the fragile capillary valves that prevents their use in the automation of multistep fluidic processes in microfluidic CDs (Gorkin III et al., 2012) . Due to the lack of a physical barrier, the capillary valves do not stop vapor transport (L. X. Kong, Parate, Abi-Samra, & Madou, 2015). Moreover, their burst frequency is a dynamic property as the contact angles of polymers surfaces changes over time. As an alternative to capillary barriers, a handful of valving techniques employ sacrificial barriers (e.g., dissolvable films and paraffin wax) to control liquid flow in the spinning CDs (L. X. Kong, Parate, et al., 2015). Some of the challenges encountered with regards to valving on microfluidic CDs are irreversibility, limited operational range of rotational frequencies, lack of versatility and the risk of evaporation and contamination.

In summary, the main limitations and challenges for liquid handling on centrifugal microfluidic platforms are:

I. The unidirectional nature of centripetal flow, and the high spinning speed, high acceleration, surface modification process and external power source required in the existing pumping mechanisms.
II. The low mixing efficiency in the micro- and nano-scale domain, and the high spinning speed, high acceleration, space occupying component and external power source required in the existing mixing mechanism.
III. The limited control over liquid retention and flow under centrifugal force, and the irreversibility, low operational range of rotational frequency and gas permeability of the previously developed microvalves.

The next section describes strategies that are proposed in this project to overcome the abovementioned limitations.

1.3 Proposed Strategy

I embedded a highly elastic latex film on a microfluidic CD to fabricate reversible and gas/liquid impermeable microballoons that can be deflected by air or liquid. The high elasticity of the microballoon allows for an efficient use of centrifugally and thermally induced forces to manipulate liquids on centrifugal microfluidic platforms. The expansion/relaxation of a microballoon allows for liquid displacement similar to the compression/expansion of an air bubble. Compared to pneumatic systems, the high elasticity of the microballoon allows us to pump and mix (reciprocate) larger liquid volumes at lower spinning speeds. To control the liquid retention and flow under centrifugal force, the same latex film is employed to develop reversible TP valves on the microfluidic CD. The high elasticity of the microballoon allows for an efficient use of an induced TP pressure to stop liquid flow. The reversible valve closes at elevated temperatures and thus prevents the evaporation of reagents in temperature controlled reactions. This is unlike the single-use valves that utilize thermal energy to remove a barrier to permit liquid flow.

1.4 Objectives

The main objectives of this project is development of reversible microballoon system for handling bioanalytical assays on centrifugal microfluidic platform. The three specific objectives that lead to achieve the main objective are:

I. Development of a micropump to displace large liquid volumes up to 90 µl against the direction of centrifugal force over a range of rotational speeds up to1500 RPM with no need for any surface modification procedure and external power source.

II. Development of a mixer to enhance dengue-ELISA detection signals by one order of magnitude in a range of rotational speeds up to 1700 rpm with no need for high acceleration, any space occupying component and peripheral equipment.

III. Development of a reversible valve to precisely control fluid retention and flow over a wide range of rotational speeds and temperatures up to 2500 RPM and 80 °C, respectively.

1.5 Scope of Research

This project focuses on the design and development liquid manipulation techniques on centrifugal microfluidic platforms for the automation of bioanalytical assays. Newtonian liquids are used for the mathematical modeling and experimental evaluation of pump, mixer and valve. Colored deionized water is implemented in pumping, siphoning, mixing, valving and continuous liquid circulation procedures and applications.

Dengue virus and extracted dengue RNA were chosen for the ELISA and PCR assays, respectively. This project does not focuses on the detection techniques on the centrifugal microfluidic platforms, and therefore resultant solutions of dengue ELISA were analyzed by a conventional well-plate reader. For the same reason, PCR resultant solutions were analyzed through agarose gel electrophoresis and a UV Transilluminator. Moreover, this project does not focuses on the development of incubator, and therefore ELISA and PCR resultant solutions are incubated inside a conventional incubator and thermal-cycler, respectively.

1.6 Thesis Organization

This thesis is comprised of six chapters. The contents of each chapter, except the current introductory *Chapter 1*, are briefly described as follows:

Chapter 2 describes the operating mechanism of micropumps, mixers and valves that are developed to manipulate liquids on centrifugal microfluidic platforms. The chapter also critically highlights the advantages and limitations of the liquid handling elements. Finally *Chapter 2* summarizes and lists the characteristics of an ideal micropump, mixer and valve.

Chapter 3 presents a centrifugally driven microballoon pump that displaces large liquid volumes towards the disc center over a low range of rotational frequencies (<1500 rpm). The chapter details the advantages of the latex material for the fabrication of the elastic microballoons, the fabrication procedure of the microballoons on microfluidic CDs, and the theoretical and experimental analysis of the microballoon pumps. Finally, the chapter illustrates a siphon priming process, which is one of the essential applications of the micropumps in bioanalytical assays, using a microballoon pump.

Chapter 4 presents a centrifugally driven microballoon based flow reciprocation mixing method. To evaluate the efficiency of the mixing technique, the chapter compares the microballoon mixer with the stopped-flow mixing method through (i)- a liquid-liquid homogenization process in a large-surface-to-volume-ratio chamber, and (ii)- biosensing enhancement of dengue detection in an immunoassay. To facilitate the use of a single microballoon for both mixing and pumping, *Chapter 4* also provides mathematical modeling of liquid displacement in mixing chambers corresponding to the changes of the disc spinning speed.

Chapter 5 presents a reversible thermo-pneumatic valve (RTPV) that is made by the latex film used for the fabrication of the microballoon mixer/pump. The chapter illustrates the fabrication procedure of RTPVs on microfluidic CDs, the mathematical modeling of the RTPV, and an application of RTPVs for continuous liquid circulation/switching. Conclusively, to illustrate the compatibility and practicality of the microballoon liquid handling elements for the implementation of bioanalytical assay on centrifugal microfluidic platforms, the chapter demonstrates and expounds a multiplexed thermally-controlled assays on a reusable microfluidic platform composed of the microballoon mixer, pump and valves.

Chapter 6 summarizes the microballoon-based liquid handling strategies presented in this thesis to overcome the problems in centrifugal microfluidics. Moreover,

the chapter describes the main limitation of the microballoon liquid handling elements and recommends several future work and related studies.

CHAPTER 2: LITERATURE REIVEW

2.1 Introduction

Over the last few decades we have seen an increasing interest in the application of Micro/Nano-fluidics in medical diagnostics technology and applications. Low sample volume, multiplexing, automation, portability, low cost and high throughput screening are among the many advantages that such platforms offer. Since emerging in the 1990s, several microfluidic and nanofluidic platforms were developed to perform various chemical and biological assays (Whitesides, 2006). Most of the reported microfluidic platforms can be classified under one of the following four main categories: Lab-On-a-Chip (LOC) (Haeberle & Zengerle, 2007), Lab-On-Paper (LOP) (Zhao & Berg, 2008), droplet-based microfluidic (droplet reactors) (Teh, Lin, Hung, & Lee, 2008), and Lab-on-a-Disc. This study focused only on Lab-on-a-Disc, which is also known as microfluidic Compact-Disc (CD) (L. X. Kong, Perebikovsky, Moebius, Kulinsky, & Madou, 2015), and the centrifugal microfluidic platform (O Strohmeier et al., 2015). A microfluidic CD is a spinning platform that relies on the centripetal force to pump liquids from side to side on the CD (M. Madou et al., 2006a).

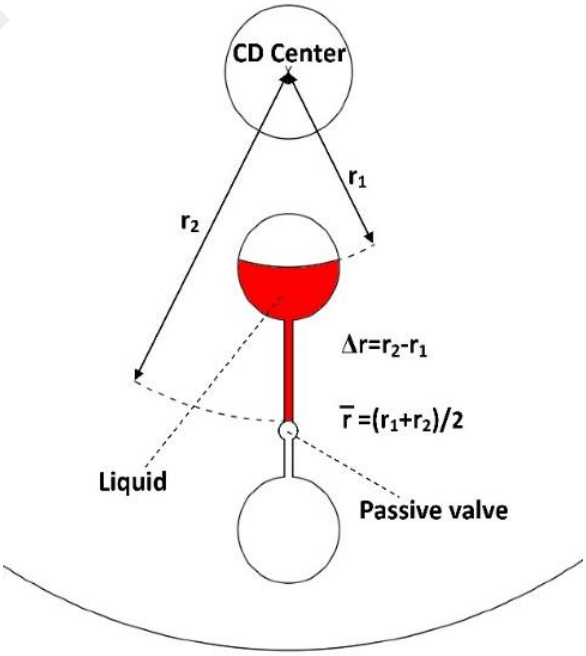

Figure 2.1: Retention of a liquid in a spinning microfluidic CD by a passive valve.

During the spinning process, all loaded liquids and particles on the CD will be affected by the centrifugal force ($P_{centrifugal}$). This force that pushes the liquids towards the outer rim of the CD can be calculated using the following equation (M. Madou et al., 2006a):

$$P_{centrifugal} = \rho\omega^2 \Delta r \bar{r} \tag{2.1}$$

where ρ is the liquid density, ω is the CD spinning speed in radian per second (rad/s), Δr is the difference between the top and bottom liquid levels at rest with respect to the CD center, and $\bar{r}$ is the average distance of the liquid from the center of the CD (see Figure 2.1). Another important force to reckon with when a liquid flows inside a microchannel is the capillary force ($P_{capillary}$). This force is calculated using the following equation (Thio, Soroori, et al., 2013):

$$P_{cap} = \frac{4\cos\theta_c \gamma_{la}}{D_h} \tag{2.2}$$

where θ_c is the liquid contact angle, γ_{la} is the liquid-air surface energy, and D_h is the channel hydraulic diameter. In the case that flow is inhibited by the capillary force, flow will only start when the centrifugal force is dominant:

$$P_{centrifugal} > P_{cap} \tag{2.3}$$

The combination of centrifugal and capillary forces allows for the passive liquid pumping and valving on the CD. However, centrifugal microfluidics suffers from several drawbacks. The unidirectional nature of the centrifugal force always pumps liquids towards the outer edge of the platform, limiting the usable space of the disc. Due to the low Reynolds number in the micro-scale domain, the dominant flow regime in microfluidic CDs is laminar. This limits the mixing to slow diffusion process, and compromises the use of smaller reagent/sample volumes on microfluidic platforms. The lack of a physical barrier in a capillary allows for vapor transportation, thus leading to cross contamination. Moreover, the burst frequency is a dynamic property as the contact

angles of polymers surfaces changes over time. Therefore to overcome this limitation, centrifugally- (passive) and externally-controlled (active) pumping, mixing and valving techniques were developed as alternatives.

Micropumps, mixers and valves are the main fluidic components in realizing automated complex bioanalytical assays in CD microfluidics. However, the developed liquid handling elements introduce serious drawbacks such as high power consumption, CD delamination, risk of contamination, and requiring an expensive high torque spindle motor or peripheral equipment. Hence, this chapter presents advances in the three liquid handling components to highlight the advantageous characteristics that make the microfluidic CD a portable, inexpensive and low-power consuming point-of-care (POC) device.

2.2 Micropumping in Centrifugal Microfluidics

The unidirectional nature of the centrifugal force pushes all on-board liquids towards the outer rim of the disc, limiting the possible number of sequential fluidic steps or the usable space on the microfluidic CDs (Abi-Samra et al., 2011; Gorkin III et al., 2010) (see Figure 2.2a). As illustrated in Figure 2.2b, the micropumps are liquid handling elements that propel liquids against the direction of centrifugal force to overcome this drawback (David J Kinahan et al., 2015; Soroori, Kulinsky, Kido, & Madou, 2013).

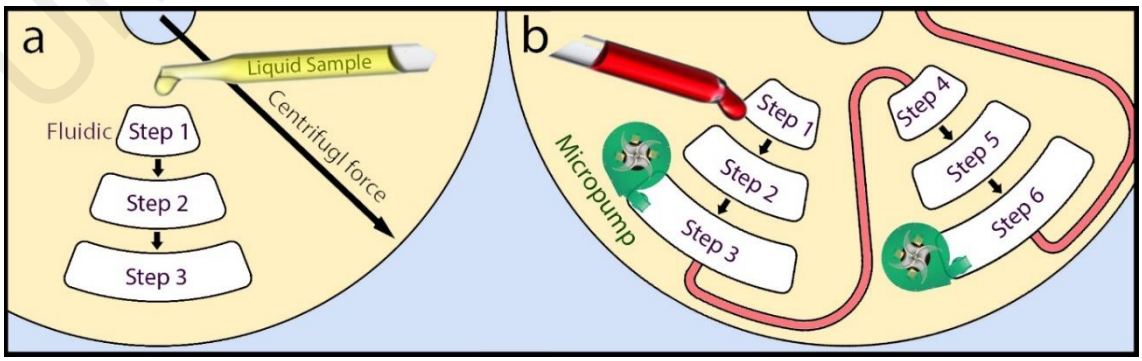

Figure 2.2: Micropump on centrifugal microfluidic platforms.

In addition, micropumps are required to prime siphon channels or siphonal flows (L. X. Kong, Perebikovsky, et al., 2015; O Strohmeier et al., 2015). In LOC microfluidics,

liquid siphoning is unique to centrifugal microfluidics, and it facilitates various pivotal laboratory protocols (e.g., plasma metering and extraction) in bioanalytical assays (Ducrée et al., 2007; Kitsara et al., 2014; Siegrist, Gorkin, Clime, et al., 2010; van Oordt, Stevens, Vashist, Zengerle, & von Stetten, 2013). A siphon microchannel allows for retaining a liquid solution inside a processing chamber at a high spinning speed (see Figure 2.3a), and then transferring a specific volume of the processed liquid (e.g., aliquoted, separated or mixed liquid) into an adjoining chamber at a lower speed (see Figure 2.3b-d). To prime a siphonal flow, a micropump propels the liquid against the direction of the centrifugal force along the siphon channel (see Figure 2.3b). Once the liquid plug passes the siphon crest, the centrifugal force drags the liquid plug towards the outer periphery of the disc (see Figure 2.3c), priming the siphonal flow (see Figure 2.3d).

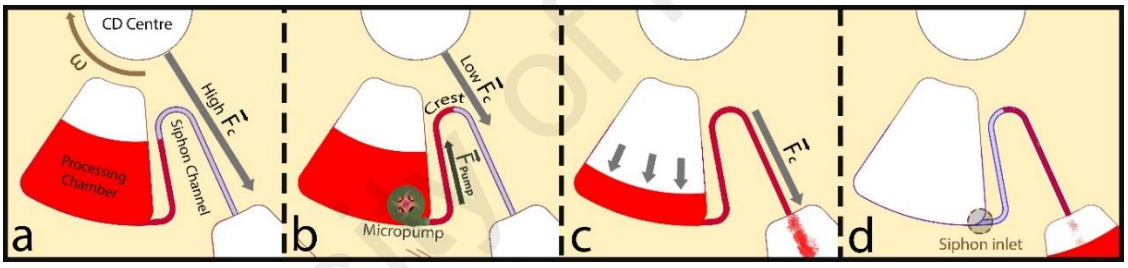

Figure 2.3: Siphoning on centrifugal microfluidic platforms.

A micropump that only propels a small liquid volume to a short distance towards the disc center can prime a siphon channel. However, it may not be able to permanently transfer a liquid to a chamber more near to the disc center. Therefore, the characteristics of micropumps that enable siphoning (i.e., siphon actuators), are not necessary similar to pumps that displace large liquid volumes to wider distances towards the center of the disc.

2.2.1 Micropumps for Actuating Siphonal Flow

2.2.1.1 Passive Siphon Actuators

Pneumatic, capillary and Euler pumps are passive liquid propulsion methods that are developed to actuate siphon channels (Deng et al., 2014; Gorkin III et al., 2010; Siegrist, Gorkin, Clime, et al., 2010) (see Figure 2.4). The pneumatic pumping mechanism is based

on the compression of an air bubble at high spinning speeds (e.g., 6000-8000 rpm), and relaxation of the bubble at a lower spin speed (see Figure 2.4A). The expansion of the bubble allows for the pumping of the liquid towards the disc center and actuating the siphonal flow (see Figure 2.4A). In pneumatic pumping method the transferring of the liquid at an elevated spin speed traps an air volume (air bubble) in the pneumatic chamber (see Figure 2.4A.i). Afterwards, at an elevated spinning speed, the induced centrifugal pressure forces the liquid into the pneumatic chamber to compress the air bubble (see Figure 2.4A.ii). Decreasing the spinning speed then allows for the air expansion, propelling liquid toward the disc center (see Figure 2.4A.iii). At the instance the liquid plug passes the pick of the siphon channel centrifugal force drags the liquid outwardly, siphon priming (see Figure 2.4A.iv).

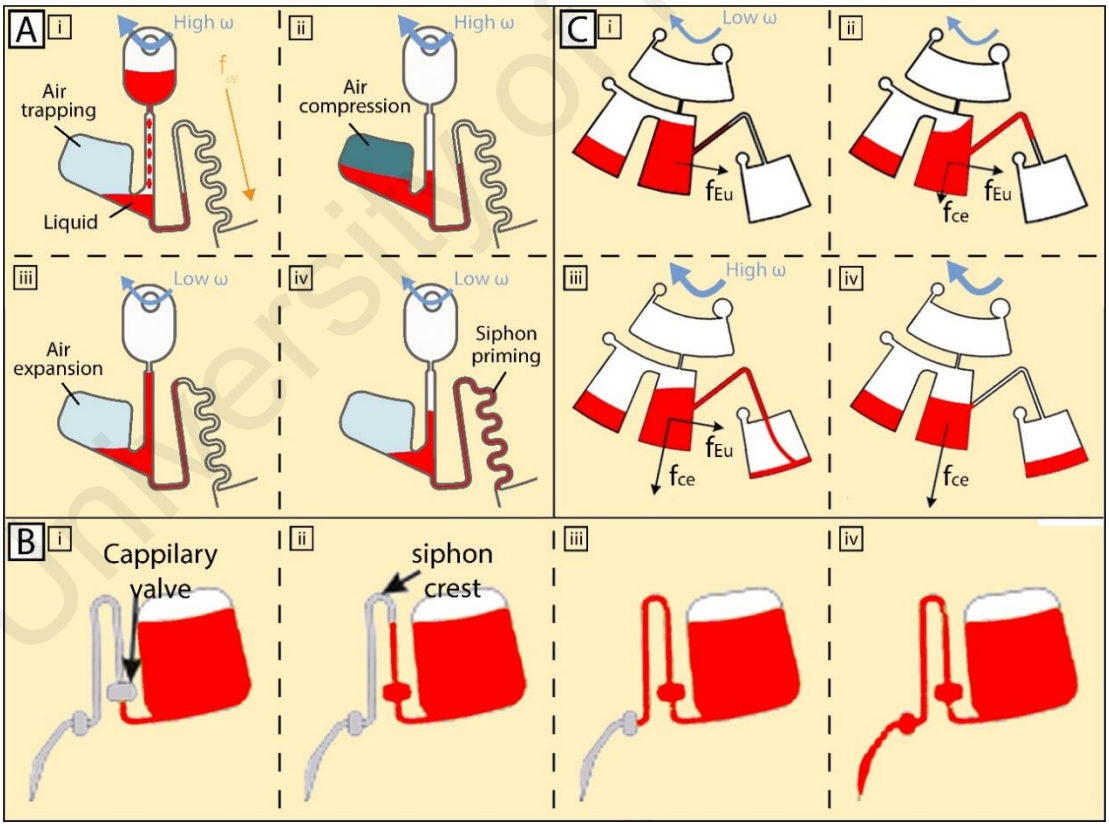

Figure 2.4: Centrifugally driven pumping techniques that enable siphonal flow in microfluidic discs.

One way to prime a siphon channel with no need for a high spinning speed is using a physically or chemically modified microchannel with high surface energy (Nwankire,

Donohoe, et al., 2013) (see Figure 2.4B). In siphoning by a hydrophilic microchannel, a capillary stops liquid entering the siphon channel to prevent unwanted actuation of the siphon (see Figure 2.4B.i). At an elevated spinning speed, the capillary valve bursts and hydrostatic equilibrium takes place (see Figure 2.4B.ii). Afterwards, at a reduced spinning speed capillary force prevails over the centrifugal force and liquid travels along the siphon channel up to the second capillary valve (see Figure 2.4B.iii). At an elevated spinning speed the second capillary valve bursts, priming the siphonal flow (see Figure 2.4B.iv). However, the nature of the hydrophilic microchannel to return to its former hydrophobic state causes instability in its pumping function over time.

To provide a long term (e.g., two months) stable increase in surface energy of the siphon microchannels, Maria Kitsara et al., spin-coated the middle layer of a CD with polymeric solution of hydroxypropyl-methyl cellulose (HPMC) and poly- vinyl alcohol (PVA) (Kitsara et al., 2014). However, the complexity and the high cost of the surface modification processes limit the use of hydrophilized microchannels in POC devices.

To prevent the need for a high spinning speed and any surface wettability procedure, Yongbo Deng et al., developed a Euler-driven siphon actuating mechanism purely based on the acceleration of the spinning disc (Deng et al., 2014) (see Figure 2.4C).As demonstrated in Figure 2.4.Ci, when a disc starts spinning at a high acceleration (i.e., $\geq$ 3000 rpm/s), in the fractions of time ($< 6 \times 10^{-1}$s) the Euler force becomes dominant and tilts the liquid towards the opposite direction of the rotation. This allows the liquid to pass the siphon crest (see Figure 4C.ii). Afterwards (i.e., $\geq 6 \times 10^{-1}$s), the centrifugal force prevails over the Euler force and drags the liquid towards the outer periphery of the disc (see Figure 4C.iii-iv). However, an expensive high torque motor that generates the adequate Euler force to tilt a liquid is not available in all spin stands, particularly in the portable platform.

2.2.1.2 Active Siphon Actuators

All active siphon actuators are constructed based on pneumatic-based systems. However, active pumps that manipulate a trapped air bubble to displace a liquid cannot actuate a siphonal flow. This is due to the expansion resistance of the air bubble that prevails over the centrifugal force, disturbing the siphoning process. To enable siphoning, two external pumps inject air into the fluidic network instead of manipulating the air trapped in the disc. The external rig of the earlier developed pump consists of i- a cylinder of compressed air/gas, ii- a rotameter for measuring the flow rate, and iii- an on/off solenoid valve (M. C. Kong & Salin, 2010) (see Figure 2.5a). Figure 2.5b demonstrates displacement of the entire liquid through pumping and siphoning.

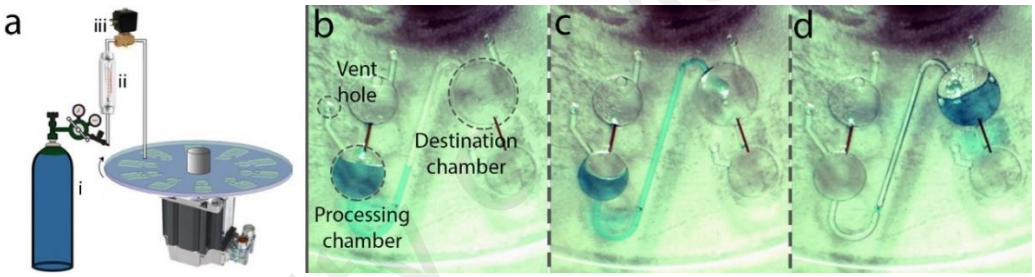

Figure 2.5: The contactless gas injection liquid pumping system.

To prevent the risk of contamination due to the injection of ambient air into the disc, Liviu Clime et al., mounted a micropump on the platform and directly connected the

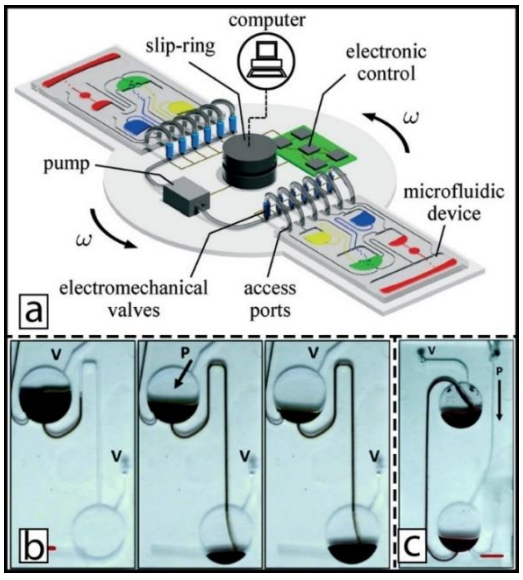

Figure 2.6: (a) Schematic of the active pneumatic pump for (b) liquid siphoning and, (c) inward pumping on centrifugal microfluidic platforms.

external pump to the fluidic network (Clime, Brassard, Geissler, & Veres, 2015) (See Figure 2.6). The authors called the on-disc micropump as the active pneumatic pump. It operates at spinning speeds up to 1000 rpm, and provides pressure lower and higher than the atmospheric pressure to, respectively, pump liquids backward and forward. However, the high cost and complexity of the micropump and the subsequent interconnects compromised the conceptual simplicity of the centrifugal microfluidic platforms.

2.2.2 Micropumps for Inward Displacement of Liquids

2.2.2.1 Passive Inward Pumps

To our knowledge, the only passive inward pump used in real life applications is the recently modified centrifugo dynamic inward (CDI) pump (Czilwik et al., 2015; Stetten, 2012). CDI pump is a pneumatic system that manipulates a liquid by the compression and the relaxation of an air bubble at a high and low spinning speed, respectively. As demonstrated in Figure 2.7A, the fluidic network of the pump includes a narrow inlet and a wider outlet channel. This allows for the propulsion of the liquid along the microchannel with the lower flow resistance when the spinning speed is rapidly reduced or the disc is abruptly stopped (Czilwik et al., 2015; Stetten, 2012) (see Figure 2.7A.ii). In general, using pneumatic pumps in temperature-controlled assays is challenging. This is due to the generation of thermo-pneumatic (TP) pressure during heating that can ruin the assay or damage the platform. To enable the use of the CDI in temperature controlled assays, Czilwik et al., separated the reaction chamber and the trapped air region by a microchannel, which is called Vapor Diffusion Barrier (VDB) (see Figure 2.7a). The CDI activates at a high spin speed (see Figure 2.7a.i), and a sudden reduction of spin speed causes the displacement of the liquid mostly through the outlet channel as it is wider than the inlet channel (see Figure 2.7a.ii). VDB minimizes the unwanted heat transfer to the air bubble (Czilwik et al., 2015). One of the serious limitations of the CDI pump is its inability to pump the entire liquid volume.

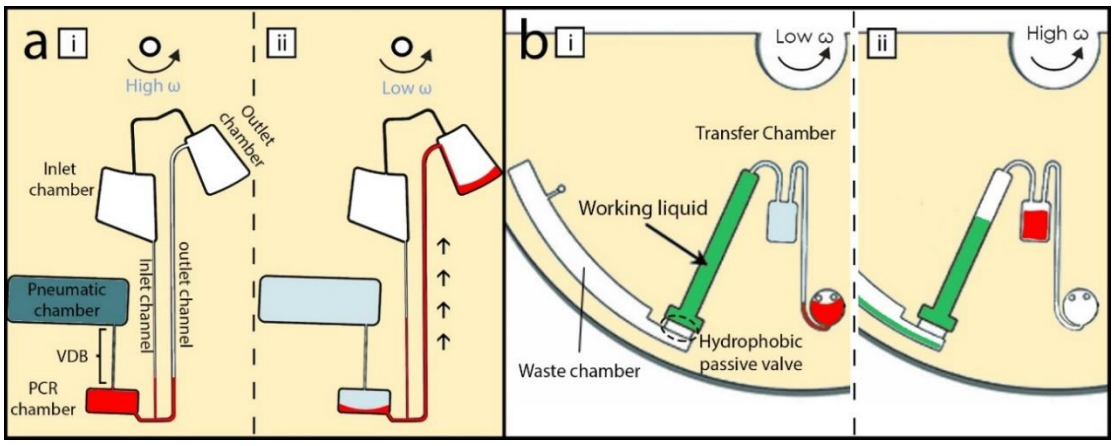

Figure 2.7: Inward pump that permanently transfer liquids from the outer to the inner rim of microfluidic discs.

To pump the entire liquid at a low spinning speed Soroori et al., developed a micro-pulley pump that operates akin to the conventional pulley system (Soroori et al., 2013). In the fluidic network of the micro-pulley an ancillary liquid, a main liquid, and an air volume between the liquids, respectively, act akin to the heavy load, the lighter load and the connecting-cable of a conventional pulley system (see Figure 2.7b.i). The micro-pulley also consists of a passive valve to retain the ancillary liquid in its respective chamber and prevent the actuation of the pump at low spinning speeds. The micro-pulley actuates at an elevated spin rate (i.e. >430 rpm) at which the passive valve bursts. At this instance, the outward displacement of the ancillary liquid pulls the trapped air into the ancillary chamber and the main liquid into the transfer chamber (Figure 2.7b.ii). It should be noted that the micro-pulley operates similar to an earlier developed pumping mechanism where an immiscible liquid was used instead of the trapped air volume to pull and push the main liquid (M. C. Kong, Bouchard, & Salin, 2011).

2.2.2.2 Active Inward Pumps

The recently developed TP and the active pneumatic pump (described in *Section 2.2.1.2*) are the only active inward pumps that are currently used in real life applications (Clime et al., 2015; Keller et al., 2015; Thio, Ibrahim, et al., 2013). However, to clarify the limitations of the micropumps, the earlier developed electrolytic-based and centrifugo-magnetic pumping mechanism are illustrated below (see Figure 2.8c). The

electrolytic pump generates oxygen and hydrogen from the electrolysis of water to induce pneumatic pressure and propel the liquid (Noroozi, Kido, & Madou, 2011) (see Figure 2.8a,b). Figure 2.8a shows peripheral setup required for the transfer of electricity to the water in the electrolysis chambers. The schematic of electrolysis pumping is demonstrated in figure 2.8b; briefly (i) when the electric potential is applied to the electrodes, (ii, iii) the pneumatic pressure induced from water electrolysis then pumped the liquid against the direction of the centrifugal force. The four stages of the centrifugo-magneto pumping are shown in Figure 2.8c. When the magnet arrives below the pump chamber, the right side of the membrane deflects and closes the inlet of the chamber (see Figure 2.8c.i). Afterwards the magnet arrives below the second steel plate and deflects

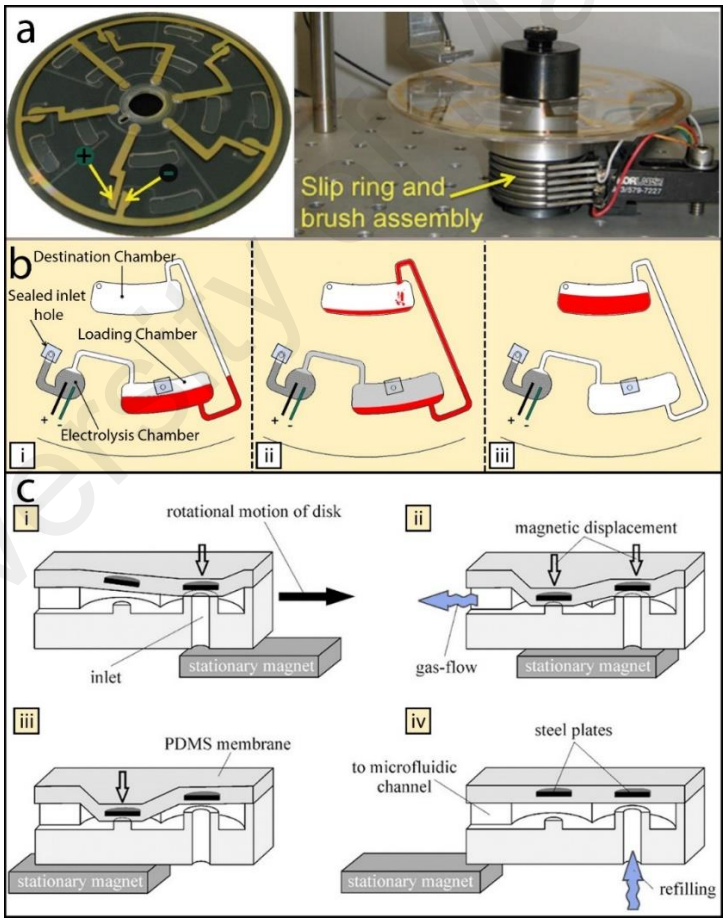

Figure 2.8: Active pneumatic pumps on centrifugal microfluidic platforms.

the other side of the membrane to push air into a fluidic network (see Figure 2.8c.ii). Then the magnet passes by the chamber, resulting in the relaxation of the membrane and refilling the pump chamber with ambient air (see Figure 2.8c.ii,iv).

To prevent the need for expensive and complex CD fabrication process and experimental setup, the centrifugo-magnetic pump employs magnetic deflection of a Polydimethylsiloxane (PDMS) membrane to inject air bubbles into the disc to propel liquids (Haeberle, Schmitt, Zengerle, & Ducrée, 2007) (see Figure 2.8c). To periodically deflect the membrane during the spinning of the disc, two steel plates were embedded on the membrane, and an external, stationary permanent magnet was located below the microfluidic disk. The continuous injection of air bubbles into the fluidic network induced an adequate pneumatic pressure to pump the liquid towards the disk center. However, the injection of ambient air into the disc increases the risk of contamination, thus preventing the pump's usage for biomedical applications.

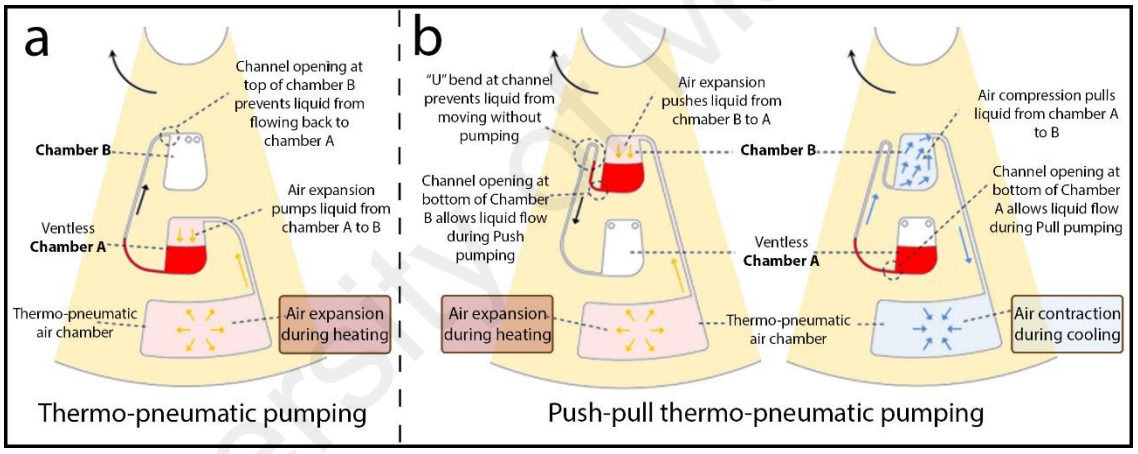

Figure 2.9: Fluidic components and the operating mechanisms of TP pumping methods.

To prevent the risk of contamination, Abi-Samra et al, utilized IR radiation of a halogen lamp to heat and expand a trapped air bubble to generate TP pressure (Abi-Samra et al., 2011) (see Figure 2.9a). Recently, Thio, Ibrahim, et al. (2013) modified the conventional TP pump to utilize the air contraction during the passive cooling of the heated disc to propel back the liquid to its initial location (see Figure 2.9b). The newly developed push-pull pump is used for a sequential washing of a reaction chamber in an immunoassay test. However, serious drawbacks of the TP pumps such as slow pumping progress and high power consumption prevents their use in POC applications.

2.2.3 Micropumps Evaluation

The large air chamber and the high spinning speed in the pneumatic pumping pose several problems such as the unwanted actuation of valves and high power consumption that limit its use in complex sequential procedures. To cope with these drawbacks, microchannels with high surface energy are used to prime siphonal flow. However, the additional necessary surface modification process increases the manufacturing complexity and the cost of platforms with such wet microchannels (Gorkin III et al., 2010). The Euler pump enables siphonal flow with no need for any additional fluidic component or high spinning speed, and any surface modification procedure. However, not all spin stands, particularly the portable and low cost spin stands can provide enough torque to tilt the liquid. Despite their limitations, due to the importance of the siphoning action in bioanalytical assays, these fluidic techniques remain the preferred micropumps in centrifugal microfluidic platforms.

In passive inward pumping category, the CDI pump with VDB enabled the implementation of temperature controlled assays i.e., PCR. However, from the inability of the CDI pump to displace an entire liquid volume it can be concluded that the pump is not able to displace small liquid volumes. Other disadvantages of the CDI pump are akin to the pneumatic pump. To overcome these drawbacks, micro-pulley pumps liquid were designed via the actuation of the ancillary liquid. However, the ancillary liquid occupies a large space on the disk and the system is not robust as it actuates at low spinning speeds.

Active pumps displace large liquid volumes with no need for changing the spinning speeds of the microfluidic CDs. However, to our knowledge, no active pump yet being used on a portable platform. The complexity of operation, high cost, slow operation, high power consumption, and risk of contamination are the main limitations of the active pumps that prevent their implementation for the development of POC devices.

2.3 Mixing in Centrifugal Microfluidics

In the micro- and nano-scale domain, the dominant flow regime is laminar, limiting the mixing efficiency and slowing chemical processes (Grumann et al., 2005; Noroozi et al., 2009; van Reenen et al., 2014). Many recent inventions pertain to enhanced mixing on a CD by the application of forces different from the centripetal force. Mixing forces are created by liquid flow across special structures inside serpentine microchannels, or by special spinning profiles and physical impacts in microchambers.

2.3.1 Mixing on Serpentine Microchannels

Mixing in a serpentine microchannel (under laminar flow) takes place via a combination of the Coriolis-driven flow, transverse secondary flow and the high inertia flow that induces stirring at the eddies of the microchannel (Di Carlo, 2009; Liu et al., 2000; Therriault, White, & Lewis, 2003) (see Figure 2.10). Geometry, length and structure are the main factors effecting the mixing efficiency of a serpentine microchannel. Kuo et al., and Ren et al., have numerically and experimentally demonstrated that square-wave serpentine microchannels provide higher mixing efficiency when compared to zig-zag and curved channels (Kuo & Jiang, 2014; Y. Ren & Leung, 2013a). The higher efficiency of the square-wave channel is due to the longer

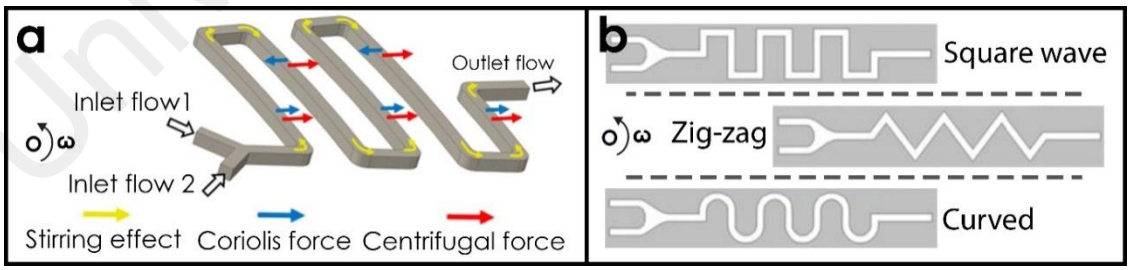

Figure 2.10: (a) In a serpentine microchannel stirring at eddies and pseudo forces accelerate the mixing process. (b) Serpentine microchannels of different geometries.

liquid pathway it provides and the stronger chaotic stirrings that occur at its sharp eddies (Kuo & Jiang, 2014). However, because their mixing efficiency and period are confined

by their length, serpentine microchannels are not appropriate mixing components in sequential bioanalytical assays e.g., immunoassays and DNA hybridization.

2.3.2 Passive and Active Mixing on Microchambers

In general, microchamber-based mixing techniques are more efficient and practical in sequential bioanalytical assays with a series of incubation periods. By using a combination of the Euler and Coriolis forces (i.e., shaking or stopped-flow) an effective mixing was demonstrated by Grumann et al. (2005) (see Figure 2.11a). The same team of researchers demonstrated that the mixing efficiency could be further enhanced by adding microbeads in the mixing chamber and/or using an external magnetic platform to stir the beads (see Figure 2.11b). Diffusive mixing, shaking, magnet stirring, and shaking with magnet stirring accomplished a same mixing process in 7 minutes, 3, 1.3, and 0.5 seconds, respectively.

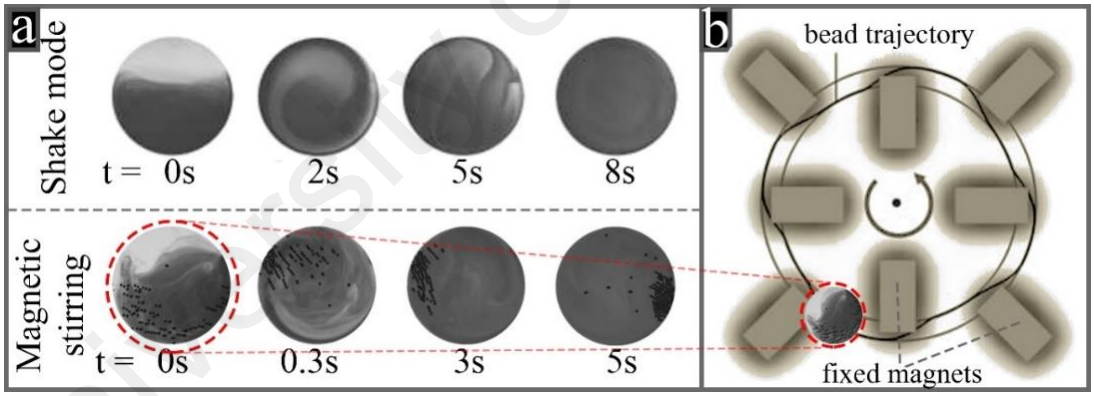

Figure 2.11: (a) Mixing progress by shaking and magnet stirring techniques. (b) The magnetic platform that was used for shifting the beads upwards and downwards.

To enhance the quality of heterogeneous immunoassays, Noroozi et al. (2009) developed a flow reciprocation mixing method based on the pneumatic pumping technique (see Figure 2.12). To use considerably less reagents for a Burkholderia immunoassay, Noroozi, Kido, Peytavi, et al. (2011) utilized the flow reciprocation to maximize hybridization efficiency between the Burkholderia antibodies and a Burkholderia-antigens-coated microarray. This reduced the required analyte volume from

300 µl to 10 µl, and the process time from 105 minutes to 10 minutes (Noroozi, Kido, Peytavi, et al., 2011). Figure 2.12b shows the operating mechanism of the flow reciprocation mixer. Frist centrifugal pressure induced at high spinning speeds compressed the trapped air in the pressure chamber and pushed the reagent into the pressure chamber (see Figure 2.12b.i). Reducing the spinning speed then allowed for the air relaxation and the air expansion pushed the reagent out of the pressure chamber (see Figure 2.12b.ii). Spin rate of the disk was continuously altered between 3500 rpm and 7000 rpm, and therefore the reagent was reciprocated over the Burkholderia microarray (see Figure 2.12b.iii). At the end of each incubation period the disk was stopped and the expanded air propelled the reagent into the upper chamber (see Figure 2.12b.iv). At this point, because the liquid level reached above the siphon crest, increasing the spin rate allowed for transferring the used reagent to the waste chamber.

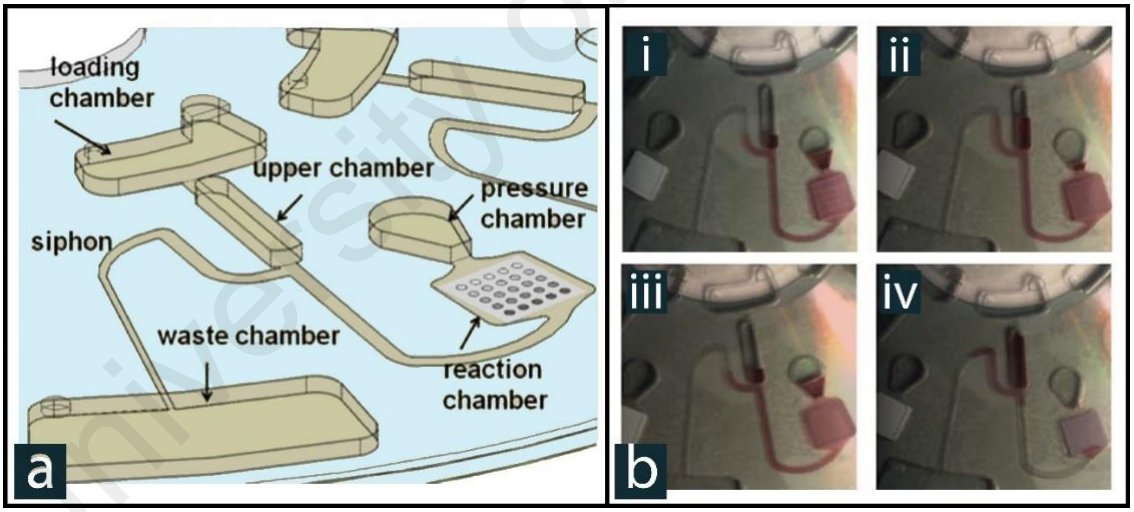

Figure 2.12: Fluidic components of a flow-reciprocating mixing unite equipped with a siphon channel.

Similar to the shaking and flow reciprocation mixing methods that are, respectively, developed based on the Euler and pneumatic pumping techniques, active mixing techniques are developed based on the active pneumatic siphon actuators (Clime et al., 2015; M. C. Kong & Salin, 2012) (see Figure 2.13).

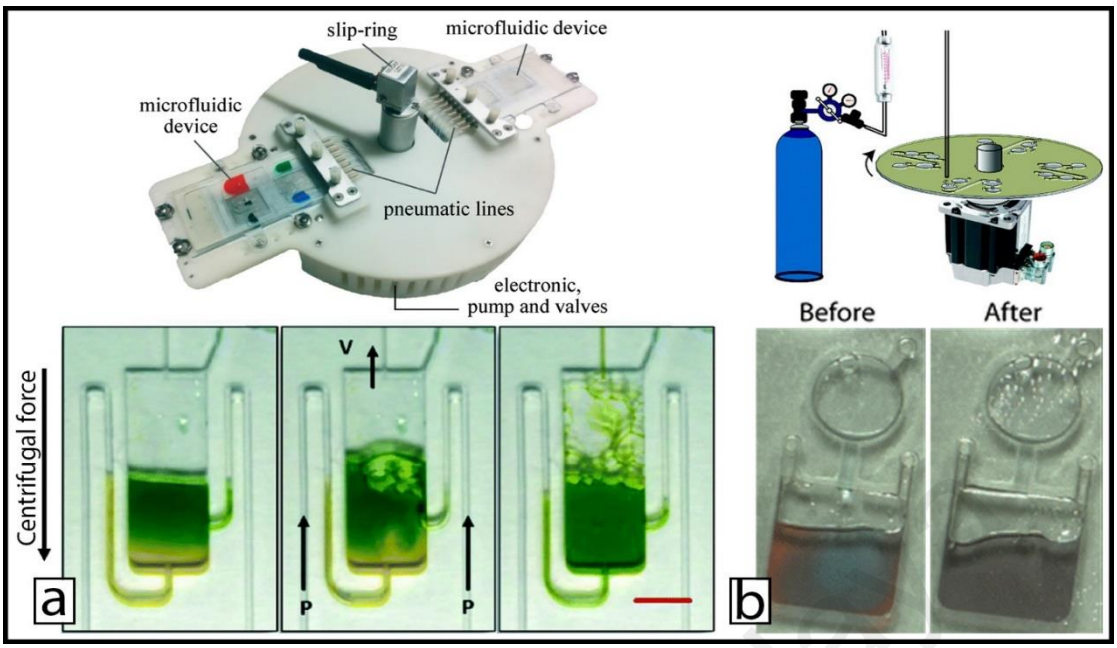

Figure 2.13: Active mixing by (a) the stationary, and (b) the on-disc pneumatic pumps that use for the actuating siphon channels.

2.3.3 Evaluation of Mixers in Centrifugal Microfluidics

Serpentine microchannels homogenize liquids with no need for any changes in the disc's spin speed or the use of any peripheral equipment. However, their limited mixing efficiency prevents their use in bioanalytical assays. Repeating a liquid manipulation action such as shaking, flow reciprocation and magnet stirring on a chamber on the other hand provides greater mixing efficiency. Among the chamber-based mixers, shaking and flow reciprocation due to their independency on any external actuator remain the preferred mixing methods in CD microfluidics (T.-H. Kim, Park, Kim, & Cho, 2014; Noroozi, Kido, Peytavi, et al., 2011; Nwankire et al., 2014; Roy et al., 2015b). Moreover, stopped-flow mixing method (shaking) makes the best use of the limited space available on the disc. However, high-torque rotating motors that can generate adequate Euler force are expensive, and are not available in all lab-based spin stands. Flow reciprocation allows for optimizing parameters such as incubation periods and the surface capture rate in heterogeneous assays. However, the high spinning speed and the large air chamber required to induce an adequate pneumatic pressure limits it use in complex sequential procedures.

Mixers that operate at low spin speeds (e.g., <1500 rpm) and accelerations with no need for any peripheral equipment provide several advantages for portable systems. This includes low power consumption and compatibility with various types of low cost spindle motors as well as other centrifugally controlled fluidic components. Moreover, when the amount of a targeted analyte is at an extremely low concentration, a large volume of a sample is needed for the analysis. In such applications (e.g., detection of rare circulating tumor cells (CTCs)), fluidic components that can pump and or mix larger liquid volumes are crucial.

2.4 Valving in Centrifugal Microfluidics

The centrifugal force generated by the spinning of the disc, pumps all the reagents residing on the spinning platform towards the disc outer periphery. This characteristics of the pseudo force enables the simultaneous handling of several fluidic steps, however, it makes the retention of liquids in different chambers and managing the sequence of their flow quite challenging. In centrifugal microfluidics, a valve is a barrier or a technique that retains a liquid experiencing centrifugal force in its respective chamber until it actuates (removes or changes) (Godino, Gorkin III, Linares, Burger, & Ducrée, 2013; Robert Gorkin et al., 2010). Valves actuate either by increasing the spinning speed of the microfluidic disc above a critical value (i.e., the burst frequency), or by an external force or stimuli e.g., magnetic force and heat (Cai, Xiang, Zhang, & Wang, 2015; Gorkin III et al., 2012; Kazemzadeh et al., 2014). As mentioned in the introduction (see *Section 2.1*), passive capillary valves are not reliable for the automation of multistep fluidic processes in portable systems. As an alternative to capillary barriers, several passive pneumatic and active valves were developed to reliably control liquid flow on microfluidic CDs. Moreover, to reduce the number of valving steps and make the microfluidic CDs reusable, one passive and one active reversible valving concept was developed. The following subsections describes the operating mechanism of these three categories of microvalves.

2.4.1 Passive Pneumatic Valves

Centrifugally driven pneumatic valves employ the compression or the expansion resistance of an air-bubble that is trapped in the vicinity of a liquid to prevent liquid flow (see Figure 2.14) (Burger, Reis, da Fonseca, & Ducrée, 2013; D. Mark et al., 2009; Oliver Strohmeier et al., 2013; Oliver Strohmeier et al., 2014). These passive valves actuate at elevated spinning speeds where the centrifugal pressure disturbs the metastable gas-liquid interface. Sealing the vent holes of a source chamber or a destination chamber by an adhesive tape is the simplest method employed for trapping an air bubble in the chamber (Burger et al., 2013). These types of valves are known as airlocks and centrifugo pneumatic (CP) valves depending on, respectively, if the expansion or compression resistance of the air bubble prevents liquid flow. Figure 2.14A demonstrates an application of the CP valve for aliquoting a master mix reagent for multiplexing a real-time PCR assay. The master mix reagent was aliquoted into the metering figures through spinning the cartridge at 396 rpm (see Figure 2.14A.i). During the filling of each finger, the air bubble (CP valves, blue color) in the reaction chambers prevented the reagent entering the reaction chambers (see Figure 2.14A.ii). Afterward, the spin rate was increased to 1632 rpm to actuate the valves (see Figure 2.14A.iii).

To develop CP valves with different burst frequencies, Ukita et al. and Wisam et al., employed ancillary liquids to create arrays of CPs and airlocks (Al-Faqheri et al., 2015; Ukita, Ishizawa, Takamura, & Utsumi) (see Figure 2.14B). The actuation mechanism of passive liquid valves (PLVs) is based on the gas-exchange between the trapped air and the ambient air through the ancillary liquid. The ancillary liquids were used to create a source chamber (S-) (see Figure 2.14B.i), and a destination chamber passive liquid valve (D-PLV) (see Figure 2.14B.ii). Actuation of the S-PLV and the D-PLV were based on air exchange between ambient air and the pneumatic region of the valves at elevated spin speeds. The burst frequency of a PLV correlates with the height

and density of the ancillary liquid, and the distance between the venting chamber (i.e., ancillary liquid chamber) and the disc center. However, these pneumatic valve are not robust over a wide range of spinning speeds, and they can only be implemented in source and destination chambers (Burger et al., 2013; Oliver Strohmeier et al., 2013).

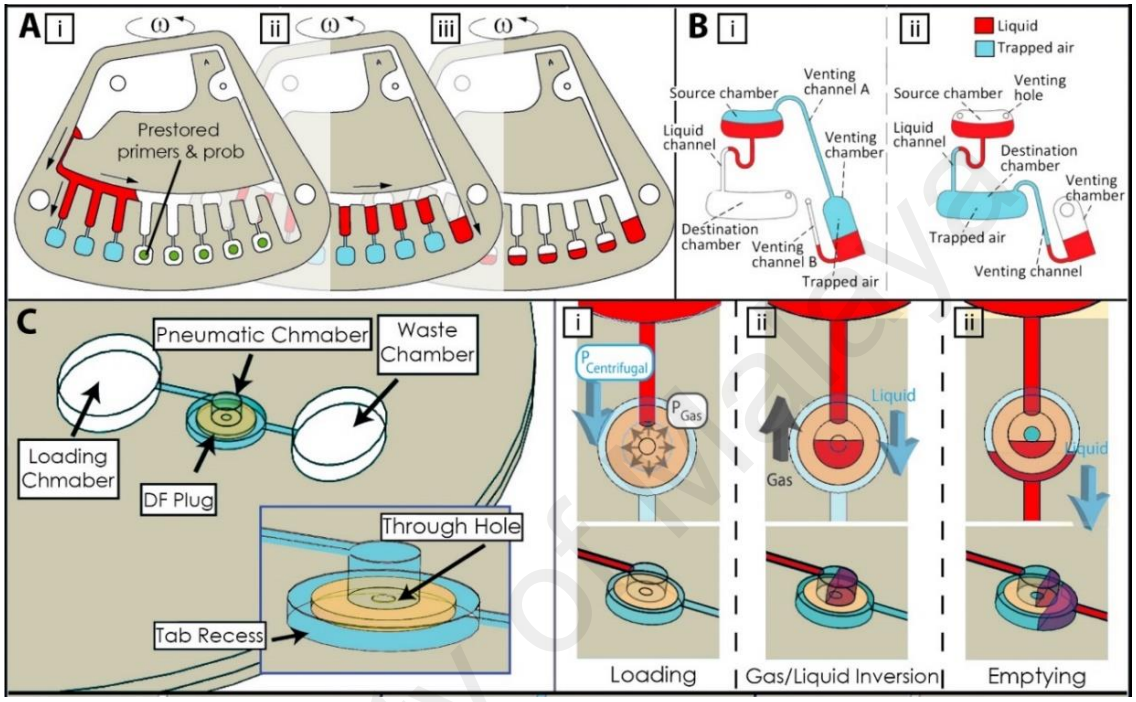

Figure 2.14: Passive pneumatic valving mechanisms.

To overcome these limitations, Gorkin III et al. (2012) employed dissolvable films (DFs) to create CP valves on any desirable location within a complex fluidic network (see Figure 2.14C). As shown in Figure 2.14C.i, an air bubble (CP valve) between the DF and liquid, prevented the liquid entering the pneumatic chamber. At an elevated spin speed (> 3500 rpm) the bubble was compressed and the CP valve actuated (see Figure 2.14C.ii). After several seconds liquid dissolved the film traveled towards the outer rim of the disc (see Figure 2.14C.iii). Unlike the conventional CP valves, the pneumatic chamber of a DF- valve is not used as a liquid processing (e.g., aliquoting and metering) chamber, and therefore its geometry can be adjusted to prevent flow over a considerably wider range of spinning speeds. However, the high tolerance in the actuation frequency (e.g., ±250 rpm (Gorkin III et al., 2012)) of DF valves limits the number valves that can

be implemented in a disc, and their use in low range of spinning speeds (David J. Kinahan, Kearney, Dimov, Glynn, & Ducree, 2014). Another drawback that is common in all pneumatic-based valves is that, the changes of ambient temperature can unwantedly actuate the trapped air and therefore the valves. This limits the use of the pneumatic valves (including DF-based valves) in POC setting in tropical and subtropical regions.

2.4.2 Active Valves

In general, active valves are more reliable for the automation of bioanalytical assay on POC devices. To develop pneumatic valves that actuate in low spinning speeds, Al-Faqheri et al. (2013) embedded wax plugs on the vent holes of a source and a destination chamber to create an active airlock and a CP valve, respectively (see Figure 2.15A). These two valves are known as vacuum and compression valves (VCVs). To actuate VCVs, an air heat gun melts the wax plugs to open their pneumatic region to the atmospheric pressure (Al-Faqheri et al., 2013). The wax plugs used in VCVs positioned far from the main liquids to minimize the risk of heat transfer to the main liquids during the actuation of the valves. However, VCVs are not robust over a wide range of rotational frequency and have the same limitations of passive pneumatic valves.

To prevent liquid flow regardless of the disc spinning speed, Park et al., developed a laser irradiated ferrowax microvalve (LIFM) to block a microchannel (see Figure 2.15B) (Park, Cho, Lee, Lee, & Ko, 2007). Recently, to enhance the compatibility of the physical barrier with organic solvents (e.g., ethanol and n-hexane), Yubin kim et al., developed a carbon dot-based valve that actuates by the same laser source used for melting the LIFM (Y. Kim, Jeong, Kim, Kim, & Cho, 2015) (see Figure 2.15C). It should be noted that Garcia-Cordero, Kurzbuch, et al. (2010) employed the laser printer lithography technology to fabricate a similar valve that actuates by the solid-state laser used in CD/DVD players. However, CDs need to be stopped in order to focus the laser irradiation

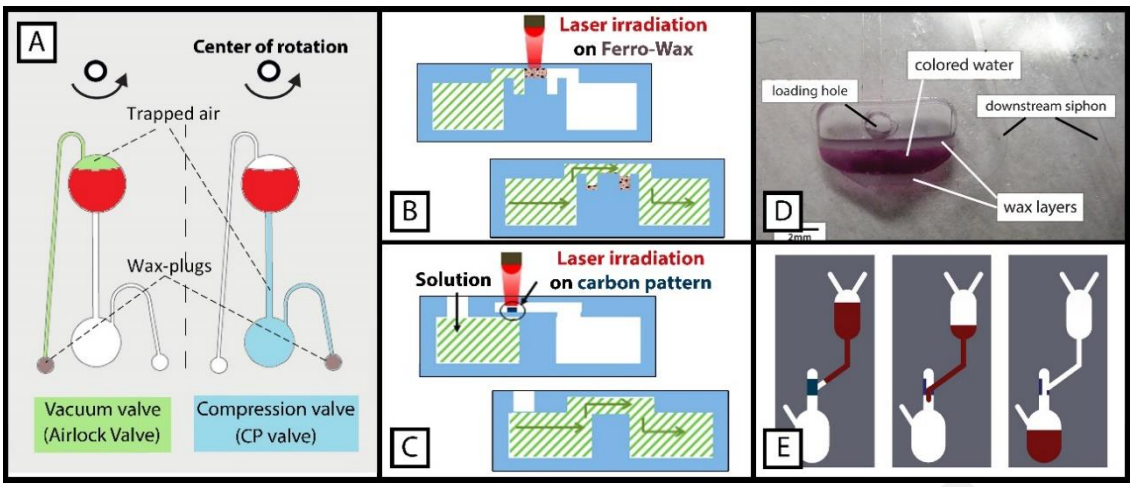

Figure 2.15: Active valving techniques on centrifugal microfluidic platforms. (A) Vacuum and compression valves (VCVs). Focused laser irradiation (B) Ferro-waxes valve, and (C) carbon printed dots. (D) The encapsulation of a reagent between two wax walls. (E) The hydrocarbon gel valve.

on the LIFMs and the carbon dots to actuate them. This disturbs other centrifugally driven fluidic procedures such as blood serum separation (Park et al., 2014).

To overcome this drawback, Ling Kong et al., encapsulated a reagent inside a paraffin-wax shell (see Figure 2.15D), and melted the wax shell to release the reagent by a focused halogen lamp during the spinning of the disc at low spinning speeds. When the valve was actuated, the melted wax because of its low density gathered at the top of the reagent and prevented the evaporation of the reagent during the thermo-cycling period (L. X. Kong, Parate, Abi-Samra, & Madou, 2014). To prevent the need for the heat, Laura Swayne et al employed a hydrocarbon gel as a physical barrier. The barrier was displaced either by the centrifugal pressure at an elevated spinning speed of 1300 rpm, or the pneumatic pressure that was generated and controlled by a stationary source of compressed air (Swayne, Kazarine, Templeton, & Salin, 2015). These valves are sacrificial or for single use only, thus a large number of them require automated fluidic procedure, and their corresponding microfluidic platforms are not reusable.

2.4.3 Reversible Valves

Reversible valves for liquid retention means that they can be repeatedly switched between their open and closed states, or have the ability of returning to their former state

after each actuation (Cai et al., 2015). Elastomeric valve, and magnetically actuated (MA) valve are two reversible valves developed on centrifugal microfluidic platforms (see Figure 2.16). The Elastomeric valve prevents liquid flow via a permanent weak adhesive force between PDMS and polycarbonate (Hwang, Kim, & Cho, 2011) (see Figure 2.16A). Since it is a physical barrier that must be continuously opened by liquid pressure in order for the liquid to pass, the valve may not open if a small volume of liquid does not provide the sufficient hydrostatic pressure. Moreover, the operating spin speed of the elastomeric valve for liquids more than 10 µl is limited to 800 RPM.

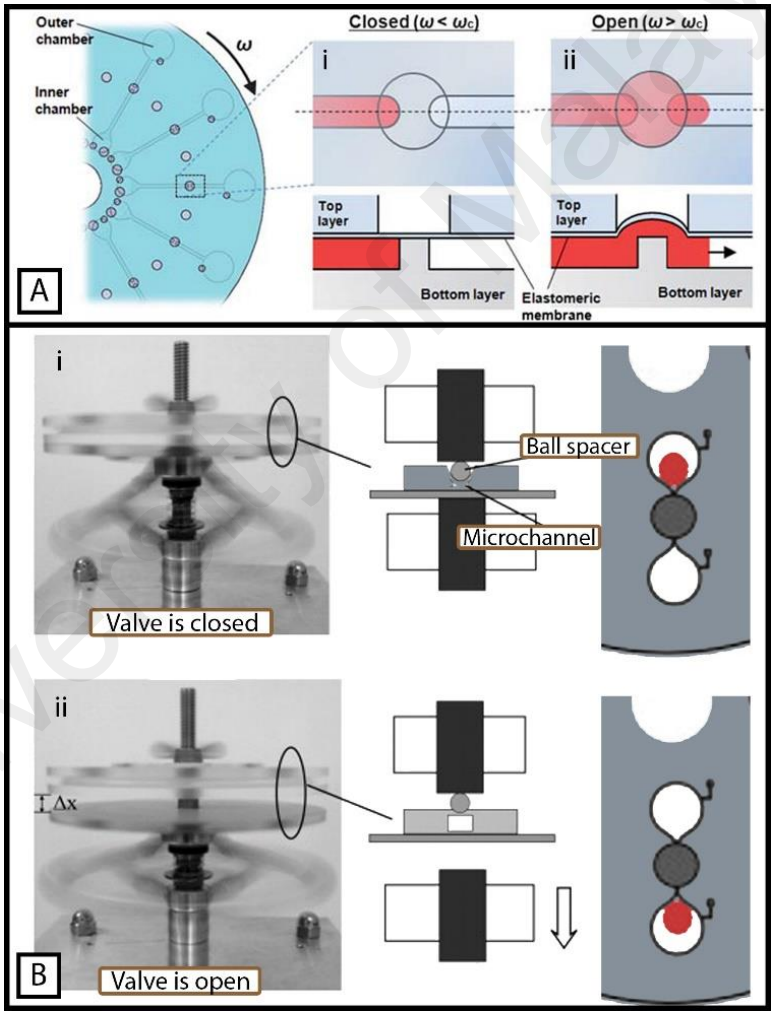

Figure 2.16: Centrifugally driven reversible valving methods. (A) The elastomeric membrane valve. (B) The magnetically actuated (MA) valve.

To cope with these drawback, Cai et al. (2015) developed MA valve with spinning range of rotational frequencies from 800 to 1600 RPM. The valve is composed of a PDMS membrane, a ball spacer, a pair of magnets (on the top and bottom of the disk), and a

flyball governor for controlling the distance between the two magnet (see Figure 2.16B). The attraction force between the two magnets forced the ball spacer to deflect the membrane into a liquid transition chamber to block it (see Figure 2.16Bi). The actuation mechanism of the valve was based on increasing the distance of the magnets to deflect back the membrane. To this end, spinning speed was increased until the enhanced centrifugal force overwhelmed the weight of the flyballs and lifted down the bottom side magnet (see Figure 2.16Bii). The bulky and complex valving mechanism and, continues interactions between multiple magnet pairs limited the number of MA valves that can be used in a disk (Cai et al., 2015).

2.4.4 Microvalves Evaluation

Passive pneumatic valves enabled the automation of laboratory functions such as separation, metering and aliquoting. DF component enabled the implementation of CP valves everywhere within a fluidic network, and the automation of more complex sequential fluidic procedures. However, the sensitivity of trapped air to the changes of temperature and the sensitivity of DF materials to the humidity introduce limitations for their use in real life applications, particularly in regions with high temperature fluctuation and humidity (Knapen, Beeldens, & Van Gemert, 2005; McCormick, Lowe, & Ayres, 2002). For similar reasons, implementation of these valves for the automation of temperature controlled reactions is quite challenging.

Robust active valves (e.g., LIFMs and carbon dots) are usually not sensitive to changes in ambient humidity and temperature and provide more precise control over the liquid retention and release. LIFM and carbon dots enable the automation immunoassays with a high number of valving steps. To cope with their drawback (i.e. the stopping of the disc) VCVs and paraffin-wax shells can be used as alternatives. However, the long microchannel required for ensuring enough distance between the reagent and the wax plug in VCVs subsequently occupied a large space of the disc. In the other technique

developed by L. X. Kong, Parate, et al. (2015), thermal manipulation of reagents during the process of reagent encapsulating and releasing limit the compatibility of the technique with different reagent materials and bioanalytical assays. The hydrocarbon gel valve prevents the need for heating the platform. However its actuation, similar to the active pneumatic pumping and mixing actions, involves the risk of contamination.

Reversible valves can be reused for multiple purposes. For instance, in heat based bioanalytical assays, reversible valves first can be used for metering and then preventing the evaporation of reagents during heat cycles. However, the elastomeric valve does not allow for the entire liquid to pass, and is as fragile (un-robust) as passive capillary valves. The bulky and mechanically complex system required for the MA valving on the other hand prevents it use on portable platforms and in real life applications. Therefore, demand for the development of simpler and more robust reversible valving systems that enable flexible and real time control of flow on centrifugal microfluidic platforms is continuing.

2.5 Summary

This section summarizes characteristics of the liquid handling elements that make a microfluidic CD a portable platform, inexpensive and low-power consuming POC device. Micropumps enabling siphonal flow are more practical in real life applications than pumps that only transfer a liquid to a chamber near the disc center. Passive pumps reliably actuate siphonal flow, thus prevent the need for any peripheral equipment. However, the high spinning speed, surface modification procedure and high torque required for the implementation of pneumatic, capillary and Euler pumps, respectively, increase the power consumption, complexity of fabrication and cost of a portable platform. On the other hand, to enable the implementation of various bioanalytical applications (e.g., immunoassay, DNA hybridization and CTC detection) on microfluidic CDs, the micropump must be able to displace various liquid volumes. From these, it can be concluded that there is a need for the development of a passive micropump that

displaces various liquid volumes at low range of spinning speed with no need for any surface modification procedure and high torque spindle motor.

Table 2.1: Technical aspects of micropumps, mixer and valves.

Microfluidic element	Mechanism	Operational spin speed	Max acceleration	Fabrication procedure	Volume	Vapor tight
Pump						
Pneumatic	Passive	8000 rpm	-	Simple	7 µl	-
Capillary	Passive	1000 rpm	-	Complex	13.5 µl	-
Euler	Passive	4000 rpm	4000 rpm/s	Simple	30 µl	-
Inward Pneumatic	Passive	2400 rpm	1800 rpm/s	Simple	240 µl (90%)	-
Thermo Pneumatic	Active	1200 rpm	-	Simple	19µl/min	-
Electrolysis Pneumatic	Active	4500 rpm	-	Complex	9µl/min	-
Centrifugo-magnetic	Active	1800 rpm	-	Highly complex	19µl/sec	-
Mixer						
Batch mode	Passive	60 rpm	1920 rpm/s	Simple	-	-
Pneumatic reciprocation	Passive	7500 rpm	-	Simple	25µl	-
Stationary pneumatic	Active	1500	-	Complex	-	-
On-disk pneumatic	Active	1200	-	Complex	-	-
Valve						
CP	Passive	1680 rpm	-	Simple	-	No
PLV	Passive	1500 rpm	-	Simple	-	No
DF valve	Passive	4400 rpm	-	Complex	-	Yes
Elastomeric	Passive	800 rpm		Complex	10 µl	Yes
LIFM	Active	*410 kPA	-	Complex	-	Yes
Hydrocarbon gel	Active	1300 rpm	-	Complex	-	Yes
MA	Active	1600 rpm	-	Complex	-	No

*Spinning speed equivalent 410 kPa.

The highly practical mixers (batch mode, and flow reciprocation mixer) use a single fluidic element to mix and then transfer (siphon) the mixed solution for further fluidic procedures. Moreover, flow reciprocation mechanism maximizes the dynamic mixing area to optimize the immobilization parameters in heterogeneous assays. However, the large air chamber required in pneumatic flow reciprocation limited it usage in complex sequential assays. For this reason, and due to the limitation of the Euler driven mixer, it can be concluded that there is a need for the development of a passive flow

reciprocation mixer that operates over a low range of spinning speeds and acceleration with no need for any additional fluidic component.

Technical aspects of the surveyed microvalves are listed in Table 2.1. Valves such as LIFM and DF-based valves that employ a physical barrier to block a microchannel are highly robust at high spinning speeds. In general, active valves are more robust than passive ones and operate over wide (low and high) range of rotational frequencies. However, LIFMs cannot be actuated during the spinning of the disc and therefore are not compatible with several lab procedures such as blood serum extraction. On the other hand, reversible valves are multifunctional and can enable the automation of bioanalytical assays with less number of valve components. Moreover, there is an absence of a valving mechanism that can be closed to seal reaction chambers at elevated temperature on centrifugal microfluidic platforms. From these it can be concluded that there is a need for the development of an active reversible valve to precisely control liquid flow over a wide range of rotational frequencies, and prevent evaporation of reagents and risk of cross-contamination in temperature controlled reactions.

CHAPTER 3: LATEX MICROBALLOON PUMPING ON CENTRIFUGAL MICROFLUIDIC PLATFORMS

3.1 Introduction

Centrifugal microfluidic platforms have emerged as point-of-care diagnostic tools. However, the unidirectional nature of the centrifugal force limits the available space for multi-stepped processes on a single microfluidics disc. To overcome this limitation, a passive pneumatic pumping method actuated at high rotational speeds has been previously proposed to pump liquid against the centrifugal force. In this study, a novel microballoon pumping method that relies on elastic energy stored in a latex membrane is introduced. It operates at low rotational speeds and pumps larger volumes of liquid towards the centre of the disc. Two different microballoon pumping mechanism have been designed to study the pump performance over a range of rotational frequencies from 0 to 1500 rpm. The behaviour of the microballoon pump on the centrifugal microfluidic platforms has been theoretically analysed and compared with the experimental data. The experimental data shows that the microballoon pump dramatically decreases the required rotational speed to propel a liquid compared to the conventional pneumatic pump. It also shows that within a range of rotational speed, desirable volume of liquid can be stored and pumped by adjusting the size of the microballoon.

3.2 Literature Review

The centrifugal microfluidic platform is an automated LOC platform that relies on the centrifugal force to manipulate the liquid movement between the microchambers through microchannels. The advantageous features of portability, disposability and full automation in these platforms have led to the research of various aspects of the centrifugal microfluidics for novel POC diagnostic (Garcia-Cordero, Barrett, O'Kennedy, & Ricco, 2010; Haeberle, Brenner, Zengerle, & Ducrée, 2006; Kazemzadeh, Ganesan, Ibrahim, He, & Madou, 2013; M. Madou et al., 2006b; Steigert et al., 2006). Over the last decade, various centrifugal microfluidic designs have replicated standard medical diagnostics

techniques such as ELISA (Lai et al., 2004), and PCR (Amasia, Cozzens, & Madou, 2012). However, the technology faces a severe implementation challenge due to the unidirectional nature of the centrifugal force, limiting the number and the performance of fluidic functions required for complex integrated assays (Gorkin, Clime, Madou, & Kido, 2010). One way to implement more fluidic functions/steps on a microfluidic disc is to provide a mechanism that pumps liquid back to the disc centre.

In recent years, a handful of liquid manipulating techniques have been introduced to overcome the unidirectional liquid flow on centrifugal microfluidic platforms. An initial study by R. Gorkin et al. (2010) used a pneumatic compression chamber to pump liquid over a short distance toward the disc centre. Zehnle et al. (2012) connected a narrow inlet and a wider outlet to a compression chamber and has used the difference between their hydrodynamic resistance to pump a large amount of liquid back towards the disc centre. In another study by Garcia-Cordero, Basabe-Desmonts, Ducrée, and Ricco (2010), hydrophilic capillary action was used to manipulate the flow direction on the disc. However, these techniques are limited either to the distance or the amount of liquid they can pump toward the disc centre. Moreover building enough pneumatic energy to pump liquid toward centre of the disc requires high rotational speed, which may prematurely burst any passive valves embedded on the disc, and making hydrophilic capillaries requires complex surface modification procedures.

An ideal pumping solution that enables the implementation of multi-stepped or complex assays would be able to move a large volume of liquid while making the efficient use of the disc limited space. To meet this requirement, a few studies have been conducted by various researchers. Haeberle et al. (2007) attached steel plates on a PDMS membrane and used an external magnetic platform to deflect the membrane. Periodical deflection of the membrane resulted in the introduction of air bubbles into the fluidic network, and the injected bubbles pumped liquid towards the centre of the disc. In a different pneumatic

based study by M. C. Kong and Salin (2010), an external source of compressed air is used instead. However, in both studies, air from the surroundings is used for pumping liquids against the direction of centrifugal force. A major drawback of these pneumatic based methods is that there is a high risk of contaminating samples or reagents in the process of pumping. In order to manipulate trapped air inside centrifugal microfluidic platforms, Kameel Abi-Samra et al. and Thio et al. employed external heating source to heat air chambers and therefore utilized air expansion inside the microfluidic system to pump liquid toward the disc centre (Abi-Samra et al., 2011; Thio, Ibrahim, et al., 2013). Drawback of these implementations is the added external features such as externally actuated magnet, air source or external heating source, which increase the complexity and cost of the device.

This chapter introduces a novel pumping technique, called latex microballoon pumping, which is capable of propelling liquid back to the disc centre without performing surface treatments or using external actuators. The microballoon pump is fabricated simply by integrating a highly flexible latex film onto a CD microfluidic. This novel latex microballoon pump operates at low rotational speeds (e.g., less than 1500 rpm) and avoids external contaminants. It pumps predictable and large volume of liquid to expected distances from the disc centre. As one of the essential applications of the micropumps in bioanalytical assays, siphon activation using the microballoon pump is demonstrated. To illustrate the suitability of using latex as a flexible membrane, latex and the more commonly used PDMS are compared.

3.3 Methods and Materials

3.3.1 Microballoon Pumping Mechanism

In this section conventional pneumatic pumping method is compared with the microballoon pumping technique to achieve a holistic overview of the microballoon function in the centrifugal microfluidic platforms. In the static pneumatic pumping

method first introduced by R. Gorkin et al. (2010) trapped air in a sealed chamber prevents liquid from entering the chamber when the rotational speed is low i.e. low centrifugal force acting on the liquid (see Figure 3.1a). At higher rotational speeds a greater centrifugal force is acting on the liquid, and therefore the liquid is forced into the sealed chamber and compresses the trapped air (see Figure 3.1b). This compression results in the pressurization of the trapped air in the sealed chamber, which acts as a kinetic energy storage device. When the rotational speed is reduced, the stored kinetic energy in the compressed air pumps the liquid back out of the sealed chamber. However, 6000 to 8000 rpm is required to effectively compress the air, and spinning the disc over high rotational frequencies disturbs other fluidic functions.

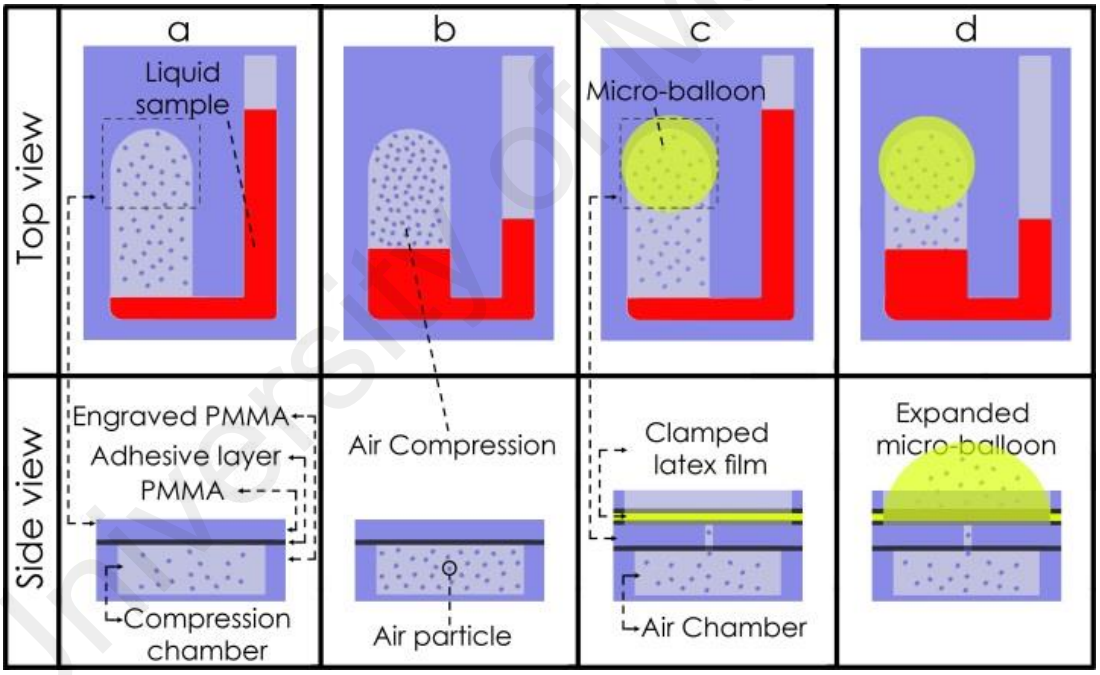

Figure 3.1: Schematic of conventional pneumatic pumping and latex microballoon pumping methods.

To achieve the equivalent kinetic energy without operating at high rotational speeds, a highly elastic microballoon is attached on the perforated air chamber (see Figure 3.1c). When the rotational speed is gradually increased, induced centrifugal pressure forced the liquid into the air chamber and pushed the air towards the microballoon. The microballoon expanded to accommodate the air displaced from the air chamber (see

Figure 3.1d). Afterwards, the expanded microballoon acts as a kinetic energy storage vault. As in the case of static pneumatic pumping, when the rotational speed is reduced, the stored kinetic energy of the expanded microballoon pushes the stored air back into the air chamber and pushes the liquid out of the chamber. This method effectively reduces the rotational speed required to pump liquid towards the disc centre.

3.3.2 Microballoon Material

Before conducting the experiments, a brief study of materials helped us to decide on the suitability of latex as compared to a silicone elastomer for fabrication of microballoons. PDMS is a silicone elastomer, which due to its excellent mechanical and chemical properties has been extensively used in advanced microfluidic platforms (Anderson, Chiu, Wu, Schueller, & Whitesides, 2000; Beebe et al., 2000; Chung et al., 2008; Cygan, Cabral, Beers, & Amis, 2005; Kaigala et al., 2008; M. S. Kim, Yeon, & Park, 2007; Tourovskaia, Figueroa-Masot, & Folch, 2004; Vollmer, Probstein, Gilbert, & Thorsen, 2005). PDMS is mainly used for fabrication of micro-pumps,(Grover, Skelley, Liu, Lagally, & Mathies, 2003; Jeong, Park, Yang, & Pak, 2005; Pan, McDonald, Kai, & Ziaie, 2005) micro-bioreactor,(Ostrovidov, Jiang, Sakai, & Fujii, 2004; Wu, Urban, Cui, & Cui, 2006) and micro-valves (Beebe et al., 2000; Go & Shoji, 2004; Grover et al., 2003; Li, Hsu, & Folch, 2005; Takao et al., 2005). For instance, Haeberle et al. (2007) employed external permanent magnets to fluctuate a PDMS film and inject air into a connected microfluidic network.

Latex films have also been used in microfluidic systems where biocompatible balloons, (Herculano, Alencar de Queiroz, Kinoshita, Oliveira Jr, & Graeff, 2011), micro-valves(Balabanian, Coutinho-Netto, Lamano-Carvalho, Lacerda, & Brentegani, 2006) and micro-pumps (Cosnier et al., 2001; Grover et al., 2003; Jeong et al., 2005; Lagally, Emrich, & Mathies, 2001; Nagayama, 1996; Pan et al., 2005; Weibel, Siegel, Lee, George, & Whitesides, 2007) were needed. Likewise to PDMS, latex has excellent

chemical and physical properties such as chemical inertness, biocompatibility, high elasticity, thermal and electrical insulation (Cosnier et al., 2001) and therefore enables a wide range of techniques and applications in microfluidic systems (Brask, Snakenborg, Kutter, & Bruus, 2006; A. Han et al., 2003; K. H. Han et al., 2007; Zhang, Xing, & Li, 2007). Some of the characteristics and applications of PDMS and latex are listed in Table 3.1. Both the latex and PDMS films are highly transparent which makes them excellent materials to be implemented in microfluidic platforms. In addition, latex films have higher elasticity in comparison to PDMS films. The Young's modulus of both latex and PDMS with thickness of 220μm is 1.2MPa and 3.1MPa, respectively (Brask et al., 2006).

Table 3.1: Brief comparison between the latex and PDMS film.

Property	**L/P**	**Characteristics**		***Applications***
Optical	Latex	Highly transparent >90%		Optical detection at wide range of wavelength
	PDMS			
Electrical	Latex	Insulator breakdown voltage	10^7-10^8 V/m (Braga, Costa, Leite, & Galembeck, 2001)	Leads to fabricate embedded circuits and intentional breakdown to open connections(McDonald, Steven, & Whitesides, 2001)
	PDMS		2×10^7 V/m (McDonald & Whitesides, 2002)	
Biocompatibility	Latex	Biocompatible		Drug delivery, catheter, balloon angioplasty(Herculano et al., 2011) (Balabanian et al., 2006).
	PDMS	Excellent Biocompatible		A wide range of applications in vivo(Bélanger & Marois, 2001; De Jong, Lammertink, & Wessling, 2006; Leclerc, Sakai, & Fujii, 2003; Whitesides, 2006)
Permeability	Latex	Water vapour impermeable (Arda & Pekcan, 2001; Grubauer, Elias, & Feingold, 1989)		Barrier for packing or sealing, also gas and liquid separation(Stephen, Ranganathaiah, Varghese, Joseph, & Thomas, 2006)
	PDMS	High gas permeable(J. E. Mark, 2009; Merkel, Bondar, Nagai, Freeman, & Pinnau, 2000)		Supply oxygen to the cells (Leclerc et al., 2003) and gas permeation pumps.
Elasticity	Latex	E- 1.2 to 3.1 Mpa (Brask et al., 2006)		Micro valve and Micro-pumping systems(Brask et al., 2006; Zhang et al., 2007)
	PDMS	E- 1.6 to 11 MPa (Brask et al., 2006)		Micro valve(Beebe et al., 2000; Go & Shoji, 2004; Grover et al., 2003; E. T. Lagally, S.-H. Lee, & H. Soh, 2005; E. T. Lagally, S. H. Lee, & H. Soh, 2005; Li et al., 2005; Takao et al., 2005)and Micro-pumping systems(Cosnier et al., 2001; Grover et al., 2003; Jeong et al., 2005; Lagally et al., 2001; Weibel et al., 2007)

In term of permeability, both the latex and PDMS films are liquid impermeable, however PDMS films due to their high gas permeability are more suitable for application in which aeration is required (Dittrich, Tachikawa, & Manz, 2006; Eddings & Gale, 2006). The oxygen permeability of PDMS at room temperature is twenty one greater than natural latex (Henrik Hillborg, 2012; H Hillborg & Gedde, 1999). Low gas permeability allows preserving the trapped air in the system and high elasticity leads to an efficient conversion of the kinetic energy to elastic energy, and conversely. Considering the higher elasticity and lower gas permeability of latex, in this study the latex film has been selected to make elastic microballoons in the centrifugal microfluidic platforms. The surface morphology of the latex material used for the fabrication of microballoons has been observed by scanning electron microscopy (SEM) (see Figure 3.2). This material does not contain pores of any significant dimensions and therefore the chosen latex material can be successfully used in our measurements.

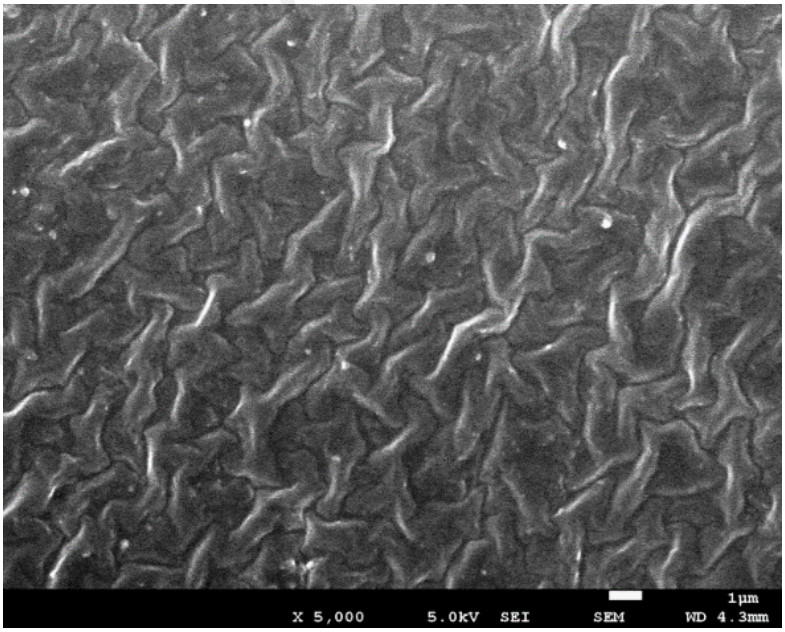

Figure 3.2: SEM image of latex surface used in all experiments.

3.3.3 CD Microfluidic Fabrication Procedure

Centrifugal microfluidic platforms were fabricated with either a seven layer design, or a three layer design. In the first design the latex film covered the whole disc to

enable the implementation of microballoon pumps in several chambers (see Figure 3.3a). In the second design a latex membrane was placed on the chamber in which the microballoon pumping was needed (see Figure 3.3b). Microfluidic CDs were fabricated using layer-by-layer assembly of polymethyl methacrylate disks (PMMA, 2 mm thick, Asia Poly Industrial Sdn. Bhd, Selangor, Malaysia.), pressure sensitive adhesive layers (PSA, 100 μm thick, FLEXmount DFM-200-Clear V-95 150 poly V-95 400 poly, FLEXcon, Spencer, MA, USA) and highly elastic latex films (~220 μm, Mister 003, SSL group, GBA Corporation Sdn. Bhd, Selangor, Malaysia). Microfeatures on the PMMA discs were either engraved or cut-out using a computer numerical controlled machine (CNC, model Vision 2525, by Vision Engraving & Routing Systems, USA). PSA microfeatures were cut-out using a cutter plotter machine (model PUMA II, by GCC, Taiwan). A custom-made spin stand that was used in this study to monitor the liquid movements in fluidic networks is comprised of a spinning motor, a laser RPM sensor, and a high-speed camera (Basler piA640-210gc, Germany). The spin stand is controlled by a custom-made LabVIEW program, and it allows for controlling the spinning speed, real time monitoring of liquid movement, and capturing an image per CD revolution.

The layers were aligned and pressed together to form a microballoon microfluidic system. Figure 3.3a shows the breakdown of the seven layer disc, comprised of three PMMA discs (each 2 mm thickness), three PSA layers (each 100 μm thickness) and a featureless latex layer (220 μm thickness) covering the whole disc area. The top PMMA disc contains only venting and loading holes, the middle layer contains the microfluidic features, while the bottom layer contains only the cut-out masks matching the sizes of the required microballoons. The top layer was first bond to the middle PMMA disc with a PSA layer with the venting and loading holes and the cut-out of chambers and channels. Two PSA layers with cut-out masks (identical to the middle PMMA disc) were used to sandwich the latex film between the middle and bottom PMMA disc.

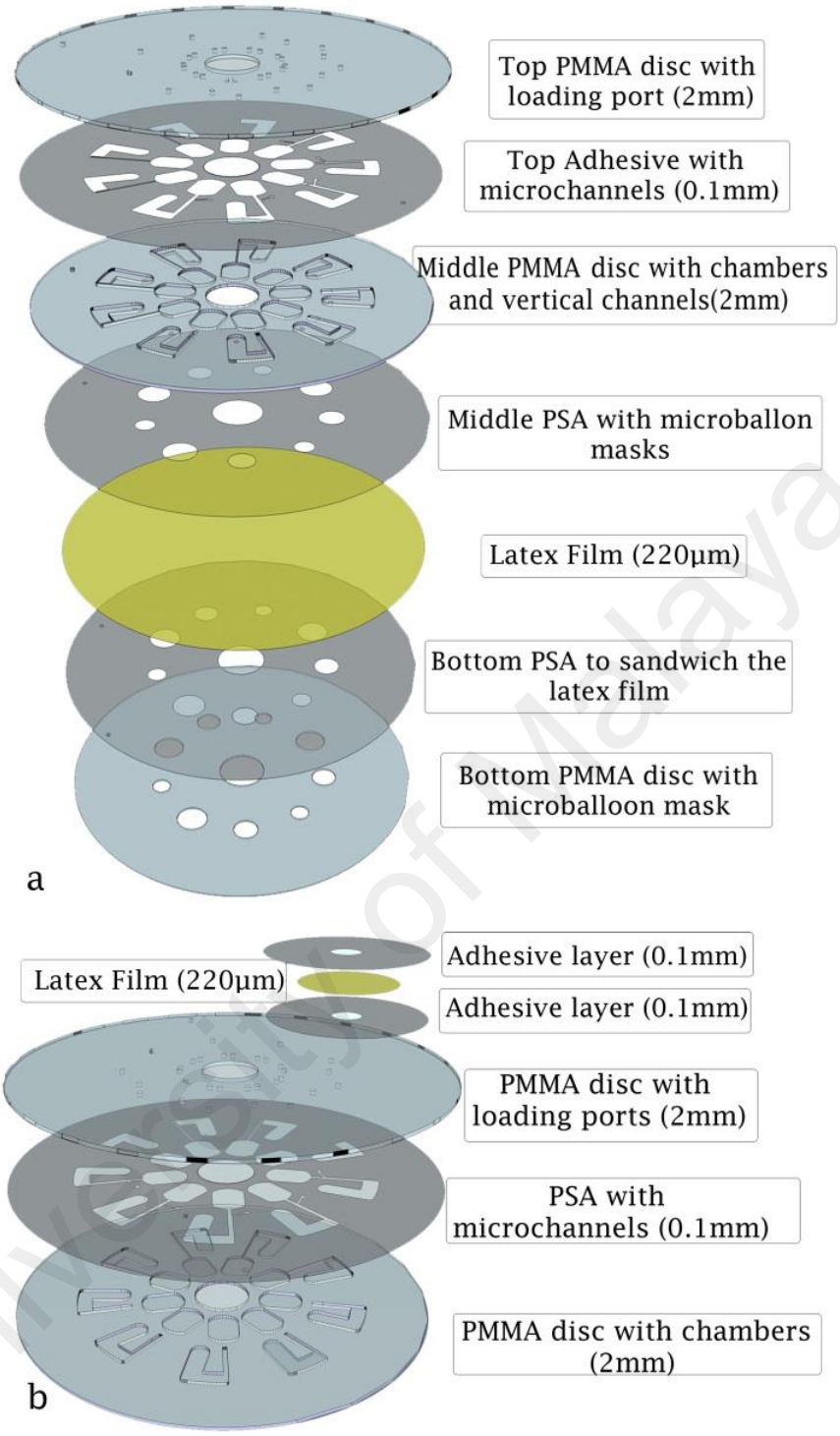

Figure 3.3: Schematics showing assemblies of microfluidic CDs. (a) A seven layer CD with an arrays of microballoons. (b) A three layer CD with a single microballoon.

Figure 3.3b shows the breakdown of the three layers disc comprising of two PMMA discs (each 2 mm thickness) and one PSA layer (100 µm thickness). The microballoon pumps in this case are fabricated individually from 2 layers of PSA (100 µm thickness) and a layer of latex (220 µm thickness). The latex layer was sandwiched between two

PSA layers with cut-out mask of any desired microballoon shape. The sandwiched latex was bonded onto the disc where required.

3.3.4 Microballoon Pumping Designs and Mechanisms

Design A (see Figure 3.4A) and Design B (see Figure 3.4B) show two microballoon pumping mechanisms that can be used for different applications. The first design was created to assess the relation between the rotational frequency and the milimetric advancement of the liquid toward the disc centre. The second design was used to measure the maximum volume of liquid that can be stored by microballoons corresponding to the rotational frequency. Design C (see Figure 3.4C) was employed to perform siphoning using microballoon pumping mechanism A.

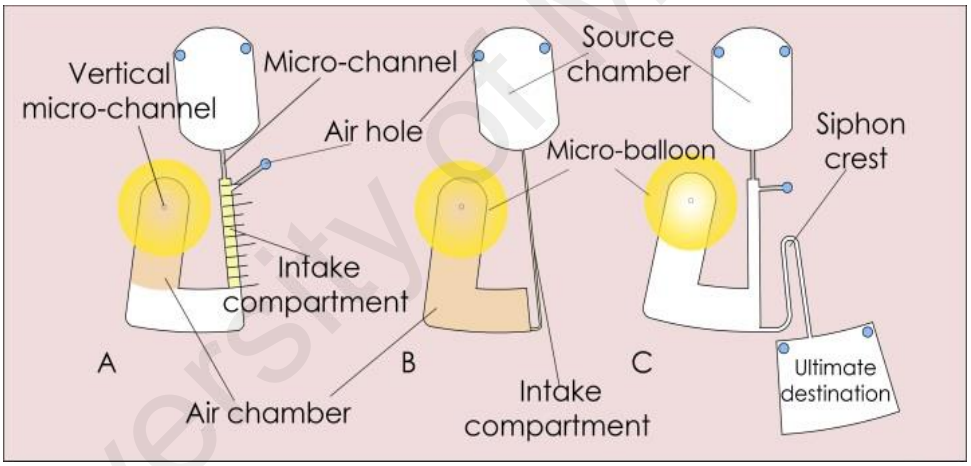

Figure 3.4: Components of Microfluidic platform designs A, B and C.

3.3.4.1 Microballoon Pumping with Design A

Design A is a pumping mechanism that allows controlling the liquid levels in a radially aligned intake by varying the rotational speed. It consists of a source chamber and a sealed U-shaped destination chamber (see Figure 3.4A). The destination chamber comprises of an intake compartment and a perforated air chamber with an attached microballoon. The source chamber is connected to the intake compartment via a microchannel. An air hole is placed on the top of the intake compartment (close to microchannel) to ensure that the air is only trapped and displaced in the air chamber. To

observe the relation between the rotational speeds and the changes of liquid level in the intake compartment, 1 mm spaced markers were engraved on the disc surface over the intake.

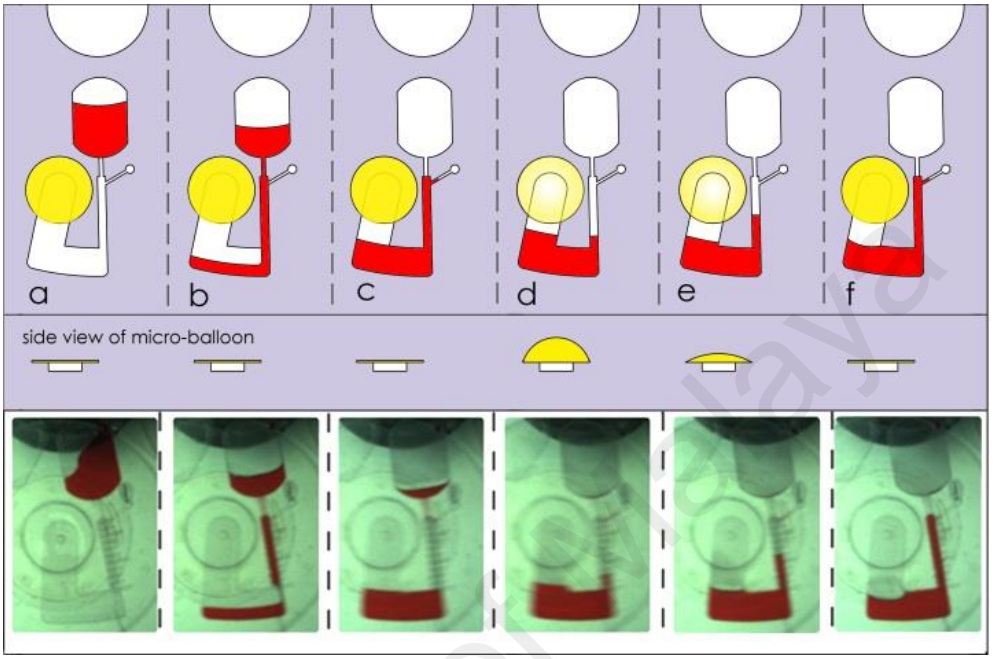

Figure 3.5: Schematic of the microballoon pumping by Design A.

A step by step description of the experiments based on Design A (see Figure 3.4A) is shown in Figure 3.5. The experiment was carried out by loading 70 µl of coloured deionized water into the source chamber (see Figure 3.5a) and spinning the disc until the liquid bursts into the destination chamber (see Figure 3.5b). During filling the destination chamber, air escaped through the air hole which was located at the top of the intake. Once the liquid has reached the bottom of the air chamber (see Figure 3.5c), air within the air chamber was trapped. The trapped air expanded the microballoon in parallel with the gradual increment of the rotational speed (see Figure 3.5d). The rotational speed was increased to 1500 rpm until entire liquid travelled into the destination chamber and the liquid level at the intake compartment nearly equalized to the liquid level at the air chamber. At this point, the rotational speed was reduced to contract the microballoon. The displaced air due to the contraction of the balloon pumped the liquid towards the disc centre. The volume of the liquid propelled towards the disc centre was controlled by

adjusting the rotational speed (see Figure 3.5e). The microballoon returned to its relaxed state when the rotational speed was reduced to zero i.e., the liquid level positioned at the nearest possible distance to the disc centre (see Figure 3.5f).

A millimeter advancement of the liquid in the intake is equal to displacement of 1.49 µl liquid. The corresponding rotational speed for each 1 mm advancement of liquid through the intake compartment was recorded during the experiment. The experiment was repeated for microballoon sizes within the range of 3 mm to 5 mm radii. A similar experiment without the implementation of microballoon was conducted to compare the performance of the microballoon pump and the conventional pneumatic pump, which was shown in Figure 3.1. The results are demonstrated and discussed in *Section 3.4.1*.

3.3.4.2 Microballoon Pumping with Design B

Design B was used for investigating the maximum volume of liquid that can be pumped by microballoons of different sizes. The design consists of a source chamber and an air chamber (see Figure 3.4B). The source chamber is connected to the air chamber via a tiny intake compartment (i.e., a microchannel). The intake compartment is connected to the bottom of the air chamber. Unlike the previous design, there is no air hole at the top of the intake compartment. This allows for utilizing the whole air volume in the air chamber to expand the microballoon.

A stage by stage observation of the experiments based on design B is shown in Figure 3.6. The experiment was carried out by loading colored deionized water samples ranging from 10 µL to 90 µL into the source chamber (see Figure 3.6a). The disc was spun to transfer the liquid into the air chamber (see Figure 3.6b). The lack of venting hole in the design caused the air to displace from the air chamber to the microballoon at the instance the liquid entered to the air chamber. Increasing the rotational speed resulted in transferring more liquid into the air chamber (see Figure 3.6c).

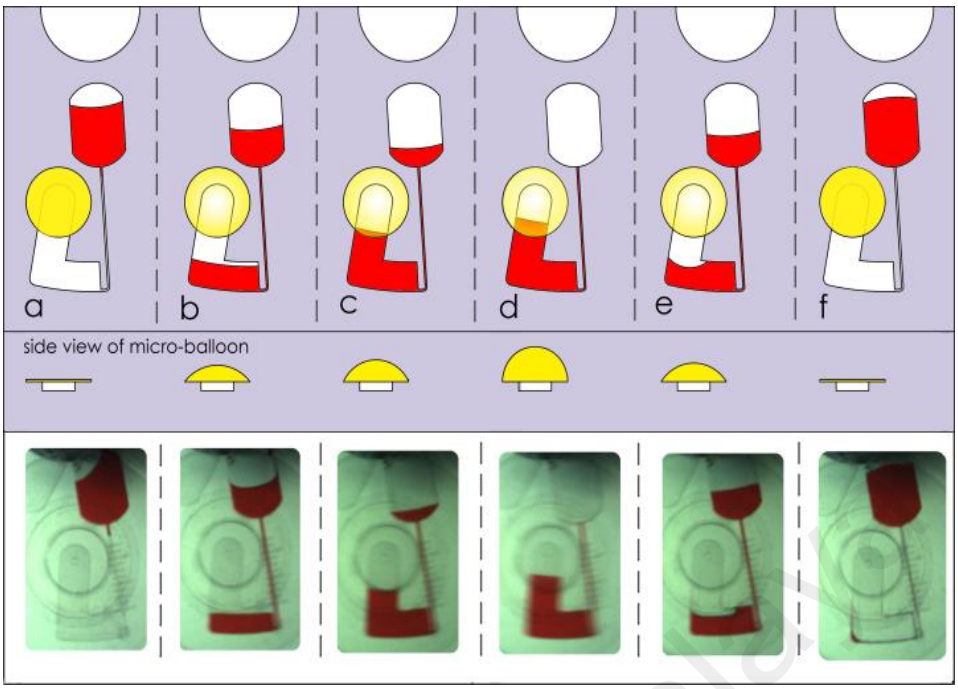

Figure 3.6: Schematic of microballoon pumping by Design B.

The rotational speeds at which the abovementioned volumes of liquid were fully drained from the source chamber (see Figure 3.6d) were recorded for different microballoon sizes (3 mm to 5 mm). At this stage, the maximum volume of liquid corresponding to rotational speed and the size of microballoon was determined. The results are shown in Figure 3.9 and discussed in the section of Results and Discussion. The rotational speed was gradually reduced to test the pumping performance of the microballoon pump (see Figure 3.6e). When the disc was stopped the microballoon pumped back the entire liquid to the source chamber (see Figure 3.6f).

3.3.4.3 Microballoon Siphoning with Design C

With design C (see Figure 3.4C) siphon process was accomplished without the need for high rotational frequencies and any microchannel surface modifications. Design C is similar to the design A except that it has a siphon channel and an ultimate destination chamber. For siphons to be primed, the liquid in the intake compartment must be pumped beyond the siphon crest. In our experiment, a 3 mm radius microballoon was installed on the air chamber. The experiment was carried out by loading 80 µL of coloured deionized water into the source chamber and spinning the disc up to 1400 rpm to transfer liquid to

destination chamber. Rotational speed was gradually reduced to propel the liquid sample towards the disc centre, until the siphon actuated and the liquid entered to the ultimate destination.

3.3.5 Mathematical Modelling of Microballoon Pumping

In this section theoretically investigates the microballoon pumping mechanisms to facilitate future implementations of this novel pumping technique in centrifugal microfluidic platforms. In general, the behaviour of the microballoon pumps can be described in terms of changes of the liquid level in the intake compartment i.e., $x=R_i - R_{i0}$ (see Figure 3.7). The liquid level in the intake compartment is a result of the equilibrium of the hydrostatic pressure and the kinetic energy stored in the microballoon.

Figure 3.7 shows the centrifugal microfluidic design that consists of a U-shaped chamber i.e., air chamber and intake compartment. Figure 3.7a shows the liquid level and the air trapped in the air chamber when the system is at rest. When the disc is spinning, due to the flexibility of the microballoon, the liquid level in the air chamber rises up, and the liquid level in the intake compartment goes down (see Figure 7.b). At this point, the microballoon expansion volume is equivalent to the amount of liquid entered the air chamber.

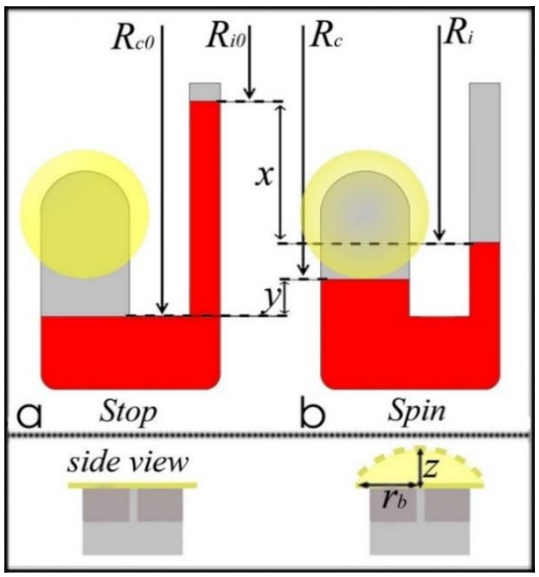

Figure 3.7: Parameters regarding to microballoon expansion volume and hydrostatic pressure when the disc is stopped and spinning.

The hydrostatic pressure acting on the liquid column in the U-shaped chamber is:

$$\Delta P(\mathrm{x}) = \frac{1}{2}\rho\omega^2\left(R_c^2 - R_i^2\right) \tag{3.1}$$

where ρ is the liquid density, ω is the rotational frequency R_c, R_i are liquid levels in the air chamber and intake compartment, respectively. Substituting R_c, R_i with R_{c0}-y and R_i=R_{i0}-x in Equation 3.1 yield:

$$\Delta P(\mathrm{x}) = \frac{1}{2}\rho\omega^2\left(R_{c0} - y + \left(R_{i0} + x\right)\right)\left(R_{c0} - y - \left(R_{i0} + x\right)\right) \tag{3.2}$$

where x and y are the respective changes in liquid levels in the intake compartment and the air chamber: x=R_i–R_{i0} and y = R_{c0}–R_c as shown in Figure 3.7. To simplify the pervious expression, the term $(R_{c0}–y+(R_{i0}+x))(R_{c0}–y–(R_{i0}+x))$ is denoted as $\varphi(x)$. Equation 3.2 is simplified to:

$$P\left(\mathrm{x}\right) = \frac{1}{2}\rho\omega^2\phi\left(x\right) \tag{3.3}$$

The pressure P represented by Equation 3.2 and 3.3 causes the expansion of the microballoon. When expanded, the pressure exerted by the microballoon $P_b(z)$ can be expressed in terms of the microballoon bulge height and initial radius as follows(Gad-el-Hak, 2010; Hohlfelder, 1999):

$$P_b\left(\mathrm{z}\right) = C_1\frac{Mtz^2}{r_b^4} + C2\frac{\sigma_0 tz}{r_b^2} \tag{3.4}$$

where M is the bi-axial modulus of elasticity, t is the thickness of the latex film, r_b is the initial microballoon radius, σ_0 is the initial film stress, z is the bulge height (microballoon height), and C_1, C_2 are constants. The thin latex film bi-axial modulus of elasticity is defined as $M=E/(1-v)$ where E is the Young's modulus of elasticity and v the Poisson's ratio.

To evaluate Equation 3.4, the bulge height z of the microballoon should be determined. The bulge height is a result of the air displaced by the liquid in the air

chamber. The relationship between the microballoon expansion volume *(V)* and the liquid level and cross-sectional areas of the compartments is defined as follows:

$$V = \frac{2}{3}\pi r_b^2 z = xS_i = yS_c \tag{3.5}$$

where *Si* and S_c are the cross-sectional areas of the two compartments. Solving Equation 3.5 allows us to determine the bulge height of the microballoon using either the volume change in the intake compartment (xS_i) or the volume in the air chamber (yS_i):

$$z = \frac{3xS_i}{2\pi r_b^2} \text{ or } z = \frac{3ySc}{2\pi r_b^2} \tag{3.6}$$

Equating 3.3) and (3.4 allows us to obtain a relationship between the liquid levels (indicated by $\varphi(x)$) and the rotational frequency of the disc:

$$\frac{1}{2}\rho\omega^2\varphi(x) = C_1\frac{Mtz^2}{r_b^4} + C2\frac{\sigma_0 tz}{r_b^2} \tag{3.7}$$

Equations 3.6 and 3.7, have been compared with the experimental data for rotational frequencies from 0 to 1500 rpm. Figure 3.8 shows the comparison between theoretical and experimental results for various microballoons. The parameters used for the evaluation of Equation 3.7 are listed in Table 3.2. The Equation 3.7 was used to analyse the performance of microballoon pump Design B at various rotational frequencies.

Table 3.2: Value of parameters used in analytical analysis.

Parameters	Value	Parameters	Value
r_b	3,4 and5mm	E	1.2 MPa
R_{i0}	25.5 mm	v	0.48
R_{c0}	36 mm	σ_0(r_b-3 mm)	0.06 MPa
t	220 µm	σ_0(r_b-4 mm)	0.058 MPa
ρ	1000 kg/m^3	σ_0(r_b-5 mm)	0.055 MPa
S_i	1.49 mm^2	S_c	6.12 mm^2

3.4 Results and Discussions

3.4.1 Microballoon Pumping with Design A

These two section evaluate the pump behaviour for two microballoon pump mechanisms or pumping with Design A and B. The effect of various microballoon sizes on the pumping behaviour of each mechanism is also discussed. In general, mechanism A is a pumping technique similar to the pneumatic pumping introduced by R. Gorkin et al. (2010). In this mechanism structure of the design and pump performance is proportional to the size of liquid volume. Figure 3.8 demonstrates the accuracy of the proposed pumping method to manipulate exact volumes of liquid. The figure illustrates the corresponding rotational speeds to the liquid level in the intake compartment.

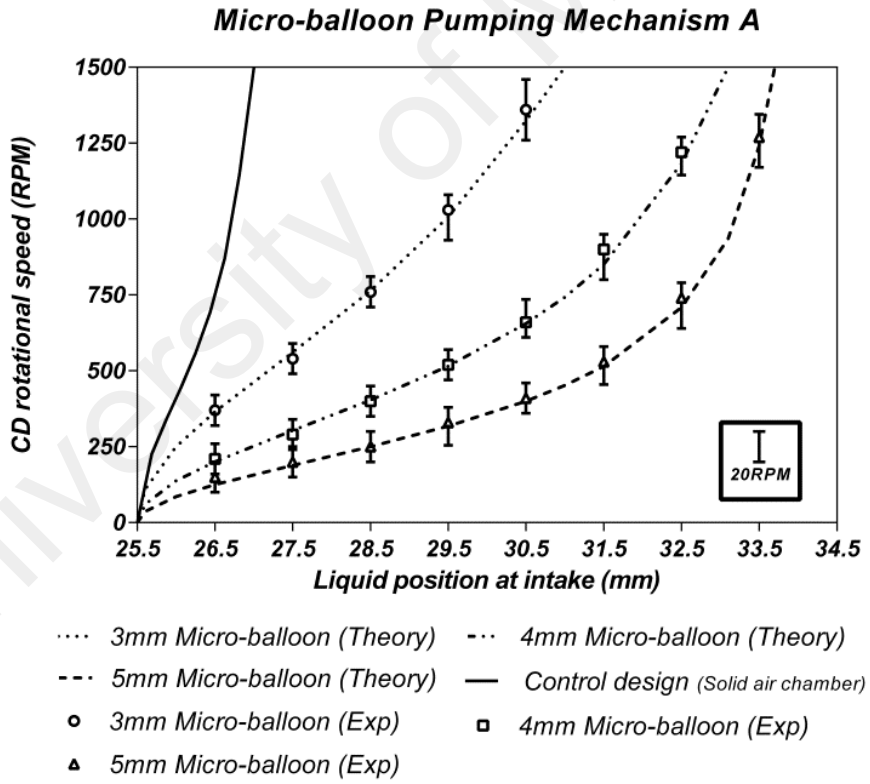

Figure 3.8: Mechanism A, the rotational frequency versus the liquid level in the intake compartment for three sizes of microballoons.

The experimental data for microballoon radii of 3-5 mm are compared with that of the control design and the theoretical expression (Equation 3.7). The results show that the liquid level is proportional to the rotational speed, liquid volume and the microballoon

size. For a certain liquid volume, increasing the microballoon radius decreases the required range of rotational speed to pump the liquid to specific distances toward the centre of the disc. All three different microballoons used in the experiment pump substantially larger volumes of the liquid i.e., up to 5 times in comparison with the control design. In order to pump such volume of liquid with the conventional pneumatic pumping methods 6000-8000 rpm is required (see ref. (R. Gorkin et al., 2010)). The experimental data shows a low variation in critical frequencies corresponding to liquid levels in the intake compartment (see Figure 3.8).

3.4.2 Microballoon Pumping with Design B

Figure 3.9 illustrates the capability of the microballoons to pump a wide range of liquid volumes. It shows that the volume of liquid that can be stored is increases with the size of the microballoon. At the rotational speed of 1500 rpm, increasing the microballoon diameter from 3 mm to 5 mm increases the amount of stored liquid from 30 µl to approximately 90 µl.

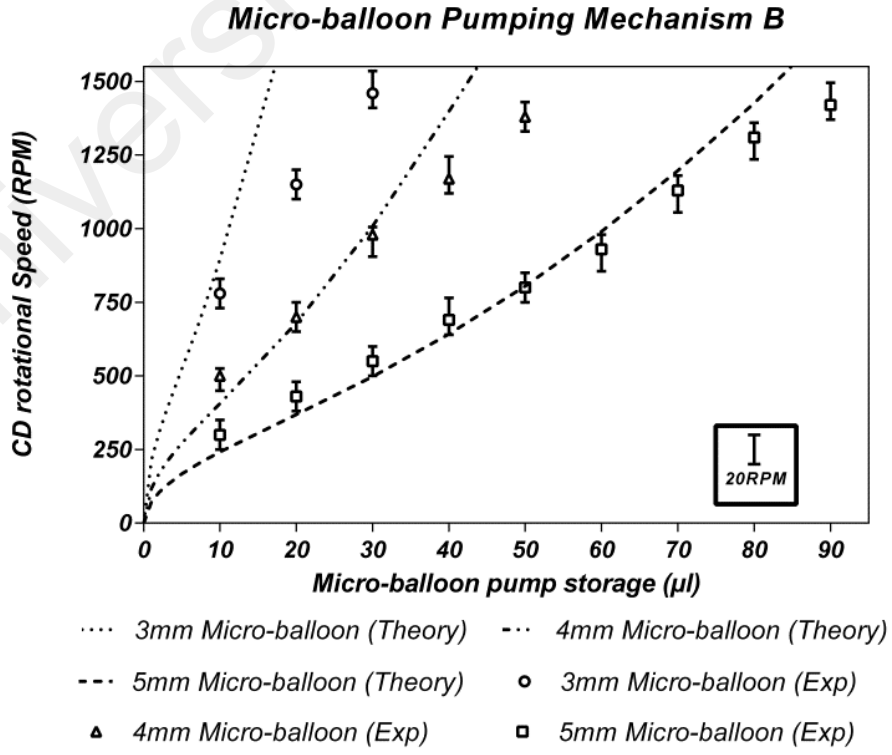

Figure 3.9: Mechanism B, the rotational speed versus the volumes of stored liquid with three sizes of microballoons.

The theoretical results are in a good agreement with the experimental results except for the smallest size of microballoons used (3 mm). Note that, the Equation 3.7 does not calculate the effect of the air compressed on the microballoon pumping mechanism. The deviation between the experimental data and the theoretical results may be due to gradual increments of air compression in the destination chambers which occur at high rotational speeds. The smaller microballoons require higher pressure to store a fixed volume of liquid and therefore, the effect of air compression is more significant on smaller microballoon sizes.

3.4.3 Microballoon Siphoning with Design C

On centrifugal microfluidic platforms, siphoning is used to transfer liquid between two chambers in a multi-steps process. The examples include the blood serum separation and the transfer of liquid from the detection chamber to the waste chamber for an ELISA, or the cascaded transfer of liquid between a series of chambers. Current centrifugal platforms either utilize microchannels surface modification or pneumatic pumping technique to implement siphon valves (Ducrée et al., 2007; Kido et al., 2007; Siegrist, Gorkin, Clime, et al., 2010). However, surface properties of polymers tend to return to its natural state over time and pneumatic pumping methods requires high rotational speeds.

The inclusion of a microballoon onto the centrifugal microfluidic platform allows for siphon actuation without the need for surface treatment or air compression. The step by step process of siphon actuation using design C (see Figure 3.3) is shown in Figure 3.10.The source chamber was initially loaded with 80 µl of the liquid sample (see Figure 3.10a). The disc spin rate was increased to transfer the liquid from the source chamber into the destination chamber (see Figure 3.10b) and to expand the microballoon by the displaced air. At rotational speed of 1400 rpm whole liquid was transferred to the destination chamber and liquid levels at the destination chamber and the siphon channel were equalized (see Figure 3.10c). At this stage, the height of the liquid in the intake com-

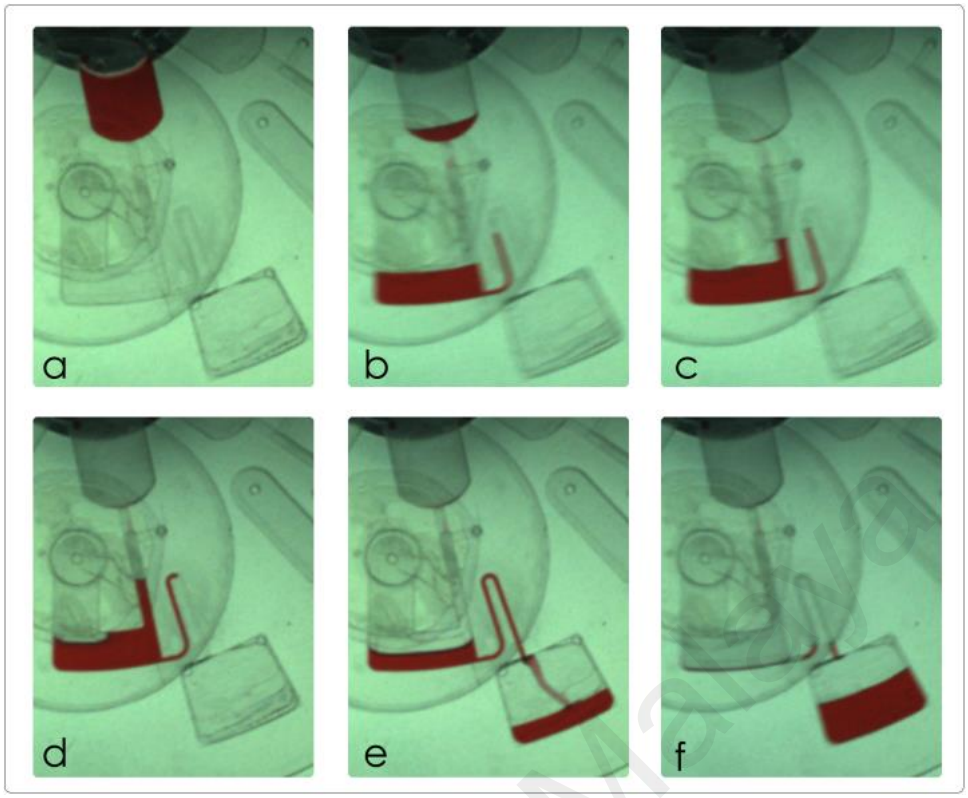

Figure 3.10: Schematic of the siphoning procedure in microfluidic Design C.

partment does not reach the top of the siphon crest and therefore siphon doesn't actuate. Rotational frequency was gradually reduced to decrease the centrifugal pressure acting on the liquid. Thus the microballoon pushed the displaced air back into the air chamber, pumping the liquid up into the adjoining intake compartment and into the siphon channel (see Figure 3.10d). Once the liquid level in the siphon channel reached the top of the crest, the siphon was actuated and the liquid was siphoned into the ultimate collection chamber (see Figure 3.10e and f). The rotational speed the siphon was actuated in our experiment was as low as 580 rpm. Unlike the conventional pneumatically actuated siphon valve, with the microballoon pump the siphon was primed at a low range of rotational speed. Another benefit of the microballoon assisted siphon is the ability to actuate the siphon under both hydrophobic and hydrophilic conditions.

3.5 Conclusions

Unidirectional nature of liquid flow within centrifugal microfluidic platforms limits the number of possible process steps before liquids reach to the rim of the disc. Microballoon

pumping, a novel technique, is created to efficiently overcome this limitation. Microballoon pumping is based on the displacement of trapped air to expand a highly elastic latex membrane and employ the stored elastic energy for pumping liquids. In comparison with other pumping methods introduced to push liquids against centrifugal force, microballoon pumping does not require surface treatment, high rotational speed or any external actuators. The microballoon pumping compared to conventional pneumatic pumping techniques is able to pump larger volume of liquids at dramatically lower the range of rotational speed. Table 3.3 shows the comparison between technical aspects of microballoon and previously developed pumping mechanism.

The microballoon mechanism was modelled and the model was confirmed by analysing rotational speed versus pumping position for three different sizes of microballoons. The model can be used to approximately predict pumping behaviour in different mechanisms with various sizes of the microballoons. As a practical application of this novel pumping mechanism, microballoon design A is used to actuate a siphon channel. Overall, the microballoon pumping is an efficient liquid propelling technique that enables more complex biochemical assays on centrifugal microfluidic platforms.

Table 3.3: Comparison between microballoon and previously developed pumps.

Pump	Operational mechanism	Operational spin speed	Max acceleration	Pumping capacity rate
Microballoon pump	Passive	1500 rpm	-	100μl
Pneumatic pump	Passive	8000 rpm	-	7 μl
Capillary pump	Passive	1000 rpm	-	13.5 μl
Euler pump	Passive	4000 rpm	4000 rpm/s	30 μl
CDI pump	Passive	2400 rpm	1800 rpm/s	*****200-300μl
TP pump	Active	1200 rpm	-	19μl/min
Electrolysis Pneumatic	Active	4500 rpm	-	9μl/min
Centrifugo-magnetic	Active	1800 rpm	-	19μl/sec

***** CDI pumps 75% for sample volume between 200 to 300 μl.

CHAPTER 4: MICROBALLOON MIXING ON CENTRIFUGAL MICROFLUIDIC PLATFORMS

4.1 Introduction

Dengue is the current leading cause of death among children in several Latin American and Asian countries. Due to poverty in areas where the disease is prevalent and the high cost of conventional diagnostic systems, low cost devices are needed to reduce the burden caused by dengue infection. Centrifugal microfluidic platforms are an alternative solution to reduce cost and increase availability of a rapid diagnostic system. The rate of chemical reactions in such devices often depends on the efficiency of mixing techniques employed in their microfluidic networks. This chapter introduces a micromixer that operates by the expansion and relaxation of a microballoon to provide for a consistent periodical 3D reciprocating flow. A microballoon reduces mixing time of 12 μl liquid in a chamber with high-surface-area-to-volume-ratio from 170 minutes, for diffusional mixing, to less than 23 seconds. This chapter also investigates the effect of the microballoon mixers in a dengue detection immunoassay. The results indicate that employing microballoon mixer enhances the detection signal of the dengue virus immunoassay by nearly one order of magnitude compared to conventional ELISA method.

4.2 Literature Review

Neglected tropical diseases (NTDs) are a category of infectious diseases that are inextricably linked to poverty that thrive in tropical and subtropical regions (Dias, Gomes-Filho, Silva, & Dutra, 2013; Linares, Pannuti, Kubota, & Thalhammer, 2013). Among the NTDs, dengue virus is of particular importance and is considered one of the major public health problems in 112 countries (Gurugama, Garg, Perera, Wijewickrama, & Seneviratne, 2010). According to WHO, in the first quarter of 2014 the dengue virus outbreak in Malaysia has affected ~ 27,500 individuals and resulted in 64 deaths (WHO, 2014). In order to reduce the economic burden caused by this disease, it is necessary to

employ a highly sensitive, rapid and low cost device as an early detection method. Introduction of such a detection system to diagnose the early stage infection where the concentration of the virus (NS1) is in the range of nanograms per milliliter range is expected to reduce the mortality rates from 20% to below 1% (Allwinn, 2011; Lapphra et al., 2008; Linares et al., 2013).

LOC devices are now revolutionizing molecular diagnostics towards a simpler and more cost effective POC diagnostic devices and this will result in tremendous advances in the detection of infectious diseases such as dengue (Chin, Linder, & Sia, 2007; Daar et al., 2002). In the LOC category, centrifugal microfluidics platform integrates and automates a sequence of laboratory unit operations (i.e., liquid metering, reagent separation and mixing) required for a chemical assay on a single platform (Kazemzadeh et al., 2013). In centrifugal microfluidics liquid is propelled through sophisticated microfluidic networks via centrifugal force generated by a spinning motor, preventing the need for an external syringe pump (Robert Gorkin et al., 2010). In centrifugal microfluidics, like in other LOC technologies, the efficiency and the rate of chemical reactions strongly depends on the efficiency of the mixing methods used in the fluidic networks (Lynn Jr et al., 2014; L. Ren et al., 2012). This is of particular importance for the diagnosis of NTD in which the concentration of virus circulated inside a patient's body in the early stages is in nano scale range.

In recent years, several active (i.e., requires an external actuator) and passive (i.e., without the need for an external actuator) mixing techniques have been introduced to cope with mixing difficulties prevalent in the predominantly laminar flow regime on centrifugal microfluidic platforms. Examples of developed active mixing techniques on centrifugal microfluidic platforms are magnet stirring and pneumatic-based mixing techniques. Chaotic advection in the first active mixer is induced by the relative motion of magnets that were embedded inside these mixing chambers, in respect to the external

magnetic forces (Ducrée et al., 2007; Grumann et al., 2005; Haeberle, Brenner, Schlosser, Zengerle, & Ducrée, 2005). Liquid manipulation in pneumatic mixing technique takes place by air/gas from an external source of compressed air/gas (M. C. Kong & Salin, 2012). Passive mixing principles that have been explored on the centrifugal microfluidic platform include reciprocating flow and stopped-flow (batch-mode) mixing (Grumann et al., 2005; Noroozi et al., 2009). Stopped-flow mixing is based on inertia induced by the reversal of the spinning direction, hence it is commonly used in complex bioassays where the efficient use of the limited space on the disk is crucial (Grumann et al., 2005) (See Figure 4.1a). In a reciprocating flow mixer, compression and expansion of air trapped inside an air chamber generates two dimensional (2D) reciprocating currents to facilitate mixing progress (See Figure 4.1b). A reciprocating flow mixer occupies quite a lot of space on the disc as an air chamber that it used to generate pneumatic energy must be accommodated. Nevertheless, by means of the same air chamber the mixer can pump the mixed liquid against the centrifugal force to other reservoirs (via siphoning) to enable more complex bioassays on the disk (Noroozi et al., 2009; Noroozi, Kido, Peytavi, et al., 2011) .

The mixing techniques on centrifugal microfluidics discussed here are useful approaches that have been employed , for example, in quantifying nitrate and nitrite levels in blood, reparatory virus detection, detection of the antibiotic resistance gene mecA of Staphylococcus aureus and several immunoassays (Focke, Kosse, et al., 2010; T.-H. Kim et al., 2013; David J Kinahan, Kearney, Dimov, Glynn, & Ducrée, 2014; B. S. Lee et al., 2011; Lutz et al., 2010; Noroozi et al., 2009; Noroozi, Kido, Peytavi, et al., 2011; Nwankire, Chan, et al., 2013; Siegrist, Gorkin, Bastien, et al., 2010).

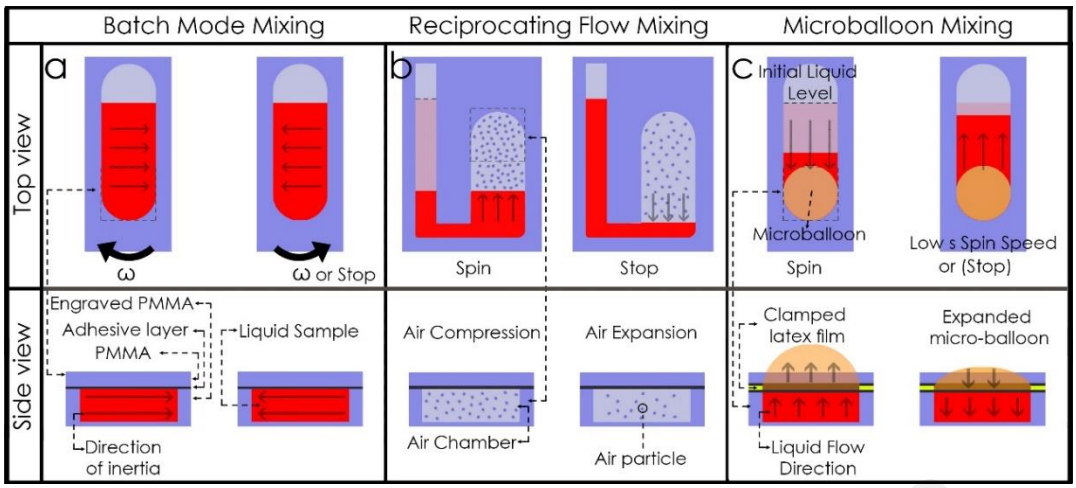

Figure 4.1: Schematic of the centrifugally driven (a) batch-mode or stopped-flow mixing, (b) pneumatic flow reciprocation mixing and (c) 3D microballoon flow reciprocation mixing mechanisms.

This Chapter introduces an advantageous microballoon-based liquid manipulation technique in centrifugal microfluidic platforms. Microballoon micromixer provides a high mixing efficiency, and operates with no need for occupying any scape of the disk, any external power source, high spinning speeds, and high accelerations. Over a low range of rotational frequencies, microballoon mixer generates three dimensional (3D) reciprocating flow in response to the changes in the platform spinning speed. A centrifugal force induced at an elevated spinning speed forces a liquid to expand a microballoon. Reducing the spinning speed then allows for the relaxation of the microballoon, pushing back the liquid back to the mixing chamber (See Figure 4.1c). Due to the mechanical properties of the microballoon, this newly introduce micromixer is also able to pump liquid similar to the reciprocating flow mixer (see *Section 2.2.1.1*), however it allow manipulating larger volumes of liquid over a dramatically lower range of spinning speeds. In this Chapter, the microballoon mixing mechanism and its efficiency are experimentally analyzed and compared with stopped-flow mixing. Finally, the effect of microballoon mixing on enhancing the detection signal in a dengue detection immunoassay is experimentally evaluated and assessed. In general, the microballoon mixer can be used in a wide range of bioanalytical applications and it is a promising

approach to help facilitate the early detection of dengue as well as other infectious diseases.

4.3 Methodology

4.3.1 Designs and Fabrications

Microfluidic Design D and Design E were created to evaluate the efficiency of the microballoon mixer in centrifugal microfluidic platforms (see Figure 4.2). Design D was introduced for three purposes; (i) evaluation of the microballoon mixing efficiency in a chamber with high-surface-area-to-volume-ratio, where diffusional mixing is time consuming, (ii) comparison of the mixing efficiency of the newly introduced technique with the established stopped-flow mixing method, and (iii) theoretical analysis of the rotational frequencies corresponding to the change of liquid levels inside a mixing chamber. The theoretical analyzing is required to enable the use of a single microballoon for both pumping and mixing. Two CD-like well plates (Design E) were fabricated to investigate the effects of microballoon mixing and stopped-flow mixing techniques in a colorimetric ELISA.

Microfluidic CDs were fabricated using layer-by-layer assembly of PMMAs, PSAs and highly elastic latex films (~140 μm thick, N. S. Uni-Gloves Sdn Bhd, Seremban, Malaysia). The mean thickness of the PSA layer that reduces by the pressure applied has been experimentally determined by the calibration of the screw pressure used for assembling platform layers. The mean thickness of PSA layer is ~60 μm that results in producing of a mixing chamber with large-surface-to-volume-ratio in Design D. The spin stand employed to monitor the liquid movements in fluidic networks is comprised of a high speed camera and a programmable spin controller system. Details of the experimental setup and the fabrication procedure of microfluidic CDs are available in *Section 3.3.3*.

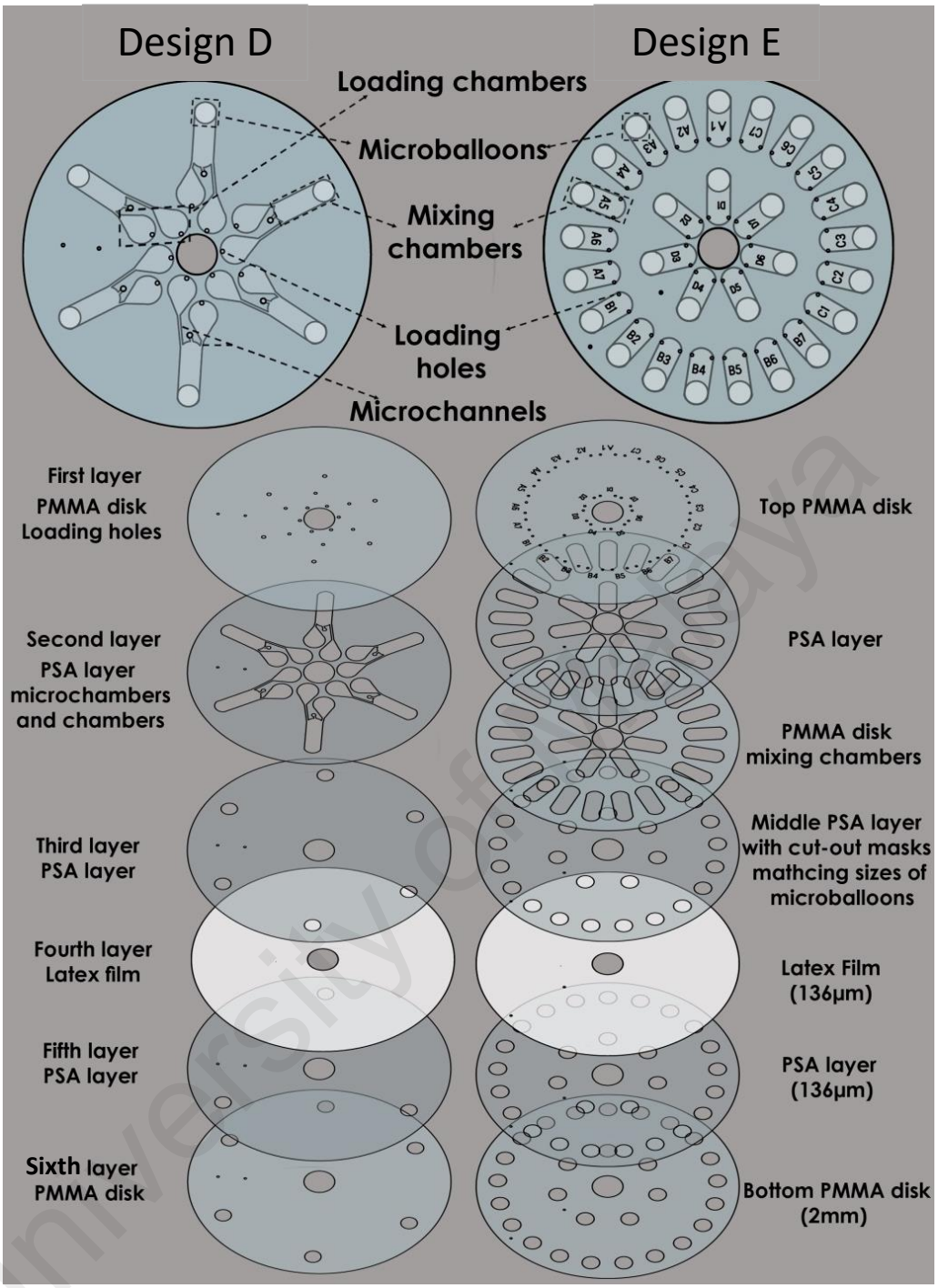

Figure 4.2: Breakdown of the CD microfluidics Design D and Design E.

Design D consists of two loading reservoirs, a mixing chamber partially covered by a latex layer, and two microchannels that connect the loading reservoirs to the mixing chamber (see Figure 4.2A). Design D is composed of two PMMA disks, three PSA layers and a latex film. In Design D, the top PMMA disk (first layer) contains venting and inlets/outlets holes. Unlike conventional microfluidic platforms, instead of using engraved chambers on plastic disk, chambers and microchannels are cut on the upper PSA

layer (second layer). Sandwiching the upper PSA layer between the top PMMA disk and the middle PSA layer (third layer) created mixing chamber of high surface-area-to-volume-ratio. In all platforms (whether ballooning action were needed or not) the masks of 4mm microballoons were cut-out in the middle PSA layer to make mixing chambers of equal liquid capacity. However, the balloon masks in the bottom PSA layers (fifth layer) were cut-out only below chambers (under latex layer) in which ballooning action was desired. Arrays of microballoons were fabricated on the platform by sandwiching a latex film (forth layer) between the middle and bottom PSA layers. Finally, a PMMA disk (sixth layer) was added to protect the chambers and balloons from accidental physical damages, which could occur during transportation (see Figure 4.2A).

Design E has an additional PMMA disk when compared to design D, increasing the thickness or liquid capacity of the reservoirs (see Figure 4.2B). Two CD-like well plates were fabricated to compare the effects of microballoon and stopped-flow mixing in the ELISA experiments. Both CD-like well plates were composed of seven layers (see Figure 4.2B), but in order to prevent ballooning action in stopped-flow mixer platform, its bottom PSA layer (fifth layer) was featureless. During the CD assembly of the both platforms, either 3x4 mm cellulose membranes (CM) or 3x4 mm polystyrenes (PS) are further attached into the specific mixing chambers (i.e., cells).

4.3.2 Microballoon Mixing in Tiny Chamber

Mixing experiments using design D was initiated with loading 11 μl deionized water into the loading chambers, and spinning the platform to transfer the liquids into their corresponding mixing microchambers. Then 1 μl black color dye was injected into another source chamber of each mixing unit. In order to transfer the color dye into the mixing chamber and conduct the first mixing cycle, the rotational frequency was increased to 810 rpm with an acceleration of 1500 rpm s^{-1}. At the rotational frequency of 810 rpm the liquid level in the mixing chamber reduced to the top of the microballoon

(see Figure 4.3a). The platform was then stopped and the stored elastic energy in the microballoon propelled the back into the mixing chamber (see Figure 4.3b).

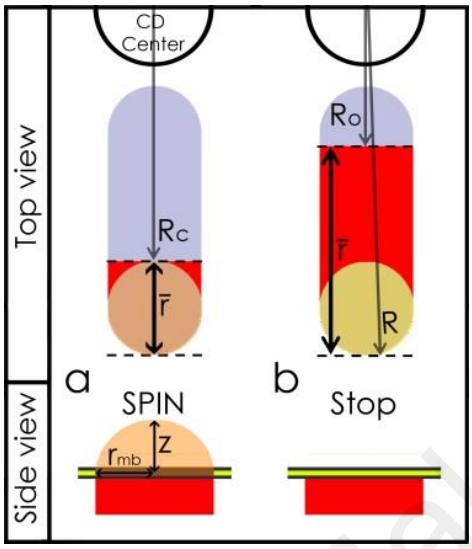

Figure 4.3: Changes of the liquid level during (a) expansion and (b) relaxation of microballoon in a mixing cycle.

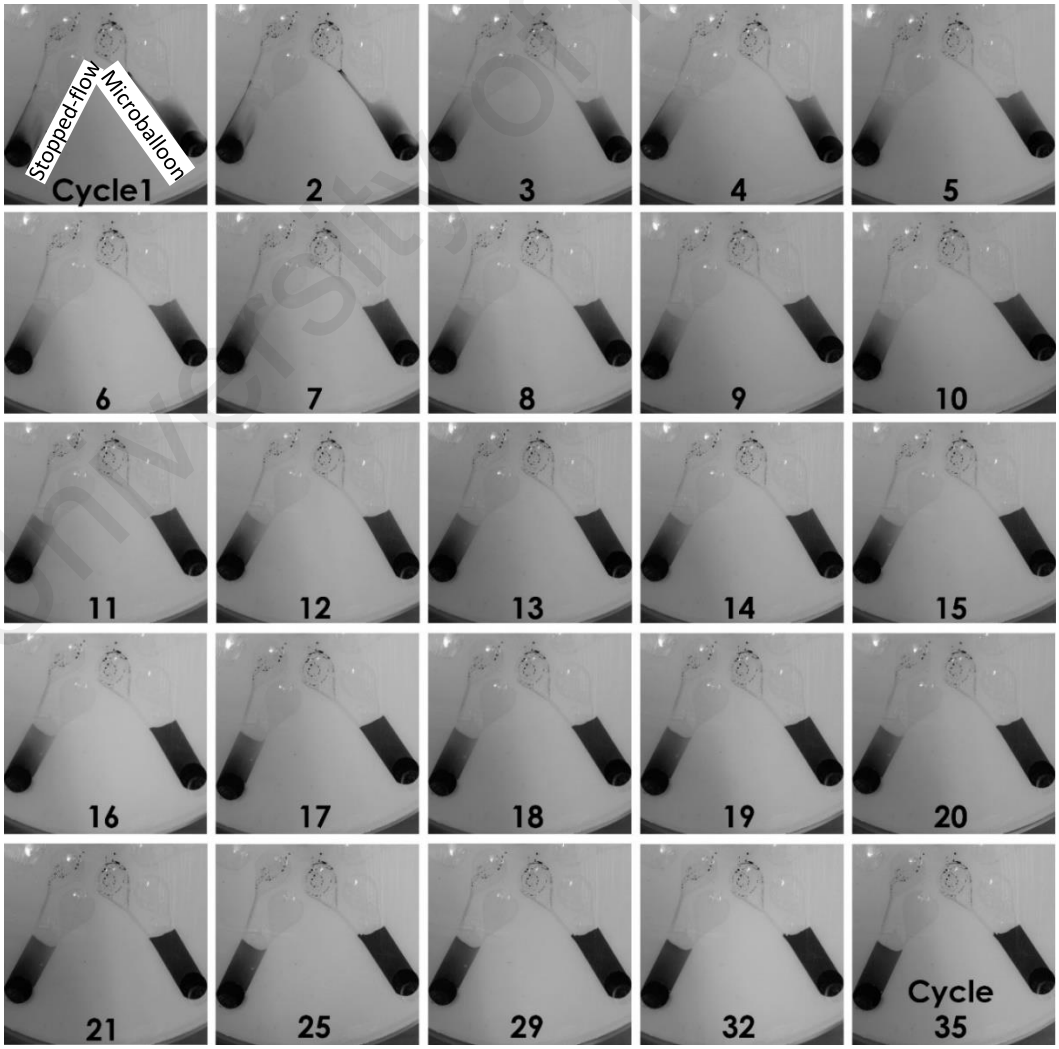

Figure 4.4: Images captured after each stopped-flow and microballoon mixing cycle.

The mixing efficiency of the liquid manipulation progress was evaluated by analyzing a series of images captured after each mixing cycle (see Figure 4.4). All images were converted and saved into 8 bit gray scale bitmaps. The section of each image that represented the mixing area was converted to an intensity histogram to measure the uniformity of the gray-scale distribution in the mixing region. The microballoon and stopped-flow mixing efficiencies under the same spinning profile are compared and the results are presented in *Section 4.4.1*.

4.3.3 ELISA in CD-Like Well Plate

Conventional colorimetric ELISA assay for the colorimetric detection of dengue virus was implemented in CD-like well plates of Design E (see Figure 4.2B). In order to assess the effect of mixing techniques on ELISA detection signal, sequential mixing cycles were applied during the assay incubation periods. During the assays incubation periods five complete mixing cycle per each three minutes was conducted. In each mixing cycle, the rotational frequency was increased to 1650 rpm with the acceleration of 1200 rpm s^{-1}, and the CD-like wells were stopped after 5 seconds of rotation. Two different mixing systems in the CDs were applied during the ELISA assay: 1) liquid mixing through ballooning action; 2) liquid mixing via stopped-flow technique. As a standard reference, conventional ELISA test was performed under the same assay protocol.

Dengue virus was used as an antigen for the ELISA assay. Dengue virus propagation in mosquito cells and titration procedures are provided in Appendix A. Microfluidic disks and micro-titration 96 well plate (SPL, life science) were filled with purified dengue virus (NS1) solution and incubated for 2 hours at 37°C. Dengue virus solution of 3.5×10^4 p.f.u/ml was prepared through serial dilution of purified dengue virus (NS1) in a coating buffer. The coating buffer was prepared by mixing 0.85 g of NaCl, 0.14 g of Na_2HPO_4, 0.02g of NaH_2PO_4 and 100 ml of PBS. Mixing chambers and well plate were charged with 200µl of AG solutions (n = 8-12), and incubated for 2 hours at

37°C. Between each step of the assay, the mixing chambers and 96 well plate were washed with PBS buffer (200 µl per chamber). Washing procedure was performed three times and each time for duration of 5 minutes in room temperature.

Blocking step was conducted to prevent non-specific binding to the active available sites, which may reduce the sensitivity of detection. Blocking buffer was prepared by adding 1 g of BSA into 100 ml of 0.05% Tween 20 in PBS and each chamber was charged with 200 µl of blocking buffer for 1 hour (37°C). After repeating the washing procedure, chambers and wells were filled with 200 µl of primary antibody against dengue virus 2 (Santa Cruz US, ICL2: sc-65725), which were diluted (0.2%) in an antibody dilution buffer. Antibody dilution buffer was prepared by mixing 36ml DI water, 4ml 10X PBS and 0.4g BSA and then adding 120 Ml Trintox-100 to the solution, under stirring condition. After 1 hour incubation at 37°C. The 96 well plate and the microfluidic disks were again washed for three times.

Secondary antibody, A1418 SIGMA, labeled with Alkaline Phosphatase (ALP), was diluted with antibody dilution buffer (2:1000). Each mixing chamber and well was charged with 200 µl of diluted IgG antibodies and incubated at room temperature. After half an hour, cells were washed out and 100 µl of ALP substrate (50% Substrate A+50% Substrate B) was charged in cells. After 20 minutes, once the transparent liquid turned to blue liquids from the mixing chambers were transferred into a new well plate, and then both well plate was transferred to the ELISA reader (Bio-Rad Model 680). The detection signal was then obtained using the micro-plate reader (at an absorbance of 570 nm).

4.3.4 Microballoon Mixer Calibration

This section theoretically describes the liquid level in a mixing chambers as a function of rotational frequency, and the maximum required rotational frequency to reduce the liquid level to the top of a microballoon. In general, the rotational frequency corresponding to the level of liquid in the mixing chamber can be described in terms of

an equilibrium present between the kinetic energy stored in the expanded microballoon and the centrifugal pressure. However, because of the difference between the geometry of the mixing chambers (Design D and E) and the chambers of Design A-C, new equations are required to evaluate liquid movement in the microballoon mixers. The maximum rotational frequency is defined when the rotational frequency increases as much as the liquid level in the mixing chamber reaches the top of the microballoon (see Figure 4.3).

The microballoon expansion volume during the spinning of the disc is equal to the change of the liquid volume in the mixing chamber. If the cross section area of the mixing chamber is denoted as *S* and microballoon expansion volume as *V*, the microballoon expansion corresponding to the changes of the liquid level in the mixing chamber is:

$$V = S(R_C - R_0) \text{ or } V = \frac{2\pi r_{mb}^2}{3} z \tag{4.1}$$

where r_{mb} is the initial radius of the microballoon, z is the height of the bulged microballoon, R_0 and R_c are corresponding liquids level in the mixing chamber when the platform is stopped and spun at the maximum required frequency of rotation, respectively. Stored kinetic energy in the expanded microballoon that is denoted with liquid volume of $S(R_c - R_0)$ is expressed in terms of bulged height of z ,which is:

$$z = \frac{3}{2\pi r_{mb}^2} V = \frac{3(R_C - R_0)}{2\pi r_{mb}^2} S \tag{4.2}$$

and the energy stored in the microballoon expanded can be described as microballoon bulge pressure (Hohlfelder, 1999; M. J. Madou, 2002):

$$P_{mb} = C_1 \frac{Mtz^3}{r_{mb}^4} + C2 \frac{\sigma_0 tz}{r_{mb}^2} \tag{4.3}$$

where C_1, C_2 are constants and M is the biaxial modulus of elasticity defined by $E(1- v)$ (E and v are the Young's modulus of elasticity and Poisson's ratio, respectively), t is the

thickness of the latex of the microballoon and σ is its initial stress. The kinetic energy stored in a bulged microballoon is generated from the centrifugal pressure that is based on the liquid density, rotational frequency, liquid length and distance from the center of the platform. Centrifugal pressure that acts on the liquids as well as the microballoon is expressed as follows:

$$P_c = \rho\omega^2 \Delta r \bar{r} \tag{4.4}$$

where ρ is the liquid density, ω is the rotational frequency of the spinning platform, Δr is the average distance of the liquid in the mixing chamber from center of the platform and $\bar{r}$ the radial length of the liquid. The density of the liquid is assumed to be constant and the changes of rotational frequency and the parameters related to the liquid position (Δr and $\bar{r}$) determine the amount of centrifugal pressure. The store kinetic energy of the microballoon in all states is proportional to the centrifugal pressure P_c=P_{mb}. Therefore, rotational frequencies corresponding to the changes of the liquid level in the mixing chamber can be yielded from equations 4.3 and 4.4 as follows:

$$\omega = \sqrt{\left(C_1 \frac{Mz^2}{r_{mb}^2} + 2C_2\sigma_0\right)\left(\frac{tz}{\rho \Delta r \bar{r} r_{mb}^2}\right)} \tag{4.5}$$

and maximum rotational frequency at which liquid level is reduced to R_c or when $\bar{r} = 2r_{mb}$ yield as :

$$\omega_{Max} = \sqrt{\left(C_1 \frac{Mz^2}{r_{mb}^2} + 2C_2\sigma_0\right)\left(\frac{tz}{2\left(\rho \Delta r r_{mb}^3\right)}\right)} \tag{4.6}$$

Employing Equation 4.5, the rotational frequencies corresponding to the change of radial length of liquid ($\bar{r}$) from R-R_0 to R-R_c was measured. In order to test the accuracy of Equation 4.5 and 6 in predicting liquid levels corresponding to rotational speeds, theoretically calculated values were compared with experimental data and the results are presented in *Section 4.4.3*. Value of the parameters used for the evaluation of Equation 4.5 and Equation 4.6 are listed in Table 4.1.

Table 4.1: Value of parameters used in theoretical analysis.

Parameters	Value	**Parameters**	Value
rmb	4 mm	**E**	3.2 MPa
R	56 mm	**ν**	0.48
R0	34 mm	**σ0**	0.55MPa
ρ	1000 kg/m3	**t**	136 µm
C1	8/3	**C2**	2

4.4 Results and Discussions

4.4.1 Microballoon Mixing in Tiny Chamber

Microballoon mixers in a similar fashion to stopped-flow mixing enables the efficient usage of the limited space of CD microfluidics. When the spinning speed was increased, the induced centrifugal pressure transferred the liquid from the high aspect ratio chamber (mixing chamber) into the microballoon. The high angular acceleration used, created a large magnitude of Euler force. The Euler force acting on the liquids generates vortices that pushes the liquid samples to the opposite direction of the disk rotation, enhancing the mixing efficiency (Grumann et al., 2005; Y. Ren & Leung, 2013b). Thereafter, the spin rate is reduced to zero with the same acceleration, therefore direction of liquid flow and Euler force were reversed. Because of the high hydraulic resistance of the chamber and the high elasticity of the microballoon the system acted as a large tank that was emptied via a leakage. The ratio of the cross-sectional area of the mixing chamber to the microballoon area is ~ 0.9% in Design D. Hence, after each mixing cycle the platform was stopped for ~ 0.5 seconds to allow for the complete relaxation of the microballoon. In addition, considering the liquid exchange between the microballoon and the ultra-thin chamber, it is gleaned that the mixing progress can be also enhanced due to the effects of liquid flowing in periodically converging-diverging passages (A1 Yong & A1 Teo, 2014; Jafari, Farhadi, & Sedighi, 2014).

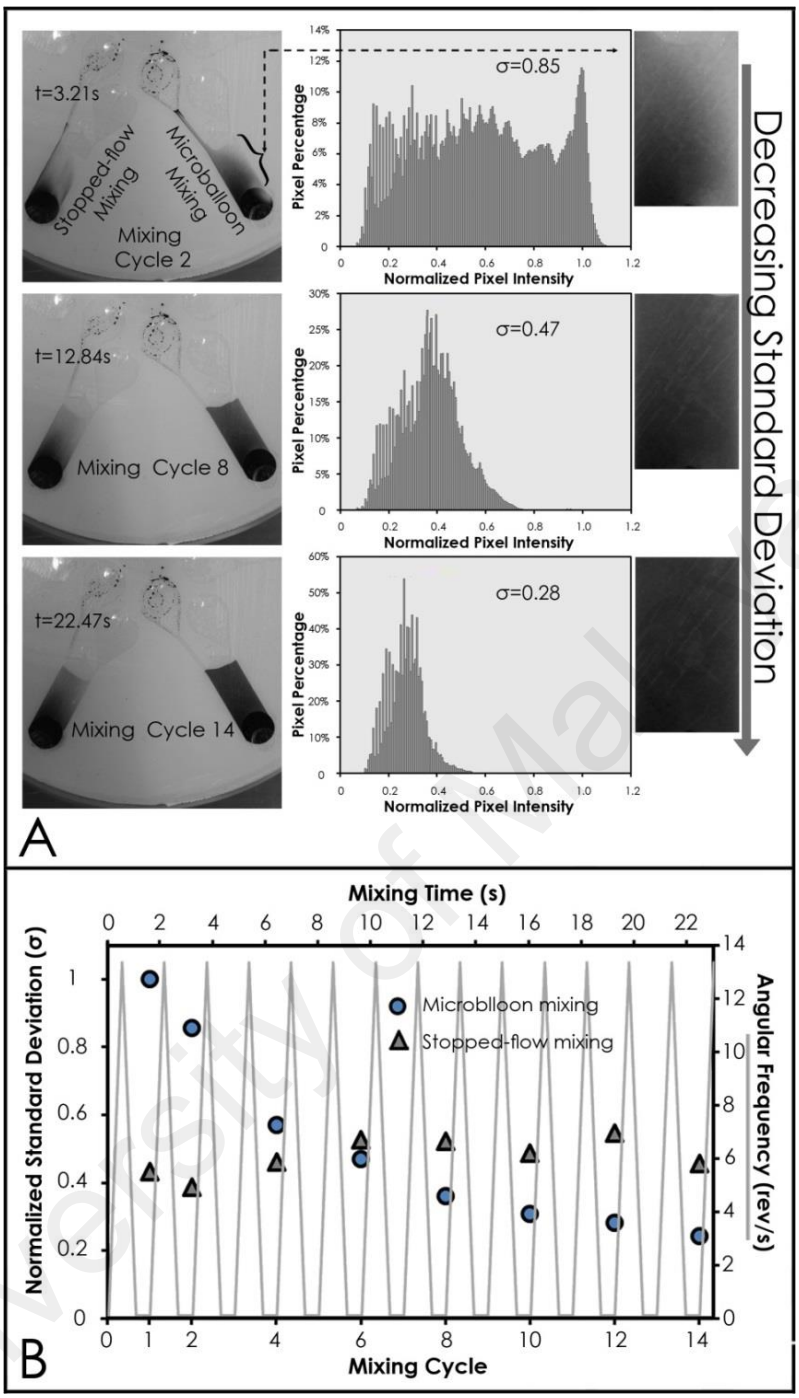

Figure 4.5: Gray color intensity histograms for evaluating the microballoon mixing efficiency.

Figure 4.5B shows the state of mixing progress after each mixing cycle demonstrated in Figure 4.4. The standard deviation obtained from the histogram was normalized according to the first microballoon mixing cycle. Shown in Figure 4.5A, distribution of pixels in the 2D-histogram which corresponded to the second mixing cycle does not flow a normal distribution, however the decreased standard deviation indicates changes in the state of mixing. Through further mixing cycles, distribution of pixel

intensities became more uniform and shifted toward the gray-scale color (see Figure 4.5A). This may be gleaned from the histograms in Figure 4.5A, showing a Gaussian distributions and the narrowing of peak width in the histograms corresponding to the eighth and fourteenth mixing cycles. Therefore, as shown in Figure 4.5B, standard deviation (σ) decreases in tandem with increasing number of efficient mixing cycles. For the experimental evaluation, mixing time at which standard deviations for both applied techniques stabilized below 0.3 are compared. As a reference, constant spinning mode (i.e. diffusional mixing) took 170 min to mix the 12 µl liquid samples. Excluding the pause times required for microballoon relaxation, stopped-flow mixing reduce the mixing time to 37.45 seconds via 35 mixing cycles. The best performance was achieved by the microballoon mixing technique, reaching a mixing time of 22.5s via 14 mixing cycles (see Figure 4.4 and 4.5).

In the case of stopped-flow mixer, the low standard deviation during the early stages of mixing progress is due to the uniformity of white color (see Figure 4.5B). As more mixing cycles is applied, the standard deviation fluctuated until cycle twelve in which the liquid color uniformly turned to gray and standard deviation continuously decreased. It has been reported that the optimum mixing in stopped-flow has been achieved via acceleration of 1920 rpm s^{-1} (Grumann et al., 2005). The Increase of acceleration/deceleration rate may intensify vortices and further improve the mixing efficiency; however the maximum angular acceleration of the spinning system used in this study is 1500 rpm s^{-1}. At low accelerations, where stopped-flow mixing becomes less effective, microballoon provides a high mixing efficiency similar to pneumatic based flow-reciprocating technique and converging-diverging passages.

4.4.2 ELISA in CD-Like Well Plate

The enhancement of the dengue virus detection signal was investigated on different substrates in CD-like well plates by using the microballoon mixing technique and the

result are presented in Figure 4.6. In order to demonstrate the cross-reactions due to the host cell proteins, the cell supernatant of non-infected cells was used as a negative control in the ELISA assay. The comparison of the positive and negative control values demonstrates the low cross-reactivity in the assay. A generally accepted approach in biomolecule immobilization relies on heterogeneous interaction between biomolecules and plastic surface. As it can be seen from Figure 4.6, the microballoon mixing procedure resulted in significantly higher detection signals when compared to stopped-flow mode mixing (regardless of the background in the ELISA experiment). The dramatic difference in the results corresponds to the type of mixing technique used in the disk. Results indicated that, 3D reciprocating flow by the ballooning action provides a higher interaction of the antigen and the surface (and the subsequent proteins attachment) compared to advective currents induced by the stopped-flow mixing technique (see Figure 4.6). This is in a direct agreement with analytical results of the mixing efficiency presented *Section 4.4.1*.

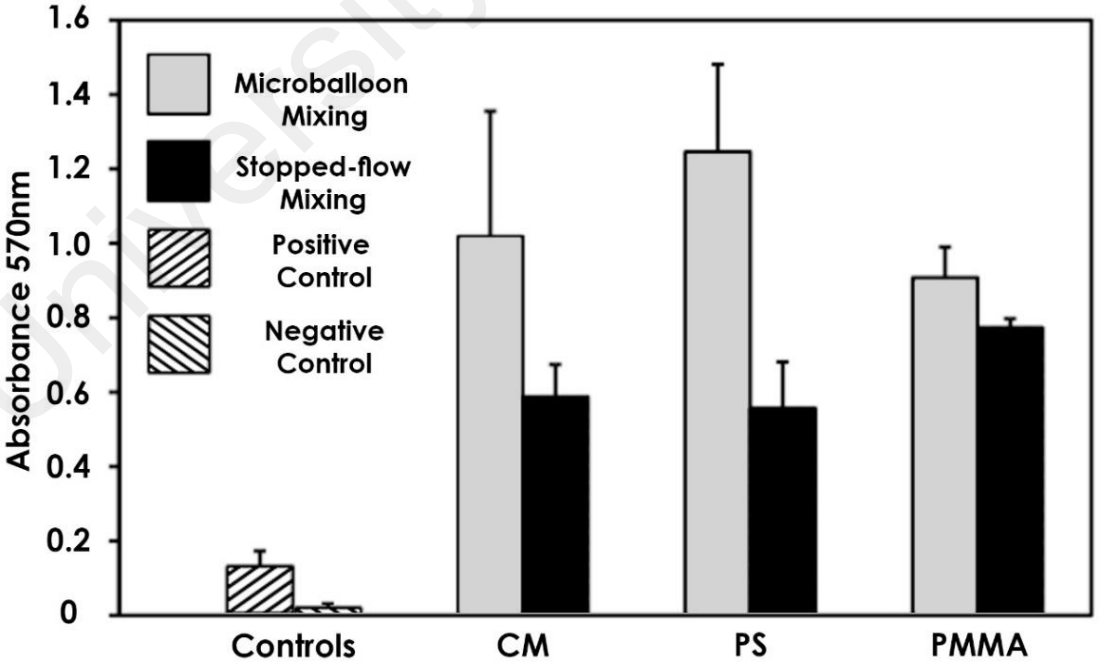

Figure 4.6: Biosensing enhancement of 3.5×10^4 p.f.u/ml NS1 in CD-like well plates using microballoon and stopped-flow mixing methods.

It is well known that proteins (or other biomolecules) have high sensitivity toward interactions with solid surfaces (Hosseini, Ibrahim, Djordjevic, & Koole, 2014). In this research only pure and non-functionalized polymeric platforms, which are used commercially to produce a variety of biosensor devices (CM, PMMA and PS), are investigated to assess the performance of the centrifugal microfluidic platforms. Possibly the most common application of those plastic materials is the production of the ELISA 96 well plates on industrial scales. Although the cellulose membrane cell has dramatically higher hydrophilicity in comparison to the other cells (PMMA and PS), results indicates that the highest detection signal was obtained from the PS cells. PMMA cells have also shown the enhanced detection signal by mixing technique, however relatively lower detection signal was generated when compared to the PS.

It is important to note that the protein attachment is not only dependent on hydrophilicity of the surface. Surface morphology and chemistry also play a crucial role at the biomolecule/plastic interface. From our results, it is obvious that cellulose membranes have adverse effect on antigen activity in comparison to flat surfaces of PMMA and PS (see Figure 4.6). The possible reason for such affinity is the higher specific surface of membranes with inter-connected fibrous morphology. For that reason antigens molecules can be trapped inside such a structure and lose the activity due to the steric interaction.

Despite the fact that the CD detection cells have been designed with a relatively similar volume as the wells of ELISA 96 well plate, it can be clearly seen form Figure 4.6, which the conventional method (ELISA or positive control) has resulted in a significantly lower intensity of detection signal. For that reason our results prove that our established microballoon mixing method can significantly enhance the detection signal of the dengue virus.

4.4.3 Microballoon Mixer Calibration

In order to facilitate the future prospect for the implementation of microballoon mixers in centrifugal microfluidic platforms, spin rate required in a mixing cycle is theoretically discussed and presented as Equation 4.6. Figure 4.7 shows the liquid levels in the mixing chamber corresponding to the rotational frequency measured with Equation 4.5. In the figure, the maximum rotational frequency calculated by Equation 4.6 is compared with the experimentally measured spinning speed of 810 rpm in design D i.e., when liquid level inside the mixing chamber reduced to the top of the microballoon. Comparing the theoretical graph with recorded liquid levels indicates the accuracy of ~ 91% and 86% for Equation 4.5 and 4.6 to the predicted levels. Note that, at the spinning speed of 810 rpm, a centrifugal pressure of ~3 KPa is induced that can be easily tolerated in our design. However, the latex high elasticity allows for withstanding dramatically higher centrifugal pressure that avoids CD delamination at high spinning speeds. For supplementary use of the same mixing system for the pumping of mixed liquids (for siphoning), Equation 4.5 which allows controlling liquid levels via rotational frequency is introduced.

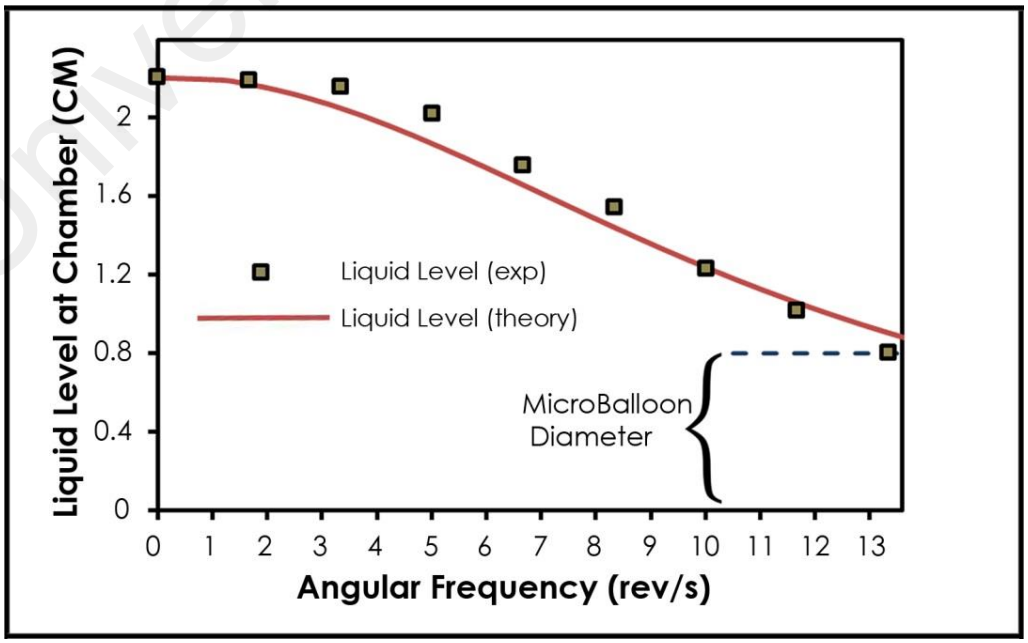

Figure 4.7: Liquid levels inside the mixing chamber corresponding to the rotational frequency (values measured for Design D).

Microballoon mixing similar to reciprocating flow enables pumping liquids toward the center of disk. As demonstrated in *Chapter 3*, microballoons are able to move large volume of liquids at lower range of rotational frequency compared to pneumatic based techniques (Aeinehvand et al. 2014). Therefore, 3D reciprocating flow by microballoons is expected to enhance the mixing efficiency at lower speeds and address the often noticed problem of CD delamination in the pneumatic flow reciprocation that occurs because of spinning high sample volumes at high spinning speeds.

4.5 Conclusions

The work presented in this Chapter offers a new method of mixing liquids on centrifugal microfluidic platforms. The microballoon mixer generates a periodical 3D reciprocating flow that accelerate mixing progression. The converging-diverging passage produced during the liquid exchange between the microchamber and the microballoon improves the mixing efficiency up to 40% compared to the stop-flow mixing method which is mainly based on Euler forces. The small space used on the disc for the control over the reciprocating flow and the operation at low rotational frequencies without any external power sources make microballoon mixer an attractive option for a wide range of applications. Details of comparison between technical aspects of microballoon and previously developed mixers is listed in table 4.2.

Table 4.2: Comparison between microballoon and previously developed mixers.

Mixer	Operational mechanism	Operational spin speed	Max acceleration	Mixer capacity
Microballoon	Passive	1650 rpm	*1500 rpm/s	200 μl
Batch mode	Passive	60 rpm	1920 rpm/s	-
Reciprocating flow	Passive	7500 rpm	-	25μl
External pneumatic	Active	1500	-	-

*Microballoon mixers operate at lower accelerations, in ELISA experiments accelerations of 1500 rpm/s was used to enable batch mode mixing in parallel with microballoon mixing.

In this study the effect of microballoon mixer in the detection of dengue virus was investigated. The results indicate that the mixing technique can dramatically enhance biomolecules reaction rates and therefore increases the detection signal of dengue virus. In general, the microballoon mixer facilitates the development of portable and low power consuming platforms for the integration of various bioanalytical applications including those involve the manipulation of large liquid volumes e.g., detection of rare circulating tumor cells.

CHAPTER 5: REVERSIBLE THERMO-PNEUMATIC VALVING ON CENTRIFUGAL MICROFLUIDIC PLATFORMS

5.1 Introduction

Centrifugal microfluidic systems utilize a conventional spindle motor to automate parallel biochemical assays on a single microfluidic disk. The integration of complex, sequential microfluidic procedures on these platforms relies on robust valving techniques that allow for the precise control and manipulation of fluid flow. The ability of valves to consistently return to their former condition after each actuation plays a significant role in the real-time manipulation of fluidic operations. This Chapter presents an active valving technique that operates based on the deflection of a latex film with the potential for real-time flow manipulation in a wide range of operational spinning speeds. The reversible thermo-pneumatic valve (RTPV) seals or reopens an inlet when a trapped air volume is heated or cooled, respectively. The RTPV is a gas-impermeable valve composed of an air chamber enclosed by a latex membrane and a specially designed liquid transition chamber that enables the efficient usage of the applied thermal energy. Inputting TP energy into the air chamber deflects the membrane into the liquid transition chamber against an inlet, sealing it and thus, preventing fluid flow. From this point, a centrifugal pressure higher than the induced TP pressure in the air chamber reopens the fluid pathway. The behaviour of this newly introduced reversible valving system on a microfluidic disk is studied experimentally and theoretically over a range of rotational frequencies from 700 RPM to 2500 RPM. Furthermore, adding a physical component (e.g., a hemispherical rubber element) to induce initial flow resistance shifts the operational range of rotational frequencies of the RTPV to more than 6000 RPM. An analytical solution for the cooling of a heated RTPV on a spinning disk is also presented, which facilitates the future development of time-programmable RTPVs. Moreover, the reversibility and gas-impermeability of the RTPV in the microfluidic networks are validated on a microfluidic disk designed for performing liquid circulation. Finally, an

array of RTPVs is integrated on a microfluidic cartridge to enable sequential aliquoting for the conversion of dengue virus RNA to cDNA and the preparation of PCR reaction mixture.

5.2 Literature Review

LOC devices utilize microfluidic elements such as pumps, mixers, and valves to miniaturize large laboratory machine functions onto small silicon or plastic substrates (Whitesides, 2006). A subcategory of LOC devices is the microfluidic disk, also known as Lab on a Disc (LOAD), which utilities pseudo forces during spinning to manipulate liquid flow within the microfluidic networks. The generated centrifugal force enables automatic parallel processing of intricate tasks on a single platform with no need for external pressure generating pumps (Abi-Samra et al., 2013; Burger & Ducrée, 2012; Park et al., 2014; Roy et al., 2015a; van Oordt et al., 2013). The arrangement of various microfluidic elements on a disk is usually designed with respect to the sequence of fluidic steps in an analytical assay. The assay on the disk is then controlled through different valving techniques and spin profiles (Nwankire, Chan, et al., 2013; Nwankire et al., 2014). Some of the challenges regarding valving on microfluidic disks are limited operational range of rotational frequencies, lack of versatility, and low reliability (Gorkin III et al., 2012; Robert Gorkin et al., 2010).

The performance of centrifugal microfluidic systems strongly depends on the ability of the passive and active valving technique present to control liquid retention and flow. Passive valves prevent flow based on surface tension or a physical gating mechanism and can be actuated using a variation in the spinning speed (Burger, Kitsara, Gaughran, Nwankire, & Ducrée, 2014; Godino et al., 2013; Kitsara et al., 2014; Nwankire, Donohoe, et al., 2013). As an example, Centrifugo-pneumatic valves utilize trapped air to prevent liquid from flowing into ventless chambers (Godino et al., 2013; Oliver Strohmeier et al., 2014). To enable the use of CP valves for a wide range of

applications, Gorkin III et al. (2012) utilized a DF as the secondary flow barrier to form similar trapped air pockets at any desirable point in the fluidic pathway. The CP valve and the DF valve are single-use valves and are unable to stop further liquid flow after the valve has been opened. Hwang et al. (2011) developed the elastomeric valve, a reversible passive valve whose closure depends on weak adhesive forces between PDMS and polycarbonate. Elastomeric valves can retain higher volumes of liquid only at low centrifugal pressure. Because it is a physical barrier that must be continuously opened by liquid pressure in order for the liquid to pass, the valve may not open if a small volume of liquid does not provide sufficient hydrostatic pressure.

Unlike passive valves, active valves can be opened or closed by external power sources (T.-H. Kim et al., 2013; L. X. Kong et al., 2014; Swayne et al., 2015). For instance, laser irradiated ferrowax microvalves and optofluidic valves are opened by focusing a heat or laser source on the sacrificial valves (Garcia-Cordero, Kurzbuch, et al., 2010; Park et al., 2007). Valves that use sacrificial barriers granted more robust and precise control of flow on disk. However, valving technologies that are reversible, (i.e., able to switch between open and closed states), make a more sophisticated and flexible flow control system. To this end, Cai et al. (2015) recently developed a magnetically actuated valve with an operating range of rotational frequencies from 800 to 1600 RPM. The magnetically actuated valve was composed of a PDMS membrane with a ball spacer on top of it, a pair of magnets (one located at the bottom of the disk and one on the top of the ball spacer), and a flyball governor for mechanically adjusting the distance between the magnets (Cai et al., 2015). At low rotational frequencies, the attraction force between two magnets deflected the membrane into the chamber and completely blocked a fluidic pathway. At higher speeds, the centrifugal force overcame the weight of the flyballs, increasing the distance between the magnets and opening the fluidic path. The distance-dependent interactions between multiple magnet pairs and their physical size limited the

number of this valve that can be embedded in a disk. Moreover, the bulky and mechanically complex actuation system used in this technique prevents the integration of other hardware components potentially needed for other on-disk processes. Therefore, complex centrifugal microfluidic processes still demand the development of simpler, reversible valving systems that enable flexible and real-time control of flow.

Develop latex microballoon pump and mixer operate without the need for surface modification, high spinning speeds, or high accelerations. However, the current chapter demonstrates an additional utility of the latex film by incorporating it into reversible, gas/liquid-impermeable microvalves designed for precise on-disk control of liquid and TP energy flow. To this end, I have developed the reversible thermo-pneumatic valve (RTPV) which is a real-time valving mechanism based on the thermal expansion or contraction of air trapped in the system and the deflection of a latex elastic membrane (i.e., microballoon). In this newly introduced valving mechanism, microfluidic pathways are closed by applying heat and reopened using a centrifugal pressure higher than the produced TP pressure.

As a normally-open valve that requires heat to be closed, the RTPV is therefore a suitable valving solution in temperature-controlled assays such as PCR and Loop mediated isothermal amplification (LAMP). Here, the RTPV mechanism is investigated experimentally and theoretically in a range of rotational frequencies up to 2500 RPM. Moreover, the cooling process of heated spinning disks is analysed to enable precise timing of the RTPV's actuation with various cooling spinning speeds. Furthermore, an application of the RTPVs for continuous flow circulation was demonstrated to verify gas-impermeability and reversibility of the valve as well as its ability to control liquid and gas flow in complex microfluidic structures. Finally, RTPVs and microballoon pump/mixer are integrated in a microfluidic cartridge to automate a fluidic procedure required for multiplexing of temperature-controlled assays. As a pilot study, the cartridge is used for

sequential aliquoting to prepare multiple separated PCR reaction mixtures for the detection of dengue virus.

5.3 Materials and Methods

5.3.1 Reversible Valving Concept and Mechanism

The mechanism of the newly introduced valving system is based on the deflection of an elastic membrane (latex membrane) that can reliably close and reopen a fluid inlet that is perpendicular to the membrane. The valve, shown in Figure 5.1a, consisted of a U-shaped transition chamber (i.e., composed of an inlet and an outlet for liquid flow), a latex membrane, and a ventless air chamber adjacent to the latex membrane to receive thermal energy. The membrane deflects when the ventless air chamber receives thermal energy and reverts back as the air chamber cools down to room temperature. Hence, the physical components capable of this phenomenon are collectively named the RTPV.

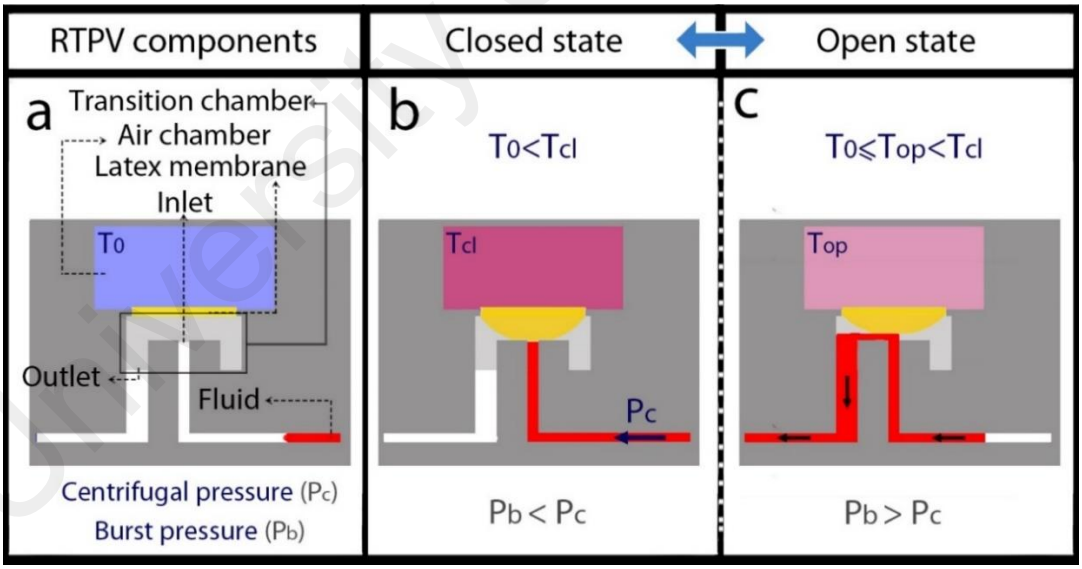

Figure 5.1: Schematic illustration of the mechanism of the reversible thermo-pneumatic valve (RTPV).

The membrane deflects into the transition chamber and pushes against the entrance of the perpendicular microchannel (inlet) to prevent fluid flow when the air chamber is heated (see Figure 5.1b). For the valve to open during spinning, the hydrostatic pressure must overcome the induced TP pressure. An optimal spinning speed can generate

sufficient centrifugal force to achieve the required hydrostatic pressure while performing passive cooling (see Figure 5.1c).

5.3.2 Microfluidic Designs and Fabrications

Three microfluidic platforms were created: Design F for the theoretical and experimental evaluation of the RTPV mechanism, and other designs (Design G and Design H) for demonstrating different applications of RTPVs on microfluidic platforms. Design F was first implemented to assess the RTPV behaviour from the closed to the open state as a function of the air chamber surface temperatures at various rotational frequencies (see Figure 5.2a). The same design was also used to theoretically and experimentally analyse the cooling of a heated spinning disk. Design F consists of a source chamber, an RTPV and a destination chamber. It is a seven-layer disk made of three PMMA disks, three PSA layers, and a latex film (See Figure 5.2b). Layer i is a PMMA disk that contains the loading/vent holes, engraved microchannels, source chamber, and destination chamber. Layer ii is an adhesive film with cut-outs in the shape of the source/destination chambers and through-holes. Layer iii is a PMMA layer with the transition chamber, and layer iv is PSA with a cut-out in the shape of the deflecting latex membrane. Layer v is a featureless, transparent, and elastic latex film. Layer vi is similar to the fourth layer, which is a PSA with a cut-out in the shape of the deflecting latex membrane, and layer vii is a PMMA disk with the engraved air chamber.

Design G is a microfluidic system specifically designed for continuous circulation and switching of two liquid samples (see Figure 5.3a). Design G was used to test the valve's reversibility, gas-impermeability, and ability to control the direction of the TP energy propagation in complex fluidic networks. The design is composed of two RTPVs, two sets of TP pumps, and two S-shaped microchannels cut out in two different PSA layers of the disk.

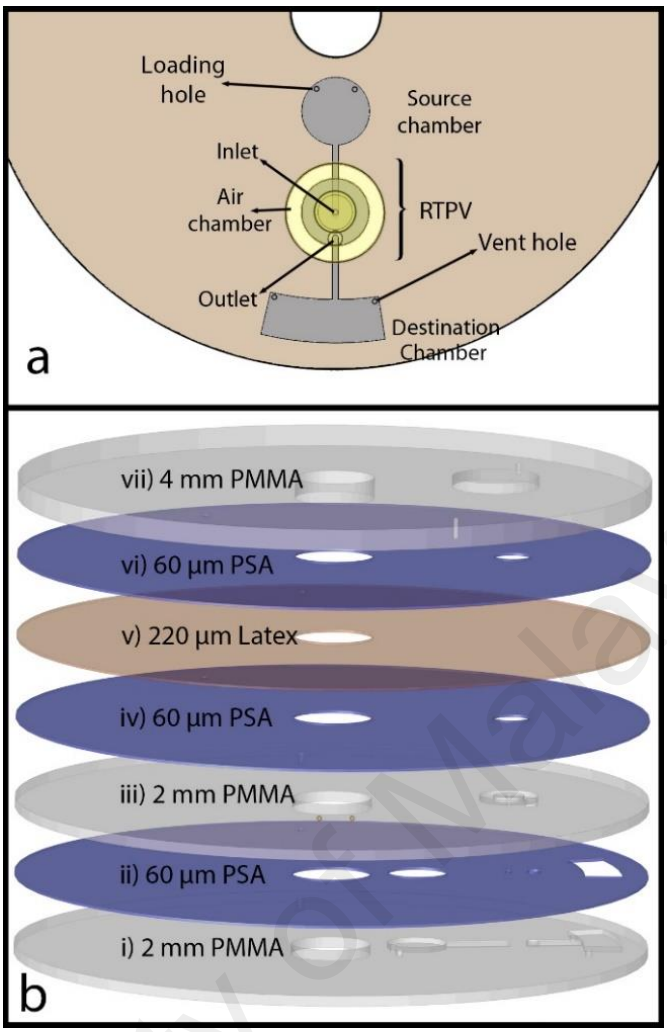

Figure 5.2: Microfluidic disk Design F was used to assess the RTPV mechanism.

The breakdown of the eleven-layer CD Design G is shown in Figure 5.3.b. Layer i is a PMMA disk with vent and loading holes. Layer ii is PSA layer with cut-outs in the shape of the loading and destination chambers and one of the two S-shaped microchannels connecting the destination chamber (right) to the loading chamber (left). Layer iii is a PMMA disk with loading and destination chambers and engraved micro-channels. Layer iv is a PSA layer with the vertically reflected features of layer ii and additional cut-outs in the shape of the inlet and outlet. Layer v is PMMA disk with the transition chambers and two through-holes to connect the upper layer air chambers to the lower layer destination chambers. Layer vi is a PSA with cut-outs matching the shapes of the elastic membranes and the through-holes. Layer vii is a featureless latex film and Layer viii is a PSA with cut-outs and through-holes similar to the layer vi. Layer ix is a PMMA disk

with cut-outs in the shapes of the ventless air chambers used for RTPVs and TP pumps. Layer x is a PSA with cut-outs in the shapes of the ventless air chambers similar to layer ix and layer xi A featureless PMMA layer that seals the air chambers from the top side of the disk. It should be noted that the top three layers could be replace by a thicker PMMA layer with engraved air chambers, but in that case, the engraved features could reduce the optical transparency of the disk. The air chambers near the centre are used to generate TP energy for valving purposes and the other two are used for pumping liquids.

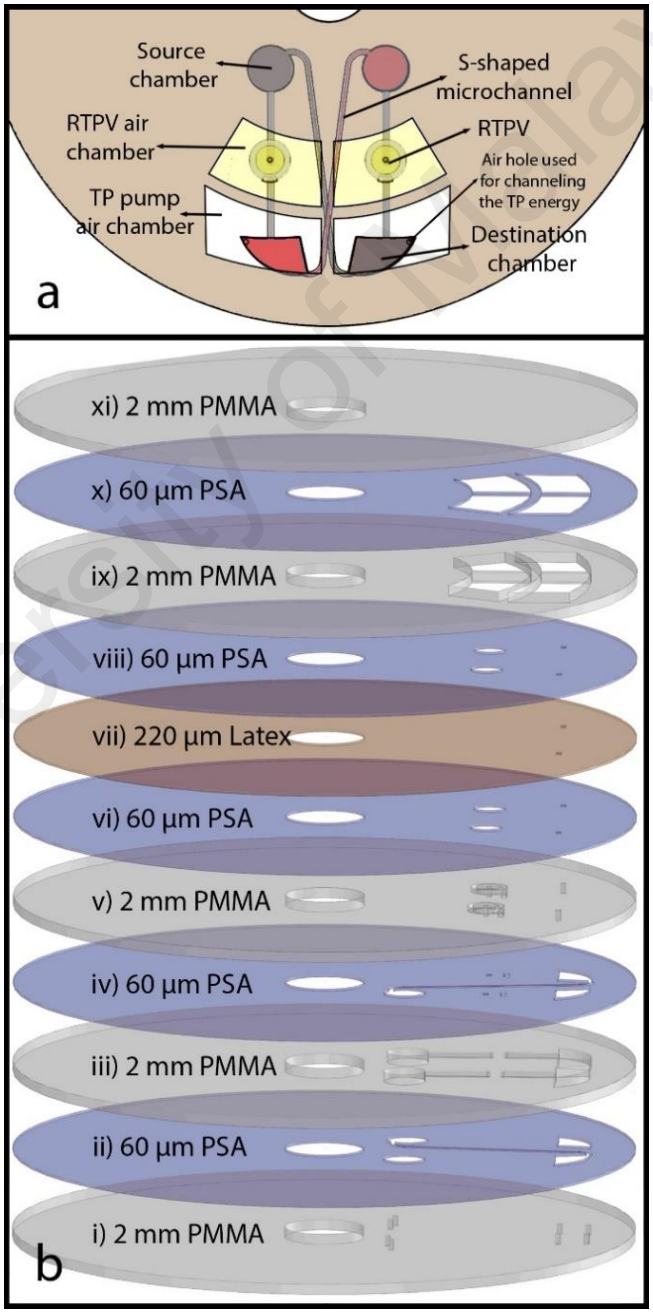

Figure 5.3: Microfluidic disk Design G is used for the continuous circulation and switching of two liquid samples.

Design H is a reusable microfluidic cartridge created for the conversion of dengue viral RNA to cDNA and the preparation of PCR reaction mixtures through the sequential aliquoting of the corresponding reagents into reaction chambers (see Figure 5.4a). Fluidic components and the breakdown of the eleven-layer cartridge, which consists of five PMMA layers, five PSA layers, and a latex film, are demonstrated in Figure 5.4b. The cartridge consisted of five PMMA layers, five PSA layers, and a latex film with a similar arrangement as Design G.

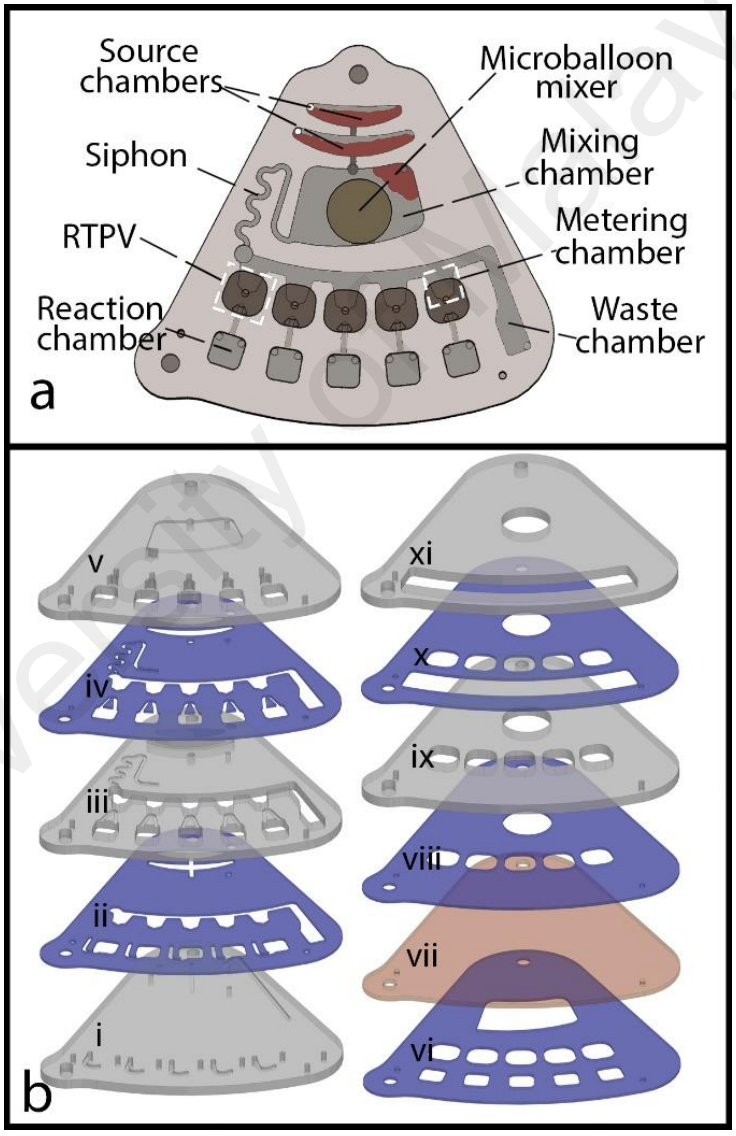

Figure 5.4: Microfluidic platform Design H is a cartridge used for preparation of PCR reaction mixture through sequential aliquoting.

Details of the experimental setup and the fabrication procedure of microfluidic CDs are available in *Section 3.3.3*. Briefly, the microfluidic platforms, are fabricated by

the manual assembly of transparent PMMA layers (2 mm thick), PSA (~60-100 μm thick), and a latex film (~220 μm thick). The micro-features were machined into the PMMA and PSA disks using the CNC and cutter plotter machines, respectively.

5.3.3 Heating Setup

A heating system used in this study is composed of a Bosch GHG 630 DCE modified industrial grade heat gun and an infrared thermometer (Smart Sensor AR550). The heat gun had a built-in digital temperature controller, which can produce air at any temperature between 50 and 500 °C. The air heat gun had to be adjusted to significantly higher temperatures than the desired constant platform temperature. The details of the heating profile of a spinning disk with a similar thickness to that of Design F were reported previously (Thio, Ibrahim, et al., 2013). The air heat gun temperature setting can be changed in steps of 10 °C, and such a heating rig does not provide a precise control over temperature of the spinning disk. Hence, the valve's actuation temperature was evaluated during a ramped cool-down of the disc.

5.3.4 RTPV Experimental Procedure

Although the air chamber adjacent to the latex membrane is ventless, a through hole was machined into the top PMMA layer and sealed just before the experimental procedure to prevent any pressure build up during the fabrication process. Then, 70 μl of coloured DI-water was dispensed into the source chamber. The experiment was initiated by spinning the disk and then heating the radial region of the valve while its surface temperature was continuously monitored. The rotational frequency was kept below 500 RPM (i.e., the average burst frequency of the valve at room temperature), and the surface temperature was heated until it reached 55 °C or 73 °C (for spin rates higher and lower than 2000 RPM, respectively) to make sure that the valves were closed by means of the deflection of the latex membrane. To characterize the conditions required to open the valve, the spinning speed was increased to a series of fixed rotational frequencies ranging

from 700 RPM to 2500 RPM, all of which were higher than the burst frequency. When a new, higher spinning speed was reached, the heat source was turned off and the cooling process was initiated (see Figure 5.5a). As soon as the pneumatic pressure in the valve dropped below the fixed centrifugally induced hydrostatic pressure, the valve was opened and liquid was transferred to the destination chamber (see Figure 5.5b). During the cooling process, the critical temperatures corresponding to the opening of the valve were recorded. The entire liquid volume was gradually and smoothly drained from the source chamber, possibly due to the simultaneous reduction of the centrifugal pressure and the TP pressure in the valve (see Figure 5.5c). The experiments were repeated five times, and the critical temperatures corresponding to the range of rotational frequencies were recorded.

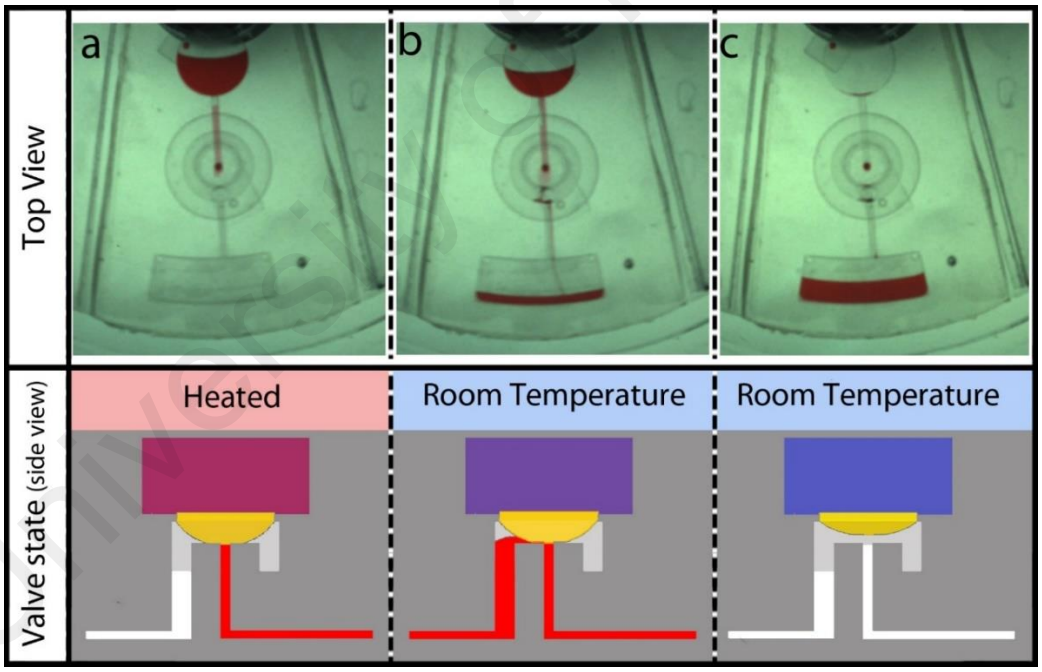

Figure 5.5: The RTPV mechanism on a microfluidic CD during changes of temperature and spinning speed.

Optimizing the spinning speed of the platform and the intensity of the heat source enabled the desired heating and cooling control of the disk, therefore allowing timing of the RTPVs' actuation. To further study and characterize cooling in the system, the times

that it took for the surface temperature of the heated spinning disk to decrease from 40 °C to 28 °C were recorded.

5.3.5 Theoretical Analysis

Characterization of the valve aids in its appropriate implementation in complex multi-step sequential assays. In this section, the RTPV actuation mechanism, which was implemented through heating and cooling on a centrifugal microfluidic platform, is theoretically analysed using the ideal gas law, the membrane deflection equation, and the equation for transient heat transfer of a freely rotating disk. The RTPV valving mechanism is characterized by calculating the valve's critical actuation temperatures and cooling time.

5.3.5.1 RTPV Actuation Temperature

When the ventless air chamber is heated, the pressure from the deflected membrane acting on the liquid inlet is equivalent to the difference between the induced *TP* pressure ΔP_{TP} and the pressure *Pm* required to deflect the membrane:

$$\Delta P_{RMV} = \Delta P_{TP} - P_m \tag{5.1}$$

According to the ideal gas law, ΔP_{TP} is given by:

$$\Delta P_{TP} = \frac{nRT}{V_{TP}} - \frac{nRT_0}{V_0} \tag{5.2}$$

where n is the number of moles, R is the ideal gas constant, T_0 and T are the temperatures at room temperature and when heated, respectively, and V_0 and V_{TP} are the volumes of the ventless air chamber at room temperature and when heated, respectively. For a known distance z between the membrane and the inlet, V_{TP} is given by:

$$V_{TP} = V_0 + V_{mb} = V_0 + \frac{2}{3}\pi r_m^{\,2} z \tag{5.3}$$

where r_m is radius of the membrane, and V_{mb} is the expanded air volume. For small value of z, where $V_0 \gg V_{mb}$, it is assumed that $V_{TP} \cong V_0$. The maximum possible value of z in

the current study is ~60 µm, and based on this, the difference between V_{TP} and V_0 is less than 0.01%. Hence, from Equation 5.3 TP pressure is given as:

$$\Delta P_{TP} = \frac{nR\Delta T}{V_{TP}} \tag{5.4}$$

The pressure required to deflect the membrane to a height z is defined by the following equation (i.e., membrane bulge equation) that is a function of the membrane's Young's modulus of elasticity E , the radius of the membrane *rm*, Poisson's ratio *v*, the thickness of the elastic membrane j, initial stress σ_0, and constants C_a and C_b (which may vary depending on the geometry of the membrane) (Aeinehvand et al., 2014; Hohlfelder, 1999; M. J. Madou, 2002):

$$P_m = C_a \frac{Ejz^3}{r_m^4(1-\upsilon)} + C_b \frac{\sigma_0 jz}{r_m^2} \tag{5.5}$$

Substituting Equations 5.4 and 5.5 into Equation 5.2, the valve pressure is then given by:

$$\Delta \mathrm{P_{RMV}} = \frac{nR\Delta T}{V_{TP}} - \left(C_a \frac{Ejz^3}{r_m^4(1-\upsilon)} + C_b \frac{\sigma_0 jz}{r_m^2} \right) \tag{5.6}$$

Except for the temperature and the height of the bulged membrane, all the parameters in the equation are constant. Assuming the valve deflection at the instant the valve actuates is insignificant ($\Delta z \approx 0$), the valve pressure varies only by the change of temperature ΔT. Therefore, the minimum increment of temperature that is required to prevent flow at a fixed rotational frequency can be predicted by equaling the valve pressure and the induced centrifugal pressure:

$$\Delta P_{\omega} = \rho\omega^2 \Delta r \bar{r} \tag{5.7}$$

where ρ is the density of liquid, $\bar{r} = (r_2 + r_1)/2$ is the average distance of the liquid from the centre of the disk, $\Delta r = (r_2 - r_1)$ is the radial length of the liquid inside the microfluidic system, and ω is the rotational frequency of the disk (see Figure 5.6).

By balancing the valve and centrifugal pressures, measured from Equation 5.6 and

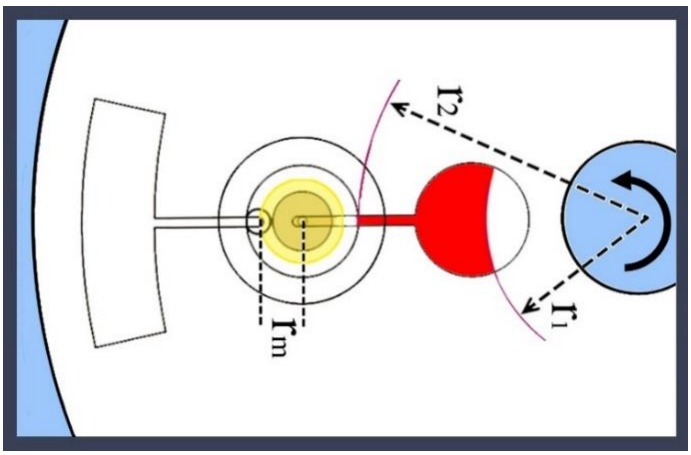

Figure 5.6: Some of the parameters used in mathematical modeling of RTPVs.

Equation 5.7, the valving condition to prevent flow can thus be characterized as:

$$\frac{nR\Delta T}{V_{TP}} - \left(C_a \frac{Ejz^3}{r_m^4(1-\upsilon)} + C_b \frac{\sigma_0 jz}{r_m^2} \right) > \rho\omega^2 \Delta r \bar{r} \qquad (5.8)$$

To simplify Equation 5.8, two constant values are defined, $K_1 = \rho \Delta r \bar{r}/2$ and $K_2 = (nR/V_{TP})$. The critical temperature required to prevent flow for a known rotational frequency and room temperature is defined as follows:

$$T > \frac{K_1\omega^2 + K_2 T_0 + P_m}{K_2} \qquad (5.9)$$

To test the accuracy of Equation 5.9, the experimentally measured actuation temperatures of a RTPV at various fixed rotational frequencies are compared to a theoretically obtained graph (see results and discussion *Section 5.4.1*).

5.3.5.2 RTPV's Cooling Time

The calculation of the passive cooling time of a heated spinning disk is based on several factors, mainly the room temperature value and the air flow regime existing around the disk at a certain spinning speed. The existing flow regime in the system depends on the range of rotational frequency and can be determined by the value of the Reynolds number given as:

$$R_e = \frac{\omega d}{\vartheta} \qquad (5.10)$$

where d and ϑ are the disk diameter and kinematic viscosity of air, respectively. In accordance with Equation 5.10, the dominant flow regime under the current testing conditions is laminar, and the heat transfer for the laminar regime around the disk is based on the "one-dimensional conduction of heat in a semi-infinite slab with a convective boundary condition" :(Indinger & Shevchuk, 2004; I. V. Shevchuk, 2006; Igor V Shevchuk, 2009)

$$\theta = \frac{T - T_\infty}{T_C - T_\infty} = e^{\gamma^2}.erfc(\gamma) \tag{5.11}$$

where, T_C is the disk surface temperature increased above the critical value T. γ is defined as:

$$\gamma = \frac{K_T k}{k_d}\sqrt{\frac{a_d \omega t}{\Pr a}} \tag{5.12}$$

where , K_T is a constant (Igor V Shevchuk, 2009), P_r is the Prandtl number of air, a and k are thermal diffusivity and thermal conductivity of air, respectively, and a_d and k_d are thermal diffusivity and thermal conductivity of the disk (PMMA), respectively. For convenience, I have defined:

$$\zeta = \frac{K_T k}{k_d}\sqrt{\frac{a_d \omega}{\Pr a}} \tag{5.13}$$

For the cooling of the rotating disk used in the current, the value of K_T can be experimentally defined:

$$K_T = A\Delta T^3 - B\Delta T^2 + C\Delta T - D \tag{5.14}$$

where, A, B, C, and D are experimentally derived constants. The following equation results upon substituting Equations 5.12, 5.13, and 5.14 into Equation 5.11:

$$1 = \frac{e^{t\zeta^2} erfc\left(\zeta t^{1/2}\right)}{\theta} \tag{5.15}$$

Table 5.1: Values of the parameters used in the theoretical analysis.

Parameters	Value	**Parameters**	Value
N	1.7488×10^{-5}	**r1**	15 mm
R	8.31 J/(Mol.K)	**r2**	32 mm
T_0	26Co	**Pr**	0.71
V_0	4.287×10^{-7} m3	**a**	2.43×10^{-5} m2/S
rm	3.5 mm	**ad**	1.2×10^{-7} m2/S
E	1.2 MPa	**k**	27×10^{-3} W/(m.k)
σ_0	0.059 MPa	**kd**	0.17 W/(m.k)
J	220 μm	**A**	0.003
N	0.48	**B**	0.0446
C_a	8/3	**C**	0.2858
C_b	4	**D**	0.2678

For fixed rotational frequencies, Equation 5.15 can be numerically solved to obtain the required cooling time for changing the surface temperature from T_C to T. A comparison between the experimentally recorded cooling times and time periods measured by Equation 5.15 is presented in Figure 5.7c (see *Section 5.4*). The values of the different parameters used in the theoretical analysis of the RTPV mechanism are listed in Table 5.1.

5.4 Results and Discussions

Several valving designs were tested to identify characteristics of the RTPV that allow for the most efficient use of the TP energy and to maximize the accessible range of rotational frequencies. The latex membrane was initially aligned parallel to a microchannel with a small opening that accommodated the deflection of the membrane. However, such an arrangement did not result in robust sealing due to the gaps remaining between the corners of the valve seat and the deflected membrane. This problem led us to use a transition chamber with a vertical microchannel (inlet) perpendicular to the latex membrane. The ultra-short distance between the membrane and the top of the inlet significantly limited the deflection of the latex membrane, allowing for the efficient use of TP energy for a robust sealing of the inlet. Efficient use of TP energy, which enables the valve to operate by small changes in temperature, is of great importance in clinical

assays, where reactions may occur near body temperature. For instance, the optimal range of operating temperature for nucleic acid sequence-based amplification (NASBA) and recombinase polymerase amplification (RPA) are within the range of 37-42 °C (T.-H. Kim et al., 2014; Lutz et al., 2010).

5.4.1 RTPV Actuation Temperature

In Figure 5.7a, the experimentally measured critical temperatures of an RTPV is compared with the theoretical graph that is obtained from Equation 5.9. Good agreement between the experimental data and the predicted values is observed from room temperature to 70 °C and at spinning speeds from 700 RPM to 2500 RPM. Hence, Equation 5.9 provides an accurate prediction of the valve's actuation temperatures at various spinning speeds. To retain liquids at higher spinning speeds, the valve requires a higher temperature that is beyond the operational temperature of the disk materials used in this study.

To circumvent these challenges, an extra hemispherical rubber seal can be embedded between the latex layer and the transition chamber, dramatically increasing the range of operational rotational frequency while also making the valve a normally-closed valve (see Figure 5.7b). Preliminary experiments show that by adding a 2 mm hemispherical rubber seal to the same radial location in the system and varying the membrane diameter (from 6 mm to 16 mm in radius), centrifugally generated hydrostatic pressures at decreasing spinning speeds of 6000 RPM down to 1300 RPM are required to open the normally-closed valve. As the membrane diameter decreases, the initial valve pressure is enhanced, and therefore, a higher spinning speed is required to actuate the RTPV (e.g., a membrane of 6 mm diameter requires 6000 RPM to open). In the designs introduced in the current study, the air chambers are located above the latex membranes; however, air chambers can be positioned anywhere in the microfluidic disk and linked with the membrane through microchannels. This facilitates the control of TP energy input

and sequential valving in multi-stage operations particularity when a set of RTPVs are aligned on the same radius of the microfluidic disk.

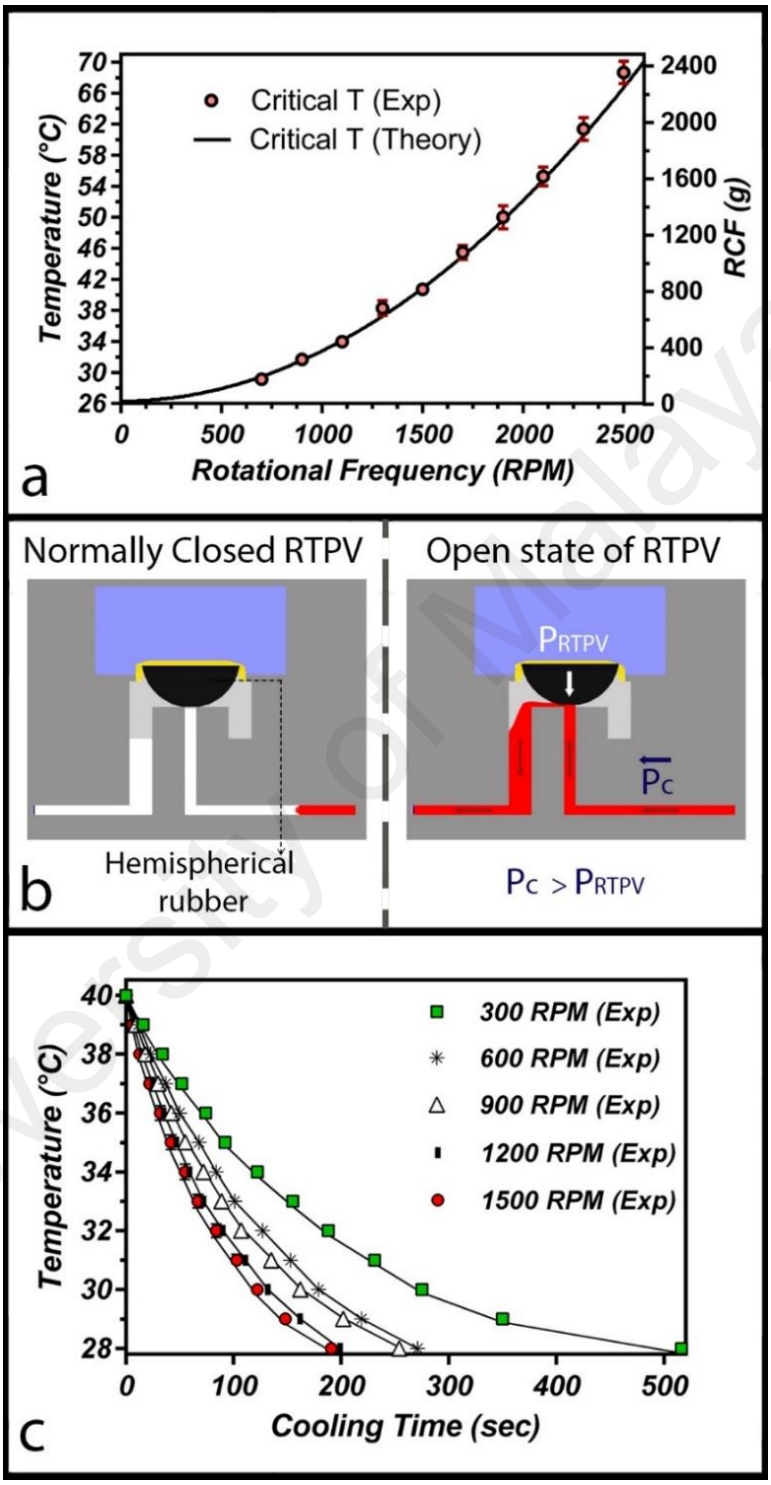

Figure 5.7: (a) The temperatures in which the centrifugal pressure is equal to RTPV pressure. (b) Schematics of closed and open state of the normally-closed RTPV with the embedded hemispherical rubber seal. (c) The cooling process of the heated disk spinning at various rotational frequencies.

5.4.2 RTPV's Cooling Time

To fully automate a sequential microfluidic procedure with RTPVs, the valves' actuation temperatures and response times needed to be controlled and predicted, respectively. Figure 5.7c shows the comparison between the cooling times recorded from experiments and those calculated at different rotational frequencies using Equation 5.15, an empirical equation. This figure shows an excellent agreement between the experimental data and the values predicted by Equation 5.15. Design G was 2.12 mm thicker than Design F and required slightly longer cooling periods. This is expected as the thermal resistance of the thicker platform is higher. In cooling experiments conducted with Design G at spin rates of 600 rpm and 1200 rpm, 10 seconds and 23 seconds longer times were required to reduce the temperature from 40 °C to 28 °C, respectively. In general, over a wider temperature range and for different disk materials and thicknesses, the parameter K_T in Equation 5.14 should be experimentally redefined. The difference between the required heating times of the two platforms, on the other hand, was negligible. This is also expected because the heating periods in these experiments, and in experiments reported in the previous study (Thio, Ibrahim, et al., 2013), are much shorter than the cooling periods.

5.4.3 RTPV Applications

The obvious limitations of the heating setup (e.g., slow operation, high power consumption, etc.) limit its usage as a thermal-cycler in assays (e.g., PCR amplification) that require rapid and precise changes of temperature. However, the aim of this study was to develop a reversible valve facilitating fluidic procedures on a microfluidic disk, which automatically closes to prevent evaporation of reagents at elevated temperatures. The RTPV is expected to operate smoothly with both contact, and non-contact heating systems such as a laser-based heating setup used for isothermal DNA amplification assays (T.-H. Kim et al., 2014), or the air-mediated heating-cooling setup used in the Rotor-Gene

2000 for real time PCR amplification (Focke, Stumpf, et al., 2010; Oliver Strohmeier et al., 2013; Oliver Strohmeier et al., 2014). Nevertheless, the heating setup was successfully used in continuous liquid circulation/switching, and sequential aliquoting applications, which are described in the next sub-sections. Sequential aliquoting allowed for the preparation of PCR reaction mixtures required for the detection of dengue virus.

5.4.3.1 Continuous Liquid Circulation/Switching

Liquid circulation in microfluidic devices is used for applications such as serial dilution (Ahrar, Hwang, Duncan, & Hui, 2014), DNA hybridization (H. H. Lee, Smoot, McMurray, Stahl, & Yager, 2006; Rodaree et al., 2011), and micromixing (Yuen, Li, Bao, & Müller, 2003). In addition, liquid circulation is widely used to control residence time distribution in chemical and biological reactors and to achieve and preserve desired flow patterns (Yerushalmi, Alimahmoodi, Behzadian, & Mulligan, 2013). In centrifugal microfluidics, continuous liquid circulation has great potential in enhancing the rate of analyte capture, leading to faster detection in bioassays (Garcia-Cordero, Basabe-Desmonts, et al., 2010).

With Design G, I have demonstrated continuous liquid circulation on a spinning disk by means of a pair of RTPVs and a pair of TP pumps. The reversibility and the gas-impermeability of the technology facilitate precise control of TP energy input and liquid flow. The vapour tight seals of RTPV enables control source chambers. A step-by-step demonstration of the liquid circulation experiment is shown in Figure 5.8. Two liquid samples, blue and red, were introduced into the source chambers (see Figure 5.8a). The disk was then spun at 900 RPM, transferring the liquids into the destination chambers (see Figure 5.8b). When the liquids were completely drained from the source chambers into the destination chambers, the rotational frequency was reduced to 300 RPM (see

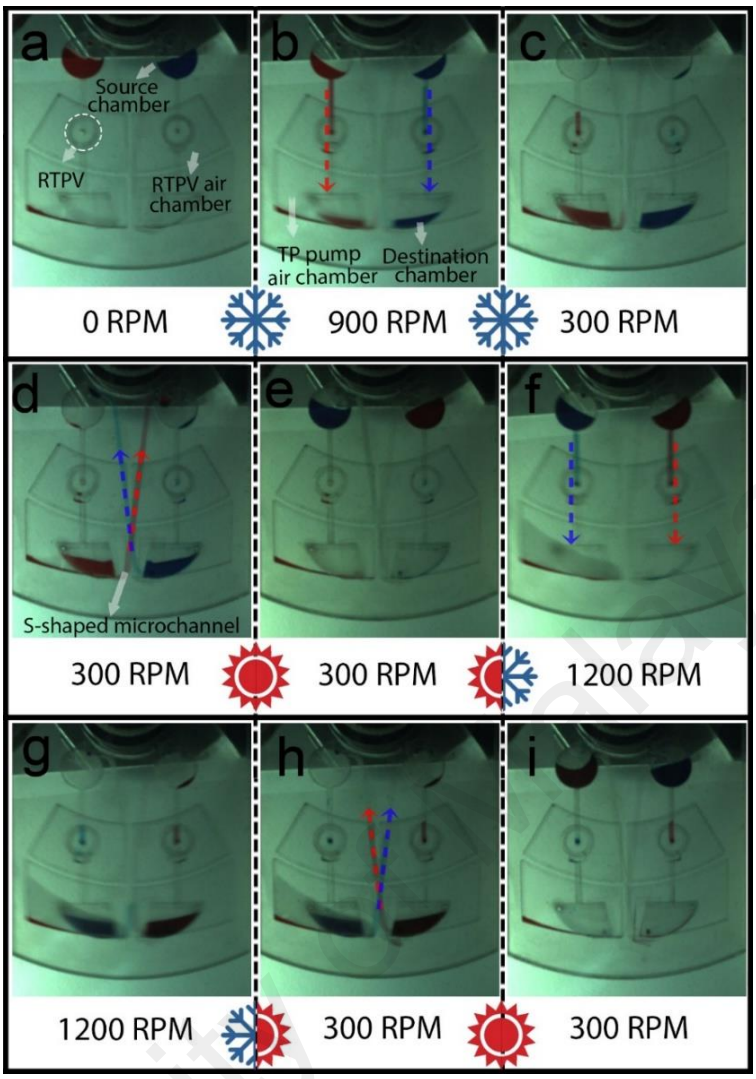

Figure 5.8: Continuous liquid circulation and switching in the microfluidic CD consisted of two RTPVs and two TP pumps.

Figure 5.8c). Due to the ultra-short distance between the liquid inlet and the membranes in the RTPVs, a small temperature increment caused the membrane to seal the inlets before the TP pumps were able to transfer the liquids towards the source chambers. A further increase in temperature actuated the TP pumps to propel the liquids towards the disk centre along the S-shaped channels (see Figure 5.8d). The disk was continuously heated until both liquids were transferred to the opposite source chambers (see Figure 5.8e). To test the reversibility of the valving system, the RTPVs were then reopened by cooling them by fast spinning (see Figure 5.8f, g). In Figures 8h to 8i, the liquids were further circulated until they were transferred back to their initial source chambers once more.

5.4.3.2 Multiplexing of Temperature Controlled Reactions

Design H is developed to demonstrate the applicability of the microballoon liquid handling elements developed in this thesis for the automation of fluidic procedures commonly required for multiplexing of heat-based assays. Aliquoting a large reagent volume into several reaction chambers by means of an array of metering fingers (chambers) and valves is the key fluidic step in multiplexing any analytical assay on a microfluidic platform. Employing gas-impermeable valves for multiplexing of the heat-based assays is considered a great advantage, preventing the evaporation of miniaturized reagents and the risk of cross-contamination (Amasia et al., 2012; Jung, Park, Oh, Choi, & Seo, 2015; L. X. Kong et al., 2014; Lutz et al., 2010). To demonstrate the compatibility and the practicality of the microballoon pump, mixer and valve in real life applications, Design H is created to automate the fluidic procedures commonly required for the multiplexing of heat-based assays. As a pilot study, Design H was used for the conversion of dengue viral RNA to cDNA, and for the preparation of PCR reaction mixtures. The reversibility of RTPVs allowed for sequential aliquoting of dengue virus RNA and PCR master mix, to multiple separated PCR reaction mixtures. Moreover, the ability of the valve to automatically close at elevated temperature prevented the evaporation of reagents during thermo-cycling period.

A step-by-step visualization of the assay integrated in the cartridge is demonstrated in Figure 5.9A. Briefly, four of the reaction chambers were loaded with 0.2 µg (2 µl) of dengue virus RNA and 2 µl DI-water was injected into the fifth reaction chamber, which was used as the negative control. Dengue virus RNA was isolated from dengue-infected cells using a commercially available kit (Promega, USA). Afterwards, 110 µl of the RT master mix (Applied Biosystem, USA) was charged into the cartridge, and all injection holes were sealed. The spin rate was immediately increased to 1800 rpm to make sure the microballoon sufficiently expanded with the reagent entering the mixing chamber,

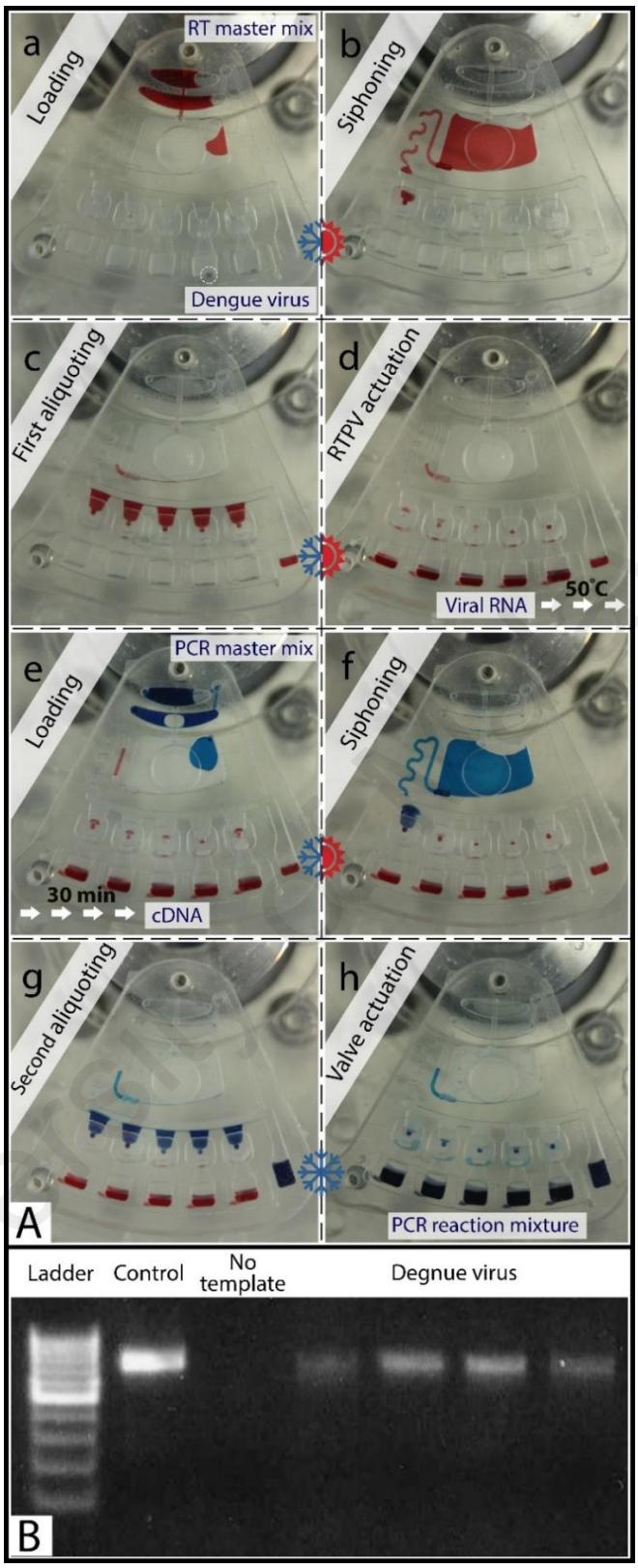

Figure 5.9: The microfluidic cartridge designed H for automation of thermally controlled assays. (A) Sequential aliquoting for preparation of PCR reaction mixture. (B) The agarose gel electrophoresis for analysing PCR reactions, and risk of cross contamination during thermocycling period.

preventing overfilling of the mixing chamber. The platform was heated to change the RTPVs from the open to the closed state. After a minute, the spin rate was reduced to 300

rpm to contract the microballoon. Releasing elastic energy of the expanded microballoon pumped the reagent against the direction of centrifugal force, increased the liquid level inside the mixing chamber and primed the siphonal flow (see Figure 5.9b). Aliquoting the master mix into the metering chambers of 20 µl occurred by increasing the spin rate to 1000 rpm (see Figure 5.9c). The heat source was powered off for 1 minute, and spin rate was increased to 3000 rpm to immediately open (actuate) the RTPVs and transfer the aliquoted reagents into their corresponding reaction chambers (see Figure 5.9d). The cartridge was then spun at 300 rpm and kept at 50 °C for 30 minutes to convert dengue viral RNA to cDNA. In the next reagent-refilling step, the components required for the preparation of 120 µl of fresh PCR master mix were distributed into the loading and mixing chambers (see Figure 5.9e). The PCR master mix contained 60 µl of 2X PCR mixture (Promega, USA), 6 µl dengue Forward primer, 6 µl dengue reverse primer, and 48 µl dH2O. The PCR master mix was prepared through microballoon mixing by altering the spin rate of the disk between 2600 and 2000 rpm for 30 seconds. In Figures 5.9.f to 5.9.h, the mixed reagent was aliquoted into the reaction chambers by the similar fluidic procedure demonstrated in Figure 5.9b to Figure 5.9d. The heating setup and platform material could not support the PCR thermal-cycling profile. Therefore, the multiplexed PCR reaction mixtures were transferred into tubes, and PCR reaction was performed in a conventional thermal-cycler to evaluate the quality of the assay. The thermal-cycling profile of the PCR reaction included 2 minutes denaturation at 95 °C, 40 cycles of 95 °C (30 seconds), 55 °C (30 seconds), and 72 °C (30 seconds), and 10 minutes extension at 72 °C. PCR products then were vitalized by agarose gel electrophoresis (Figure 5.9B). The agarose gel electrophoresis analysis indicated that reaction in the 4 wells was successful and there was no cross-contamination during the thermocycling period, since there is no band in the negative control. In addition, the PCR product of the positive

control (the conventional method of reverse transcription and PCR) showed a similar result compared to our methods as evidenced by the gel image.

At elevated temperatures, built-up TP pressure in the air chambers of RTPVs suppresses the rising pressure inside the heated reaction chambers, preventing the evaporation of reagents and cross-contamination. Perhaps no evaporation of reagents was observed or even expected at 50 ° for 30 minutes. Therefore, the efficiency of the RTPV to prevent evaporation of reagent at more elevated temperatures was demonstrated by using the thermocycling profile of a LAMP assay, i.e., 1 hour of 65 °C (see Figure 5.10), followed by 2 minutes at 80 °C (see Figure 5.10c).

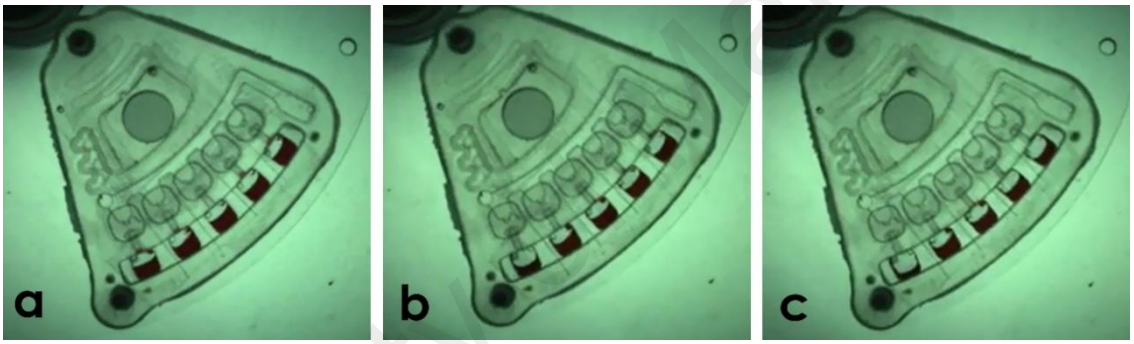

Figure 5.10: Comparison between evaporation of reagents in an open chamber and four chambers sealed with RTPVS.

In general, the reversibility of RTPVs and their sensitivity to changes in temperature creates a unique valving system to automate fluidic procedures required for multiplexing of temperature-controlled assays.

5.5 Conclusions

RTPV is a novel active valve on centrifugal microfluidic platforms that operates based on the thermal expansion of trapped air and the deflection of an embedded elastic membrane. Unlike conventional, single-use active valves that utilize thermal energy to remove barriers to permit liquid flow, the RTPV is a reversible mechanism that manipulates thermal energy to reversibly block or open microchannels. The air expansion in the heated air chamber deflects the latex membrane, sealing the inlet and preventing

fluid flow. The valving mechanism was modelled and experimentally investigated over a range of rotational speeds from 700 to 2500 RPM, and temperatures from 26 to ~70 °C. The ability of the valve to prevent flow during heating makes RTPVs suitable for use in heat-based applications such as PCR, LAMP and NASBA. Particularly, the small magnitude of temperature changes involved in the closed state of the RTPV accommodates valving needs in diagnostic assays where biological reactions occur near body temperature. Table 5.2 demonstrates the comparison between technical aspects of RTPV and previously developed microvalves.

Defining an empirical equation that predicts the cooling process of a heated disk during spinning enabled the development of time-programmable RTPVs. The usability of the valving mechanism in various applications such as micromixing and DNA hybridization are demonstrated through continuous liquid circulation and sequential aliquoting of reagents, respectively. Overall, RTPV offers unique advantages for controlling fluid flow that facilitate the integration of intricate biochemical assays on microfluidic disk.

Table 5.2: Comparison between microballoon and previously developed valves.

Valve	Operational mechanism	Operational spin speed	Single use or Reversible	Vapor tight
RTPV	Active	2500 rpm	Reversible	Yes
CP	Passive	1680 rpm	Single use	No
PLV	Passive	1500 rpm	Single use	No
DF valve	Passive	4400 rpm	Single use	Yes
Elastomeric	Passive	800 rpm	Reversible	Yes
LIFM	Active	*410 kPA	Single use	Yes
Hydrocarbon gel	Active	1300 rpm	Single use	Yes
MA	Active	1600 rpm	Reversible	No

CHAPTER 6: CONCLUSION AND RECOMMENDATIONS FOR FUTURE STUDY

6.1 Introduction

The aim of this project was to develop a reversible microfluidic system to facilitate the automation of bioanalytical assays on portable centrifugal microfluidic platforms. Therefore this thesis served to develop reversible microballoon pumps, mixers and valves to:

i. overcome the unidirectional nature of centripetal flow with no need for high spinning speeds, high acceleration, surface modification of microchannels and any external power source,
ii. enhance the mixing efficiency in the micro- and nano-scale domain without the need for high spinning speeds, high acceleration, space occupying component and any external power source, and
iii. precisely control liquid retention and flow over a wide range of rotational speeds and temperatures.

6.2 Conclusion

Reversible microballoons allow an efficient use of centrifugally and thermally induced forces to manipulate liquids on centrifugal microfluidic platforms. Due to the high elasticity, transparency, and gas impermeability of latex film in comparison to PDMS film, latex film was selected to make microballoons on the microfluidic platforms. The microballoon pump employs elastic energy stored in the latex membrane to displace various liquid volumes towards the disc center. In comparison with passive pneumatic pumps, the microballoon pump displaces and siphons liquid over considerably (e.g., up to 6000 rpm) lower range of spinning speeds. The microballoon mixer operates based on the expansion and relaxation of the latex membrane by the liquid at a high and a low spinning speed, respectively. Alternating the spinning speed generated a periodical 3D

reciprocating flow regime that reduced the mixing time of 12 µl liquid in a chamber with high-surface-area-to-volume-ratio from 170 minutes, for diffusional mixing, to less than 23 seconds. The microballoon mixer enhanced the detection signal of the dengue virus immunoassay by nearly one order of magnitude compared to the conventional ELISA method. Therefore microballoon mixer may facilitate the early detection of infectious diseases in POC settings.

Microballoon pumping and mixing at low spin speeds with no need for high accelerations and any peripheral equipment provides several advantages for portable systems. This includes low power consumption and compatibility with various types of low cost spindle motors as well as other centrifugally controlled fluidic components. Moreover, microballoon pump and mixer facilitate the manipulation of large liquid volumes. This is crucial in applications such as the detection of CTCs, when the amount of a targeted analyte is at an extremely low concentration and a large volume of a sample is needed for the analysis.

The reversible valve (i.e., RTPV) employs the deflection of a latex membrane to control liquid flow and prevent evaporation of reagents over the range of rotational speeds and temperatures up to 2500 rpm and 80 °C, respectively. It seals or reopens an inlet when a trapped air volume is heated or cooled, respectively. The ability of the valve to prevent flow during heating makes RTPVs suitable for use in heat-based applications such as PCR, LAMP and NASBA. The ability of the valve to automatically close at elevated temperatures prevents the evaporation of reagents during the thermo-cycling period.

Design H was created to demonstrate the compatibility and practicality of the microballoon liquid handling elements for the implementation of bioanalytical assay on centrifugal microfluidic platforms. The portable microfluidic cartridge automates fluidic procedures commonly required to multiplex temperature controlled reactions. In this thesis, the platform was used for the conversion of dengue viral RNA to cDNA, and

reused for the preparation of PCR reaction mixtures. Overalls, reversible microballoon system offer unique advantages that facilitate the implementation of intricate biochemical assays on centrifugal microfluidic platforms.

6.3 Future Work

Analysis of the microballoon mixing efficiency in term of Reynolds number is crucial for the optimization of the flow regime for different applications. Microballoon mixers provide the 3D reciprocating flow regime to accelerate bioreactions and subsequently enhance the detection signals in heterogeneous assays. Future studies are recommended to explore the ability of microballoon mixer to optimize required reagent volumes and incubation periods in various immunoassays.

It was mentioned that the microfluidic cartridge Design H can enable the automation of various temperature controlled assays. Implementation of a similar microfluidic cartridge for the automation of multiplexed LAMP and RPA assay in future studies is highly recommended.

REFERENCES

A1 Yong, J. Q., & A1 Teo, C. J. (2014). T1 Mixing and Heat Transfer Enhancement in Microchannels Containing Converging-Diverging Passages. *JF Journal of Heat Transfer, 136*(4).

Abi-Samra, K., Clime, L., Kong, L., Gorkin III, R., Kim, T.-H., Cho, Y.-K., & Madou, M. (2011). Thermo-pneumatic pumping in centrifugal microfluidic platforms. *Microfluidics and nanofluidics, 11*(5), 643-652.

Abi-Samra, K., Kim, T.-H., Park, D.-K., Kim, N., Kim, J., Kim, H., . . . Madou, M. (2013). Electrochemical velocimetry on centrifugal microfluidic platforms. *Lab on a Chip, 13*(16), 3253-3260.

Aeinehvand, M. M., Ibrahim, F., Al-Faqheri, W., Thio, T. H. G., Kazemzadeh, A., & Madou, M. (2014). Latex micro-balloon pumping in centrifugal microfluidic platforms. *Lab on a Chip, 14*(5), 988-997.

Ahrar, S., Hwang, M., Duncan, P. N., & Hui, E. E. (2014). Microfluidic serial dilution ladder. *Analyst, 139*(1), 187-190.

Al-Faqheri, W., Ibrahim, F., Thio, T. H. G., Bahari, N., Arof, H., Rothan, H. A., . . . Madou, M. (2015). Development of a Passive Liquid Valve (PLV) Utilizing a Pressure Equilibrium Phenomenon on the Centrifugal Microfluidic Platform. *Sensors, 15*(3), 4658-4676.

Al-Faqheri, W., Ibrahim, F., Thio, T. H. G., Moebius, J., Joseph, K., Arof, H., & Madou, M. (2013). Vacuum/compression valving (VCV) using parrafin-wax on a centrifugal microfluidic CD platform. *PloS one, 8*(3), e58523.

Allwinn, R. (2011). Significant increase in travel-associated dengue fever in Germany. *Medical microbiology and immunology, 200*(3), 155-159.

Amasia, M., Cozzens, M., & Madou, M. J. (2012). Centrifugal microfluidic platform for rapid PCR amplification using integrated thermoelectric heating and ice-valving. *Sensors and Actuators B: Chemical, 161*(1), 1191-1197.

Anderson, J. R., Chiu, D. T., Wu, H., Schueller, O. J. A., & Whitesides, G. M. (2000). Fabrication of microfluidic systems in poly (dimethylsiloxane). *Electrophoresis, 21*, 27-40.

Andreasen, S. Z., Kwasny, D., Amato, L., Brøgger, A. L., Bosco, F. G., Andersen, K. B., . . . Boisen, A. (2015). Integrating electrochemical detection with centrifugal microfluidics for real-time and fully automated sample testing. *RSC Advances, 5*(22), 17187-17193.

Arda, E., & Pekcan, Ö. (2001). Time and temperature dependence of void closure, healing and interdiffusion during latex film formation. *Polymer, 42*(17), 7419-7428.

Balabanian, C. A. C. A., Coutinho-Netto, J., Lamano-Carvalho, T. L., Lacerda, S. A., & Brentegani, L. G. (2006). Biocompatibility of natural latex implanted into dental alveolus of rats. *Journal of Oral Science, 48*(4), 201-205.

Beebe, D. J., Moore, J. S., Yu, Q., Liu, R. H., Kraft, M. L., Jo, B.-H., & Devadoss, C. (2000). Microfluidic tectonics: a comprehensive construction platform for microfluidic systems. *Proceedings of the National Academy of Sciences, 97*(25), 13488-13493.

Bélanger, M. C., & Marois, Y. (2001). Hemocompatibility, biocompatibility, inflammatory and in vivo studies of primary reference materials low-density polyethylene and polydimethylsiloxane: A review. *Journal of biomedical materials research, 58*(5), 467-477.

Braga, M., Costa, C. A. R., Leite, C. A. P., & Galembeck, F. (2001). Scanning electric potential microscopy imaging of polymer latex films: detection of supramolecular domains with nonuniform electrical characteristics. *The Journal of Physical Chemistry B, 105*(15), 3005-3011.

Brask, A., Snakenborg, D., Kutter, J. P., & Bruus, H. (2006). AC electroosmotic pump with bubble-free palladium electrodes and rectifying polymer membrane valves. *Lab on a Chip, 6*(2), 280-288.

Briand, S., Bertherat, E., Cox, P., Formenty, P., Kieny, M.-P., Myhre, J. K., . . . Dye, C. (2014). The International Ebola Emergency. *New England Journal of Medicine*.

Burger, R., & Ducrée, J. (2012). Handling and analysis of cells and bioparticles on centrifugal microfluidic platforms.

Burger, R., Kitsara, M., Gaughran, J., Nwankire, C., & Ducrée, J. (2014). Automation of immunoassays through centrifugal lab-on-a-disc platforms.

Burger, R., Reis, N., da Fonseca, J. G., & Ducrée, J. (2013). Plasma extraction by centrifugo-pneumatically induced gating of flow. *Journal of Micromechanics and Microengineering, 23*(3), 035035.

Cai, Z., Xiang, J., Zhang, B., & Wang, W. (2015). A magnetically actuated valve for centrifugal microfluidic applications. *Sensors and Actuators B: Chemical, 206*, 22-29.

Chin, C. D., Linder, V., & Sia, S. K. (2007). Lab-on-a-chip devices for global health: Past studies and future opportunities. *Lab on a Chip, 7*(1), 41-57.

Chowell, D., Castillo-Chavez, C., Krishna, S., Qiu, X., & Anderson, K. S. (2015). Modelling the effect of early detection of Ebola. *The Lancet Infectious Diseases, 15*(2), 148-149.

Chung, S., Sudo, R., Mack, P. J., Wan, C. R., Vickerman, V., & Kamm, R. D. (2008). Cell migration into scaffolds under co-culture conditions in a microfluidic platform. *Lab Chip, 9*(2), 269-275.

Clime, L., Brassard, D., Geissler, M., & Veres, T. (2015). Active pneumatic control of centrifugal microfluidic flows for lab-on-a-chip applications. *Lab on a Chip, 15*(11), 2400-2411.

Cosnier, S., Szunerits, S., Marks, R. S., Novoa, A., Puech, L., Perez, E., & Rico-Lattes, I. (2001). A comparative physical study of two different hydrophilic synthetic latex matrices for the construction of a glucose biosensor. *Talanta, 55*(5), 889-897.

Cygan, Z. T., Cabral, J. T., Beers, K. L., & Amis, E. J. (2005). Microfluidic platform for the generation of organic-phase microreactors. *Langmuir, 21*(8), 3629-3634.

Czilwik, G., Schwarz, I., Keller, M., Wadle, S., Zehnle, S., von Stetten, F., . . . Paust, N. (2015). Microfluidic vapor-diffusion barrier for pressure reduction in fully closed PCR modules. *Lab on a Chip, 15*(4), 1084-1091.

Daar, A. S., Thorsteinsdóttir, H., Martin, D. K., Smith, A. C., Nast, S., & Singer, P. A. (2002). Top ten biotechnologies for improving health in developing countries. *Nature genetics, 32*(2), 229-232.

De Jong, J., Lammertink, R., & Wessling, M. (2006). Membranes and microfluidics: a review. *Lab Chip, 6*(9), 1125-1139.

Deng, Y., Fan, J., Zhou, S., Zhou, T., Wu, J., Li, Y., . . . Wu, Y. (2014). Euler force actuation mechanism for siphon valving in compact disk-like microfluidic chips. *Biomicrofluidics, 8*(2), 024101.

Dhillon, R. S., Srikrishna, D., Garry, R. F., & Chowell, G. (2015). Ebola control: rapid diagnostic testing. *The Lancet Infectious Diseases, 15*(2), 147-148.

Di Carlo, D. (2009). Inertial microfluidics. *Lab on a Chip, 9*(21), 3038-3046.

Dias, A. C., Gomes-Filho, S. L., Silva, M., & Dutra, R. F. (2013). A sensor tip based on carbon nanotube-ink printed electrode for the dengue virus NS1 protein. *Biosensors and Bioelectronics, 44*, 216-221.

Dittrich, P. S., & Manz, A. (2006). Lab-on-a-chip: microfluidics in drug discovery. *Nature Reviews Drug Discovery, 5*(3), 210-218.

Dittrich, P. S., Tachikawa, K., & Manz, A. (2006). Micro total analysis systems. Latest advancements and trends. *Analytical Chemistry, 78*(12), 3887-3908.

Ducrée, J., Haeberle, S., Lutz, S., Pausch, S., Von Stetten, F., & Zengerle, R. (2007). The centrifugal microfluidic Bio-Disk platform. *Journal of Micromechanics and Microengineering, 17*(7), S103.

Eddings, M. A., & Gale, B. K. (2006). A PDMS-based gas permeation pump for on-chip fluid handling in microfluidic devices. *Journal of Micromechanics and Microengineering, 16*(11), 2396.

Focke, M., Kosse, D., Müller, C., Reinecke, H., Zengerle, R., & von Stetten, F. (2010). Lab-on-a-Foil: microfluidics on thin and flexible films. *Lab on a Chip, 10*(11), 1365-1386.

Focke, M., Stumpf, F., Faltin, B., Reith, P., Bamarni, D., Wadle, S., . . . Francois, P. (2010). Microstructuring of polymer films for sensitive genotyping by real-time PCR on a centrifugal microfluidic platform. *Lab on a Chip, 10*(19), 2519-2526.

Gad-el-Hak, M. (2010). *MEMS: Design and fabrication* (Vol. 2): CRC press.

Garcia-Cordero, J. L., Barrett, L. M., O'Kennedy, R., & Ricco, A. J. (2010). Microfluidic sedimentation cytometer for milk quality and bovine mastitis monitoring. *Biomedical microdevices, 12*(6), 1051-1059.

Garcia-Cordero, J. L., Basabe-Desmonts, L., Ducrée, J., & Ricco, A. J. (2010). Liquid recirculation in microfluidic channels by the interplay of capillary and centrifugal forces. *Microfluidics and nanofluidics, 9*(4-5), 695-703.

Garcia-Cordero, J. L., Kurzbuch, D., Benito-Lopez, F., Diamond, D., Lee, L. P., & Ricco, A. J. (2010). Optically addressable single-use microfluidic valves by laser printer lithography. *Lab on a Chip, 10*(20), 2680-2687.

Go, J. S., & Shoji, S. (2004). A disposable, dead volume-free and leak-free in-plane PDMS microvalve. *Sensors and Actuators A: Physical, 114*(2), 438-444.

Godino, N., Gorkin III, R., Linares, A. V., Burger, R., & Ducrée, J. (2013). Comprehensive integration of homogeneous bioassays via centrifugo-pneumatic cascading. *Lab on a Chip, 13*(4), 685-694.

Gorkin III, R., Clime, L., Madou, M., & Kido, H. (2010). Pneumatic pumping in centrifugal microfluidic platforms. *Microfluidics and Nanofluidics, 9*(2-3), 541-549.

Gorkin III, R., Nwankire, C. E., Gaughran, J., Zhang, X., Donohoe, G. G., Rook, M., . . . Ducrée, J. (2012). Centrifugo-pneumatic valving utilizing dissolvable films. *Lab on a Chip, 12*(16), 2894-2902.

Gorkin, R., Clime, L., Madou, M., & Kido, H. (2010). Pneumatic pumping in centrifugal microfluidic platforms. *Microfluidics and Nanofluidics*, *9*(2), 541-549.

Gorkin, R., Park, J., Siegrist, J., Amasia, M., Lee, B. S., Park, J.-M., . . . Cho, Y.-K. (2010). Centrifugal microfluidics for biomedical applications. *Lab on a Chip, 10*(14), 1758-1773.

Grover, W. H., Skelley, A. M., Liu, C. N., Lagally, E. T., & Mathies, R. A. (2003). Monolithic membrane valves and diaphragm pumps for practical large-scale integration into glass microfluidic devices. *Sensors and Actuators B: Chemical, 89*(3), 315-323.

Grubauer, G., Elias, P. M., & Feingold, K. R. (1989). Transepidermal water loss: the signal for recovery of barrier structure and function. *Journal of Lipid Research, 30*(3), 323-333.

Grumann, M., Geipel, A., Riegger, L., Zengerle, R., & Ducrée, J. (2005). Batch-mode mixing on centrifugal microfluidic platforms. *Lab on a Chip, 5*(5), 560-565.

Gurugama, P., Garg, P., Perera, J., Wijewickrama, A., & Seneviratne, S. L. (2010). Dengue viral infections. *Indian journal of dermatology, 55*(1), 68.

Haeberle, S., Brenner, T., Schlosser, H. P., Zengerle, R., & Ducrée, J. (2005). Centrifugal micromixery. *Chemical engineering & technology, 28*(5), 613-616.

Haeberle, S., Brenner, T., Zengerle, R., & Ducrée, J. (2006). Centrifugal extraction of plasma from whole blood on a rotating disk. *Lab on a Chip, 6*(6), 776-781.

Haeberle, S., Schmitt, N., Zengerle, R., & Ducrée, J. (2007). Centrifugo-magnetic pump for gas-to-liquid sampling. *Sensors and Actuators A: Physical, 135*(1), 28-33.

Haeberle, S., & Zengerle, R. (2007). Microfluidic platforms for lab-on-a-chip applications. *Lab on a Chip, 7*(9), 1094-1110.

Han, A., Wang, O., Graff, M., Mohanty, S. K., Edwards, T. L., Han, K. H., & Frazier, A. B. (2003). Multi-layer plastic/glass microfluidic systems containing electrical and mechanical functionality. *Lab on a Chip, 3*(3), 150-157.

Han, K. H., McConnell, R. D., Easley, C. J., Bienvenue, J. M., Ferrance, J. P., Landers, J. P., & Frazier, A. B. (2007). An active microfluidic system packaging technology. *Sensors and Actuators B: Chemical, 122*(1), 337-346.

Herculano, R. D., Alencar de Queiroz, A. A., Kinoshita, A., Oliveira Jr, O. N., & Graeff, C. F. (2011). On the release of metronidazole from natural rubber latex membranes. *Materials Science and Engineering: C, 31*(2), 272-275.

Hillborg, H. (2012). *Loss and recovery of hydrophobicity of polydimethylsiloxane after exposure to electrical discharges*: GRIN Verlag.

Hillborg, H., & Gedde, U. (1999). Hydrophobicity changes in silicone rubbers. *Dielectrics and Electrical Insulation, IEEE Transactions on, 6*(5), 703-717.

Hohlfelder, R. J. (1999). *Bulge and blister testing of thin films and their interfaces*.

Hosseini, S., Ibrahim, F., Djordjevic, I., & Koole, L. H. (2014). Recent advances in surface functionalization techniques on polymethacrylate materials for optical biosensor applications. *Analyst*.

Hwang, H., Kim, H.-H., & Cho, Y.-K. (2011). Elastomeric membrane valves in a disc. *Lab on a Chip, 11*(8), 1434-1436.

Indinger, T., & Shevchuk, I. V. (2004). Transient laminar conjugate heat transfer of a rotating disk: theory and numerical simulations. *International Journal of Heat and Mass Transfer, 47*(14–16), 3577-3581.

Jafari, M., Farhadi, M., & Sedighi, K. (2014). Heat Transfer Enhancement in a Corrugated Channel Using Oscillating Flow and Nanoparticles: An LBM Approach. *Numerical Heat Transfer, Part A: Applications, 65*(6), 601-626.

Jeong, O. C., Park, S. W., Yang, S. S., & Pak, J. J. (2005). Fabrication of a peristaltic PDMS micropump. *Sensors and Actuators A: Physical, 123*, 453-458.

Jung, J. H., Park, B. H., Oh, S. J., Choi, G., & Seo, T. S. (2015). Integrated centrifugal reverse transcriptase loop-mediated isothermal amplification microdevice for influenza A virus detection. *Biosensors and Bioelectronics, 68*, 218-224.

Kaigala, G. V., Hoang, V. N., Stickel, A., Lauzon, J., Manage, D., Pilarski, L. M., & Backhouse, C. J. (2008). An inexpensive and portable microchip-based platform for integrated RT–PCR and capillary electrophoresis. *Analyst, 133*(3), 331-338.

Kazemzadeh, A., Ganesan, P., Ibrahim, F., Aeinehvand, M. M., Kulinsky, L., & Madou, M. J. (2014). Gating valve on spinning microfluidic platforms: A flow switch/control concept. *Sensors and Actuators B: Chemical, 204*, 149-158.

Kazemzadeh, A., Ganesan, P., Ibrahim, F., He, S., & Madou, M. J. (2013). The effect of contact angles and capillary dimensions on the burst frequency of super hydrophilic and hydrophilic centrifugal microfluidic platforms, a CFD study. *PloS one, 8*(9), e73002.

Keller, M., Wadle, S., Paust, N., Dreesen, L., Nuese, C., Strohmeier, O., . . . von Stetten, F. (2015). Centrifugo-thermopneumatic fluid control for valving and aliquoting applied to multiplex real-time PCR on off-the-shelf centrifugal thermocycler. *RSC Advances, 5*(109), 89603-89611.

Kido, H., Micic, M., Smith, D., Zoval, J., Norton, J., & Madou, M. (2007). A novel, compact disk-like centrifugal microfluidics system for cell lysis and sample homogenization. *Colloids and Surfaces B: Biointerfaces, 58*(1), 44-51.

Kim, M. S., Yeon, J. H., & Park, J. K. (2007). A microfluidic platform for 3-dimensional cell culture and cell-based assays. *Biomedical Microdevices, 9*(1), 25-34.

Kim, T.-H., Abi-Samra, K., Sunkara, V., Park, D.-K., Amasia, M., Kim, N., . . . Cho, Y.-K. (2013). Flow-enhanced electrochemical immunosensors on centrifugal microfluidic platforms. *Lab on a Chip, 13*(18), 3747-3754.

Kim, T.-H., Park, J., Kim, C.-J., & Cho, Y.-K. (2014). Fully Integrated Lab-on-a-Disc for Nucleic Acid Analysis of Food-Borne Pathogens. *Analytical chemistry, 86*(8), 3841-3848.

Kim, Y., Jeong, S.-N., Kim, B., Kim, D.-P., & Cho, Y.-K. (2015). Rapid and Automated Quantification of Microalgal Lipids on a Spinning Disc. *Analytical chemistry, 87*(15), 7865-7871.

Kinahan, D. J., Burger, R., Vembadi, A., Kilcawley, N., Lawlor, D., Glynn, M., & Ducrée, J. (2015). Baking-powder driven centripetal pumping controlled by event-triggering of functional liquids.

Kinahan, D. J., Kearney, S. M., Dimov, N., Glynn, M. T., & Ducree, J. (2014). Event-triggered logical flow control for comprehensive process integration of multi-step assays on centrifugal microfluidic platforms. *Lab on a Chip, 14*(13), 2249-2258.

Kinahan, D. J., Kearney, S. M., Dimov, N., Glynn, M. T., & Ducrée, J. (2014). Event-triggered logical flow control for comprehensive process integration of multi-step assays on centrifugal microfluidic platforms. *Lab on a Chip*.

Kitsara, M., Nwankire, C. E., Walsh, L., Hughes, G., Somers, M., Kurzbuch, D., . . . Ducrée, J. (2014). Spin coating of hydrophilic polymeric films for enhanced centrifugal flow control by serial siphoning. *Microfluidics and nanofluidics, 16*(4), 691-699.

Knapen, E., Beeldens, A., & Van Gemert, D. (2005). Water-soluble polymeric modifiers for cement mortar and concrete. *Proc. Con. Mat*.

Kong, L. X., Parate, K., Abi-Samra, K., & Madou, M. (2014). Multifunctional wax valves for liquid handling and incubation on a microfluidic CD. *Microfluidics and nanofluidics*, 1-7.

Kong, L. X., Parate, K., Abi-Samra, K., & Madou, M. (2015). Multifunctional wax valves for liquid handling and incubation on a microfluidic CD. *Microfluidics and Nanofluidics, 18*(5-6), 1031-1037.

Kong, L. X., Perebikovsky, A., Moebius, J., Kulinsky, L., & Madou, M. (2015). Lab-on-a-CD A Fully Integrated Molecular Diagnostic System. *Journal of laboratory automation*, 2211068215588456.

Kong, M. C., Bouchard, A. P., & Salin, E. D. (2011). Displacement pumping of liquids radially inward on centrifugal microfluidic platforms in motion. *Micromachines, 3*(1), 1-9.

Kong, M. C., & Salin, E. D. (2010). Pneumatically pumping fluids radially inward on centrifugal microfluidic platforms in motion. *Analytical chemistry, 82*(19), 8039-8041.

Kong, M. C., & Salin, E. D. (2012). Micromixing by pneumatic agitation on continually rotating centrifugal microfluidic platforms. *Microfluidics and nanofluidics, 13*(3), 519-525.

Kuo, J.-N., & Jiang, L.-R. (2014). Design optimization of micromixer with square-wave microchannel on compact disk microfluidic platform. *Microsystem Technologies, 20*(1), 91-99.

Lagally, E. T., Emrich, C. A., & Mathies, R. A. (2001). Fully integrated PCR-capillary electrophoresis microsystem for DNA analysis. *Lab Chip, 1*(2), 102-107.

Lagally, E. T., Lee, S.-H., & Soh, H. (2005). Integrated microsystem for dielectrophoretic cell concentration and genetic detection. *Lab on a Chip, 5*(10), 1053-1058.

Lagally, E. T., Lee, S. H., & Soh, H. (2005). Integrated microsystem for dielectrophoretic cell concentration and genetic detection. *Lab on a Chip, 5*(10), 1053-1058.

Lai, S., Wang, S., Luo, J., Lee, L. J., Yang, S.-T., & Madou, M. J. (2004). Design of a compact disk-like microfluidic platform for enzyme-linked immunosorbent assay. *Analytical chemistry, 76*(7), 1832-1837.

Lapphra, K., Sangcharaswichai, A., Chokephaibulkit, K., Tiengrim, S., Piriyakarnsakul, W., Chakorn, T., . . . Thamlikitkul, V. (2008). Evaluation of an NS1 antigen

detection for diagnosis of acute dengue infection in patients with acute febrile illness. *Diagnostic microbiology and infectious disease, 60*(4), 387-391.

Leclerc, E., Sakai, Y., & Fujii, T. (2003). Cell culture in 3-dimensional microfluidic structure of PDMS (polydimethylsiloxane). *Biomedical Microdevices, 5*(2), 109-114.

Lee, B. S., Lee, Y. U., Kim, H.-S., Kim, T.-H., Park, J., Lee, J.-G., . . . Cho, Y.-K. (2011). Fully integrated lab-on-a-disc for simultaneous analysis of biochemistry and immunoassay from whole blood. *Lab on a Chip, 11*(1), 70-78.

Lee, H. H., Smoot, J., McMurray, Z., Stahl, D. A., & Yager, P. (2006). Recirculating flow accelerates DNA microarray hybridization in a microfluidic device. *Lab on a Chip, 6*(9), 1163-1170.

Li, N., Hsu, C. H., & Folch, A. (2005). Parallel mixing of photolithographically defined nanoliter volumes using elastomeric microvalve arrays. *Electrophoresis, 26*(19), 3758-3764.

Linares, E. M., Pannuti, C. S., Kubota, L. T., & Thalhammer, S. (2013). Immunospot assay based on fluorescent nanoparticles for Dengue fever detection. *Biosensors and Bioelectronics, 41*, 180-185.

Liu, R. H., Stremler, M., Sharp, K. V., Olsen, M. G., Santiago, J. G., Adrian, R. J., . . . Beebe, D. J. (2000). Passive mixing in a three-dimensional serpentine microchannel. *Microelectromechanical Systems, Journal of, 9*(2), 190-197.

Lutz, S., Weber, P., Focke, M., Faltin, B., Hoffmann, J., Müller, C., . . . Armes, N. (2010). Microfluidic lab-on-a-foil for nucleic acid analysis based on isothermal recombinase polymerase amplification (RPA). *Lab on a Chip, 10*(7), 887-893.

Lynn Jr, N. S., Martínez-López, J.-I., Bocková, M., Adam, P., Coello, V., Siller, H. R., & Homola, J. (2014). Biosensing enhancement using passive mixing structures for microarray-based sensors. *Biosensors and Bioelectronics, 54*, 506-514.

Madou, M., Zoval, J., Jia, G., Kido, H., Kim, J., & Kim, N. (2006a). Lab on a CD. *Annual Review of Biomedical Engineering 8, 8*, 601-628.

Madou, M., Zoval, J., Jia, G., Kido, H., Kim, J., & Kim, N. (2006b). Lab on a CD. *Annu. Rev. Biomed. Eng., 8*, 601-628.

Madou, M. J. (2002). *Fundamentals of microfabrication: the science of miniaturization*: CRC press.

Mark, D., Metz, T., Haeberle, S., Lutz, S., Ducrée, J., Zengerle, R., & von Stetten, F. (2009). Centrifugo-pneumatic valve for metering of highly wetting liquids on centrifugal microfluidic platforms. *Lab on a Chip, 9*(24), 3599-3603.

Mark, J. E. (2009). *Polymer data handbook* (Vol. 2): Oxford University Press New York.

McCormick, C. L., Lowe, A. B., & Ayres, N. (2002). Water-soluble polymers. *Encyclopedia of Polymer Science and Technology*.

McDonald, J. C., Steven, J., & Whitesides, G. M. (2001). Fabrication of a configurable, single-use microfluidic device. *Analytical chemistry, 73*(23), 5645-5650.

McDonald, J. C., & Whitesides, G. M. (2002). Poly (dimethylsiloxane) as a material for fabricating microfluidic devices. *Accounts of chemical research, 35*(7), 491-499.

Merkel, T., Bondar, V., Nagai, K., Freeman, B., & Pinnau, I. (2000). Gas sorption, diffusion, and permeation in poly (dimethylsiloxane). *Journal of Polymer Science Part B: Polymer Physics, 38*(3), 415-434.

Nagayama, K. (1996). Two-dimensional self-assembly of colloids in thin liquid films. *Colloids and Surfaces A: Physicochemical and Engineering Aspects, 109*, 363-374.

Noroozi, Z., Kido, H., & Madou, M. J. (2011). Electrolysis-induced pneumatic pressure for control of liquids in a centrifugal system. *Journal of The Electrochemical Society, 158*(11), P130-P135.

Noroozi, Z., Kido, H., Micic, M., Pan, H., Bartolome, C., Princevac, M., . . . Madou, M. (2009). Reciprocating flow-based centrifugal microfluidics mixer. *Review of Scientific Instruments, 80*(7), 075102.

Noroozi, Z., Kido, H., Peytavi, R., Nakajima-Sasaki, R., Jasinskas, A., Micic, M., . . . Madou, M. J. (2011). A multiplexed immunoassay system based upon reciprocating centrifugal microfluidics. *Review of Scientific Instruments, 82*(6), 064303.

Nwankire, C. E., Chan, D.-S. S., Gaughran, J., Burger, R., Gorkin, R., & Ducrée, J. (2013). Fluidic automation of nitrate and nitrite bioassays in whole blood by dissolvable-film based centrifugo-pneumatic actuation. *Sensors, 13*(9), 11336-11349.

Nwankire, C. E., Czugala, M., Burger, R., Fraser, K. J., Glennon, T., Onwuliri, B. E., . . . Ducrée, J. (2014). A portable centrifugal analyser for liver function screening. *Biosensors and Bioelectronics, 56*, 352-358.

Nwankire, C. E., Donohoe, G. G., Zhang, X., Siegrist, J., Somers, M., Kurzbuch, D., . . . Hearty, S. (2013). At-line bioprocess monitoring by immunoassay with rotationally controlled serial siphoning and integrated supercritical angle fluorescence optics. *Analytica chimica acta, 781*, 54-62.

Ostrovidov, S., Jiang, J., Sakai, Y., & Fujii, T. (2004). Membrane-based PDMS microbioreactor for perfused 3D primary rat hepatocyte cultures. *Biomedical microdevices, 6*(4), 279-287.

Pan, T., McDonald, S. J., Kai, E. M., & Ziaie, B. (2005). A magnetically driven PDMS micropump with ball check-valves. *Journal of Micromechanics and Microengineering, 15*(5), 1021.

Park, J.-M., Cho, Y.-K., Lee, B.-S., Lee, J.-G., & Ko, C. (2007). Multifunctional microvalves control by optical illumination on nanoheaters and its application in centrifugal microfluidic devices. *Lab on a Chip, 7*(5), 557-564.

Park, J.-M., Kim, M. S., Moon, H.-S., Yoo, C. E., Park, D., Kim, Y. J., . . . Kim, S. S. (2014). Fully automated circulating tumor cell isolation platform with large-volume capacity based on lab-on-a-disc. *Analytical chemistry*, *86*(8), 3735-3742.

Ren, L., Wang, J.-C., Liu, W., Tu, Q., Liu, R., Wang, X., . . . Li, L. (2012). An enzymatic immunoassay microfluidics integrated with membrane valves for microsphere retention and reagent mixing. *Biosensors and Bioelectronics*, *35*(1), 147-154.

Ren, Y., & Leung, W. W.-F. (2013a). Flow and mixing in rotating zigzag microchannel. *Chemical Engineering Journal*, *215*, 561-578.

Ren, Y., & Leung, W. W.-F. (2013b). Numerical and experimental investigation on flow and mixing in batch-mode centrifugal microfluidics. *International Journal of Heat and Mass Transfer*, *60*, 95-104.

Rodaree, K., Maturos, T., Chaotheing, S., Pogfay, T., Suwanakitti, N., Wongsombat, C., . . . Lomas, T. (2011). DNA hybridization enhancement using piezoelectric microagitation through a liquid coupling medium. *Lab on a Chip*, *11*(6), 1059-1064.

Roy, E., Stewart, G., Mounier, M., Malic, L., Peytavi, R., Clime, L., . . . Veres, T. (2015a). From cellular lysis to microarray detection, an integrated thermoplastic elastomer (TPE) point of care Lab on a Disc. *Lab on a Chip*, *15*(2), 406-416.

Roy, E., Stewart, G., Mounier, M., Malic, L., Peytavi, R., Clime, L., . . . Veres, T. (2015b). From cellular lysis to microarray detection, an integrated thermoplastic elastomer (TPE) point of care Lab on a Disc. *Lab on a Chip*.

Shevchuk, I. V. (2006). Unsteady conjugate laminar heat transfer of a rotating non-uniformly heated disk: Application to the transient experimental technique. *International Journal of Heat and Mass Transfer*, *49*(19–20), 3530-3537.

Shevchuk, I. V. (2009). *Convective heat and mass transfer in rotating disk systems* (Vol. 45): Springer.

Siegrist, J., Gorkin, R., Bastien, M., Stewart, G., Peytavi, R., Kido, H., . . . Madou, M. (2010). Validation of a centrifugal microfluidic sample lysis and homogenization platform for nucleic acid extraction with clinical samples. *Lab on a Chip*, *10*(3), 363-371.

Siegrist, J., Gorkin, R., Clime, L., Roy, E., Peytavi, R., Kido, H., . . . Madou, M. (2010). Serial siphon valving for centrifugal microfluidic platforms. *Microfluidics and nanofluidics*, *9*(1), 55-63.

Soroori, S., Kulinsky, L., Kido, H., & Madou, M. (2013). Design and implementation of fluidic micro-pulleys for flow control on centrifugal microfluidic platforms. *Microfluidics and nanofluidics*, 1-13.

Steigert, J., Grumann, M., Brenner, T., Riegger, L., Harter, J., Zengerle, R., & Ducrée, J. (2006). Fully integrated whole blood testing by real-time absorption measurement on a centrifugal platform. *Lab Chip*, *6*(8), 1040-1044.

Stephen, R., Ranganathaiah, C., Varghese, S., Joseph, K., & Thomas, S. (2006). Gas transport through nano and micro composites of natural rubber (NR) and their blends with carboxylated styrene butadiene rubber (XSBR) latex membranes. *Polymer, 47*(3), 858-870.

Stetten, F. (2012). Centrifugo-dynamic inward pumping of liquids on a centrifugal microfluidic platform. *Lab on a Chip, 12*(24), 5142-5145.

Strohmeier, O., Keller, M., Schwemmer, F., Zehnle, S., Mark, D., von Stetten, F., . . . Paust, N. (2015). Centrifugal microfluidic platforms: advanced unit operations and applications. *Chemical Society Reviews*.

Strohmeier, O., Laßmann, S., Riedel, B., Mark, D., Roth, G., Werner, M., . . . von Stetten, F. (2013). Multiplex genotyping of KRAS point mutations in tumor cell DNA by allele-specific real-time PCR on a centrifugal microfluidic disk segment. *Microchimica Acta*, 1-8.

Strohmeier, O., Marquart, N., Mark, D., Roth, G., Zengerle, R., & von Stetten, F. (2014). Real-time PCR based detection of a panel of food-borne pathogens on a centrifugal microfluidic "LabDisk" with on-disk quality controls and standards for quantification. *Analytical Methods, 6*(7), 2038-2046.

Swayne, L., Kazarine, A., Templeton, E. J., & Salin, E. D. (2015). Rapid prototyping of pneumatically actuated hydrocarbon gel valves for centrifugal microfluidic devices. *Talanta, 134*, 443-447.

Takao, H., Miyamura, K., Ebi, H., Ashiki, M., Sawada, K., & Ishida, M. (2005). A MEMS microvalve with PDMS diaphragm and two-chamber configuration of thermo-pneumatic actuator for integrated blood test system on silicon. *Sensors and Actuators A: Physical, 119*(2), 468-475.

Teh, S.-Y., Lin, R., Hung, L.-H., & Lee, A. P. (2008). Droplet microfluidics. *Lab on a Chip, 8*(2), 198-220.

Templeton, E. J., & Salin, E. D. (2014). A novel filtration method integrated on centrifugal microfluidic devices. *Microfluidics and nanofluidics, 17*(1), 245-251.

Therriault, D., White, S. R., & Lewis, J. A. (2003). Chaotic mixing in three-dimensional microvascular networks fabricated by direct-write assembly. *Nature materials, 2*(4), 265-271.

Thio, T. H. G., Ibrahim, F., Al-Faqheri, W., Moebius, J., Khalid, N. S., Soin, N., . . . Madou, M. (2013). Push pull microfluidics on a multi-level 3D CD. *Lab on a Chip, 13*(16), 3199-3209.

Thio, T. H. G., Soroori, S., Ibrahim, F., Al-Faqheri, W., Soin, N., Kulinsky, L., & Madou, M. (2013). Theoretical development and critical analysis of burst frequency equations for passive valves on centrifugal microfluidic platforms. *Medical & Biological Engineering & Computing, 51*(5), 525-535.

Tourovskaia, A., Figueroa-Masot, X., & Folch, A. (2004). Differentiation-on-a-chip: a microfluidic platform for long-term cell culture studies. *Lab Chip, 5*(1), 14-19.

Ukita, Y., Ishizawa, M., Takamura, Y., & Utsumi, Y. *Internally Triggered Multistep Flow Sequencers using Clepsydra.* Paper presented at the 16th International Conference on Miniaturized Systems for Chemistry and Life Sciences (μTAS 2012), Okinawa, Japan, Oct.

van Oordt, T., Stevens, G. B., Vashist, S. K., Zengerle, R., & von Stetten, F. (2013). Rapid and highly sensitive luciferase reporter assay for the automated detection of botulinum toxin in the centrifugal microfluidic LabDisk platform. *RSC Advances, 3*(44), 22046-22052.

van Reenen, A., de Jong, A. M., den Toonder, J. M., & Prins, M. W. (2014). Integrated lab-on-chip biosensing systems based on magnetic particle actuation–a comprehensive review. *Lab on a Chip, 14*(12), 1966-1986.

Vollmer, A. P., Probstein, R. F., Gilbert, R., & Thorsen, T. (2005). Development of an integrated microfluidic platform for dynamic oxygen sensing and delivery in a flowing medium. *Lab on a Chip, 5*(10), 1059-1066.

Weibel, D. B., Siegel, A. C., Lee, A., George, A. H., & Whitesides, G. M. (2007). Pumping fluids in microfluidic systems using the elastic deformation of poly (dimethylsiloxane). *Lab on a Chip, 7*(12), 1832-1836.

Whitesides, G. M. (2006). The origins and the future of microfluidics. *Nature, 442*(7101), 368-373.

WHO. (2014, 22.04.2014). Dengue Situation Updates. *Emerging disease surveillance and response.* Retrieved 05.08.2014, 2014, from http://www.wpro.who.int/emerging_diseases/DengueSituationUpdates/en/

Wu, M. H., Urban, J. P., Cui, Z., & Cui, Z. F. (2006). Development of PDMS microbioreactor with well-defined and homogenous culture environment for chondrocyte 3-D culture. *Biomedical microdevices, 8*(4), 331-340.

Yerushalmi, L., Alimahmoodi, M., Behzadian, F., & Mulligan, C. N. (2013). Mixing characteristics and liquid circulation in a new multi-environment bioreactor. *Bioprocess and biosystems engineering, 36*(10), 1339-1352.

Yuen, P. K., Li, G., Bao, Y., & Müller, U. R. (2003). Microfluidic devices for fluidic circulation and mixing improve hybridization signal intensity on DNA arrays. *Lab on a Chip, 3*(1), 46-50.

Zehnle, S., Schwemmer, F., Roth, G., von Stetten, F., Zengerleabc, R., & Pausta, N. (2012). Centrifugo-dynamic inward pumping of liquids on a centrifugal microfluidic platform. *Lab on a Chip, 12*(24), 5142-5145.

Zhang, C., Xing, D., & Li, Y. (2007). Micropumps, microvalves, and micromixers within PCR microfluidic chips: Advances and trends. *Biotechnology advances, 25*(5), 483-514.

Zhao, W., & Berg, A. (2008). Lab on paper. *Lab on a Chip, 2008*(8), 1988-1991.

LIST OF PUBLICATIONS AND PAPERS PRESENTED

Articles in Academic Journals (Published)

1. **Aeinehvand, M. M**., Ibrahim, F., Harun, S. W., F., Al-Faqheri, W., Thio, T. H. G., Kazemzadeh, A., & Madou, M. (2014). Latex micro-balloon pumping in centrifugal microfluidic platforms. **Lab on a Chip**, 14(5), 988-997.

2. **Aeinehvand, M. M**., Ibrahim, F., Harun, S. W., Djordjevic, I., Hosseini, S., Rothan, H. A., . . . Madou, M. J. (2015). Biosensing Enhancement of dengue virus using microballoon Mixers on centrifugal microfluidic Platforms. **Biosensors and Bioelectronics**, 67, 424-430.

3. **Aeinehvand, M. M**., Ibrahim, F., Harun, S. W., Kazemzadeh, A., Rothan, H. A., Yusof, R., & Madou, M. (2015). Reversible thermo-pneumatic valves on centrifugal microfluidic platforms. **Lab on a Chip**, 15(16), 3358-3369.

4. Hosseini, S., **Aeinehvand, M. M**., Uddin, S. M., Benzina, A., Rothan, H. A., Yusof, R., . . . Ibrahim, F. (2015). Microsphere integrated microfluidic disk: synergy of two techniques for rapid and ultrasensitive dengue detection. **Scientific reports**, 5, 16485. (Q1, IF 5.578)

5. Al-Faqheri, W., Ibrahim, F., Thio, T. H. G., **Aeinehvand, M. M**., Arof, H., & Madou, M. (2015). Development of novel passive check valves for the microfluidic CD platform. **Sensors and Actuators A: Physical**, 222, 245-254.

6. Kazemzadeh, A., Ganesan, P., Ibrahim, F., **Aeinehvand, M. M**., Kulinsky, L., & Madou, M. J. (2014). Gating valve on spinning microfluidic platforms: A flow switch/control concept. **Sensors and Actuators B: Chemical**, 204, 149-158.

7. Hosseini, S., Ibrahim, F., Djordjevic, I., **Aeinehvand, M. M**., & Koole, L. H. (2014). Structural and end-group analysis of synthetic acrylate co-polymers by matrix-assisted laser desorption time-of-flight mass spectrometry: Distribution of pendant carboxyl groups. **Polymer Testing**, 40, 273-279.

8. Irawati, N., John, V., **Aeinehvand, M**., Ibrahim, F., Ahmad, H., & Harun, S. (2014). Evanescent wave optical trapping and transport of polystyrene microspheres on microfibers. **Microwave and Optical Technology Letters**, 56(11), 2630-2634.

Proceeding

Aeinehvand, M. M., Ibrahim, F., & Madou, M. J. (2016). A New Approach for Reagent Storage-Releasing on Centrifugal Microfluidic Platforms Using Bubblewrap and Latex Membrane. In F. Ibrahim, J. Usman, M. S. Mohktar & M. Y. Ahmad (Eds.), International Conference for Innovation in Biomedical Engineering and Life Sciences (Vol. 56, pp. 269-271): Springer Singapore.

APPENDIX A: DENGUE VIRUS PROPAGATION

A clinical isolate of Dengue serotype 2 from a patient's serum sample (DENV2-isolate Malaysia M2, Gen Bank Toxonomy No.: 11062) was used for virus propagation by a single passage on C6/36 mosquito cells. The Dengue-infected cells with obvious cytopathic effects (CPE) were lysed using the freeze and thaw cycle, then the culture medium was centrifuged at 1800 rpm for 10 mins to remove cell debris. Afterwards the solution was filtered (0.2 µm), portioned into aliquots, and stored at -80°C until it was used. The viral titer of the Dengue suspension was established by serial dilutions on Vero cells using the plaque assay. Briefly, a 10-fold serial dilution of medium supernatant was added to new Vero cells grown in a 24-well plate (1.5 x105 cells) and incubated for 1 h at 37°C. The cells were then overlaid with DMEM medium containing 1.1% methylcellulose. Viral plaques were stained with naphthol blue-black dye after incubation for 5 days. Virus titers were calculated according to the following formula: Titer (pfu/ml) = number of plaques / volume of diluted virus added to the well × dilution factor of the virus used to infect the well in which the plaques were enumerated. The titer of DV that was used in the following experiments of fluorescence ELISA was 3.5×107 p.f.u/ml and these serial dilutions were prepared in PBS.

APPENDIX B: PLATFORM SPECIFICATION

Design A	Depth of intake 700 μm	Depth of air chamber 700 μm	Air hole D 1 mm	Width of intake 2 mm
Design B	Depth of intake 700 μm	Depth of air chamber 700 μm	Air hole D 1 mm	Width of intake 400 μm
Design C	Depth of intake 700 μm	Depth of air chamber 700 μm	Depth of destination chamber 700 μm	Width of siphon channel 700 μm
Design D	Depth of mixing chamber 60 μm	Width of mixing chamber 4 mm		Microballoon Diameter 4 mm
Design E	Depth of mixing chamber 2 mm	Width of mixing chamber 4 mm		Microballoon Diameter 4 mm
Design F	Depth of source chamber 2 mm	Depth of destination chamber 2 mm	Outlet diameter 2.5 mm	Depth of air chamber 2 mm
Design G	Depth of source chamber 2 mm	Depth of destination chamber 2 mm	width of S microchannel 1 mm	Depth of air chamber 2 mm
Design D	Depth of source chamber 2 mm	Depth of reaction chamber 2 mm	Depth of mixing chamber 700 μm	Depth of metering fingers 2 mm